Computer Aided Diagnosis in Breast Ultrasound Imaging

Ruey-Feng Chang **(張瑞峰)**
Department of Computer Science and Information Engineering (資訊系)
Graduate Institute of Biomedical Electronics and Bioinformatics (生醫電資所)
National Taiwan University(國立台灣大學), Taiwan

Yi-Hong Chou **(周宜宏)**
Veterans General Hospital, Taiwan
Chiun-Sheng Huang **(黃俊升)**
National Taiwan University Hospital, Taiwan
Yeun-Chung Chang **(張允中)**
National Taiwan University Hospital, Taiwan

Jeon-Hor Chen **(陳中和)**
University of California, Irvine, USA

Woo Kyung Moon
Seoul National University Hospital, Korea

Etsuo Takada
Dokkyo University, Japan

Contents

- 2-D Breast US CADx
- Elastography CADx
- 3-D Breast US/ABUS CADx
- ABUS CADe
- ABUS/MRI Density Analysis
- MRI CADe/CADx

NTU CAD Lab

1997 — 2-D US

- 1997 Aloka SSD 1200
- 2003 Acuson, GE, Medison, ATL, Philips

2000 — 3-D US

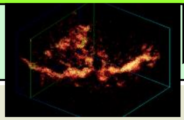

- 1999 Free-hand 3D US
- 2000 Voluson 530
- 2002 GE 730
- 2010 GE E8 and E6

2002 — Whole Breast

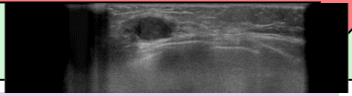

- 2002 Free-hand
- 2003 Aloka ABUS
- 2005 U-systems

2004 — PC-based US

- 2004 Telemed, Lithuania Echo Blaster 128
- 2005 Terason t3000

National Taiwan University

2006 — Elastography

- 2006 Hitachi Elastography
- 2010 Siemens Elastography

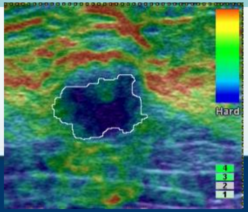

2008 — MRI

- 2008 Morphology, Kinetic
- 2009 Tofts Model
- 2010 DWI

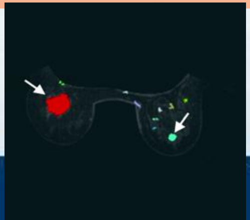

2011 — Automated US

- 2011 Siemens ABVS

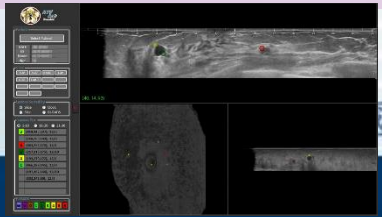

2011, 2013 — 2D/3D Shearwave

- 2010 Siemens ARFI
- 2011 Supersonic Shearwave
- 2013 3D Elastography

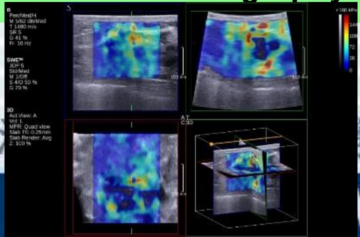

Introduction

- For 2D breast US, the physician has detected the tumor and only the computer-aided diagnosis (CADx) is needed for the tumor.

- For the new automated whole breast US (ABUS), the computer-aided detection (CADe) is needed for detecting the tumors, just like mammography CAD.

Technology Development Program for Academic (TDPA, 學界科專)

- This TDPA project was supported by the Ministry of Economic Affairs (MOEA) to develop
  - a CADe system for ABUS
  - a CADx system for B-mode US/elastography
  - breast US GPS/recoding System
- The Co-PIs are Dr. Chou from VGH, Dr. Huang, and Dr. Chang from NTUH.
- 8 PhD students worked on this project.

Technology Development Program for Academic (TDPA, 學界科專)

- Two patents have been applied.
  - Breast Ultrasound Scanning and Diagnosis Aid System
  - Ultrasound Imaging Breast Tumor Detection and Diagnostic System and Method
- 25 international journals and 12 international conference papers
  - Three IEEE Trans. MI papers have been published.
- The CADe and CADx systems have been transferred to TaiHao Medical Inc. (http://taihaomed.com/)

CADx for TDPA

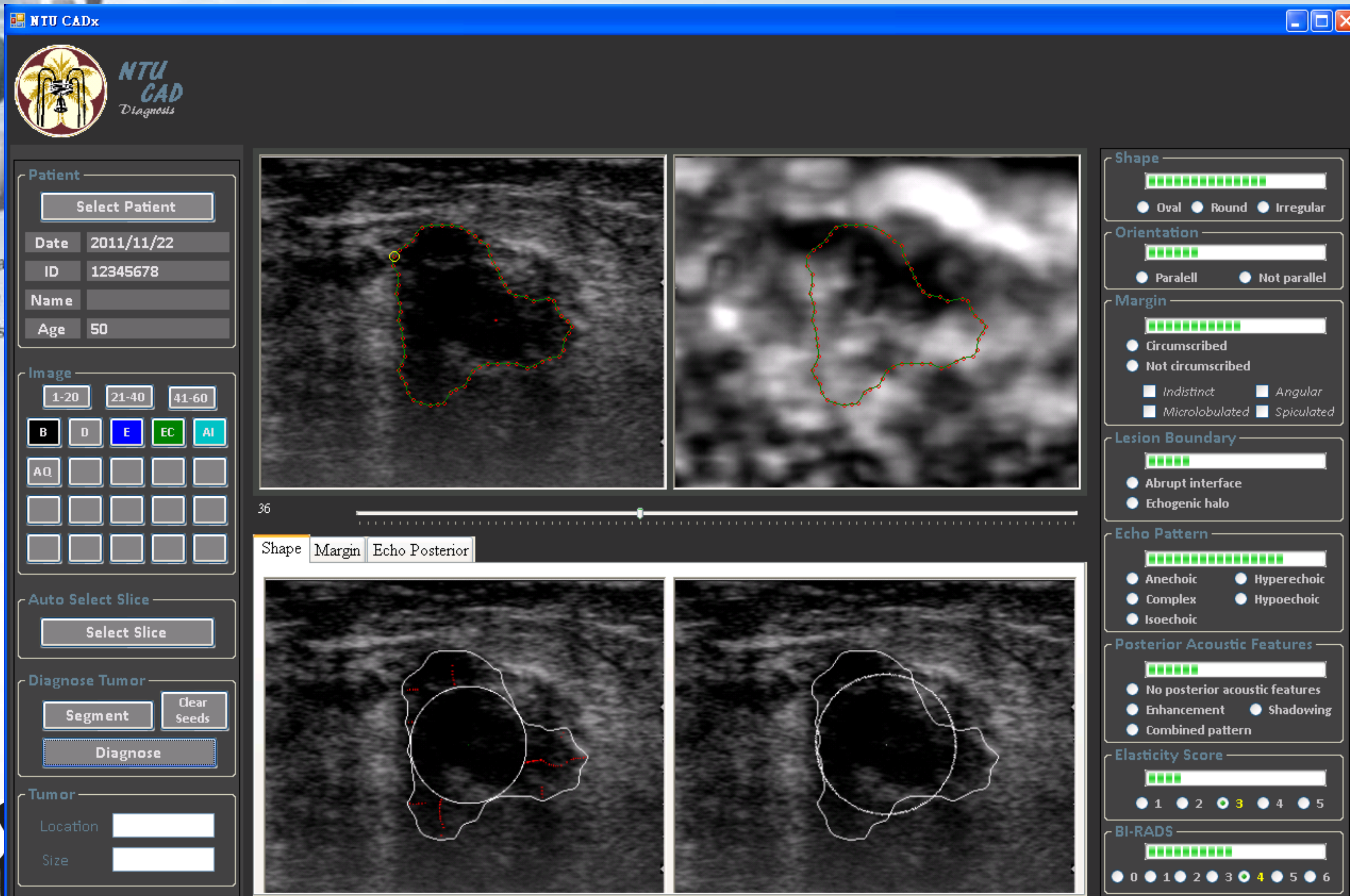

CADx for TDPA

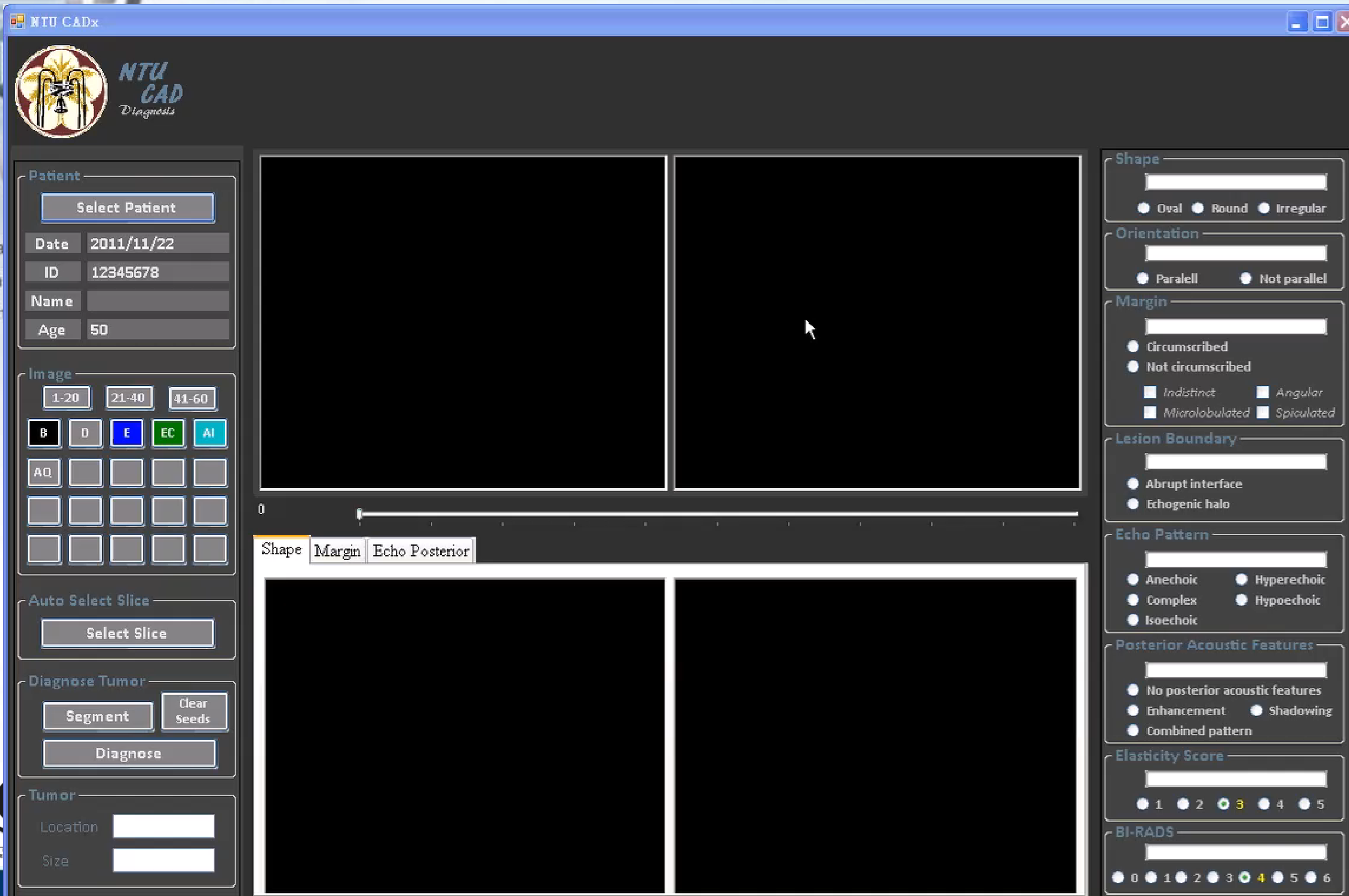

ABUS CADe

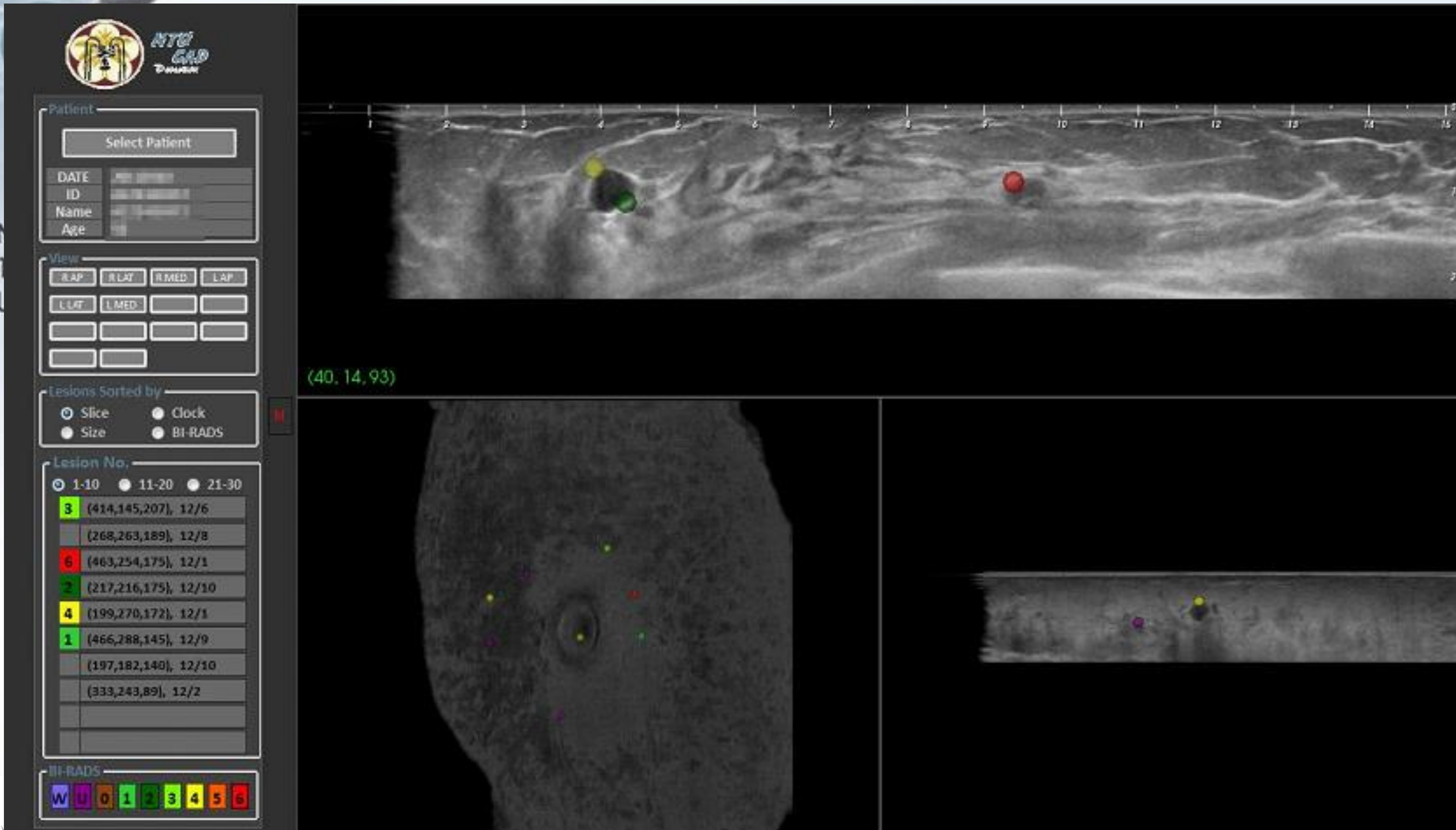
NTU CAD
Patient
Select Patient
DATE
ID
Name
Age
View
R AP
R LAT
R MED
L AP
L LAT
L MED
(40, 14, 93)
Lesions Sorted by
Slice
Clock
Size
BI-RADS
Lesion No.
1-10
11-20
21-30
3 (414,145,207), 12/6
(268,263,189), 12/8
6 (463,254,175), 12/1
2 (217,216,175), 12/10
4 (199,270,172), 12/1
1 (466,288,145), 12/9
(197,182,140), 12/10
(333,243,89), 12/2
BI-RADS
W U 0 1 2 3 4 5 6

DEMO

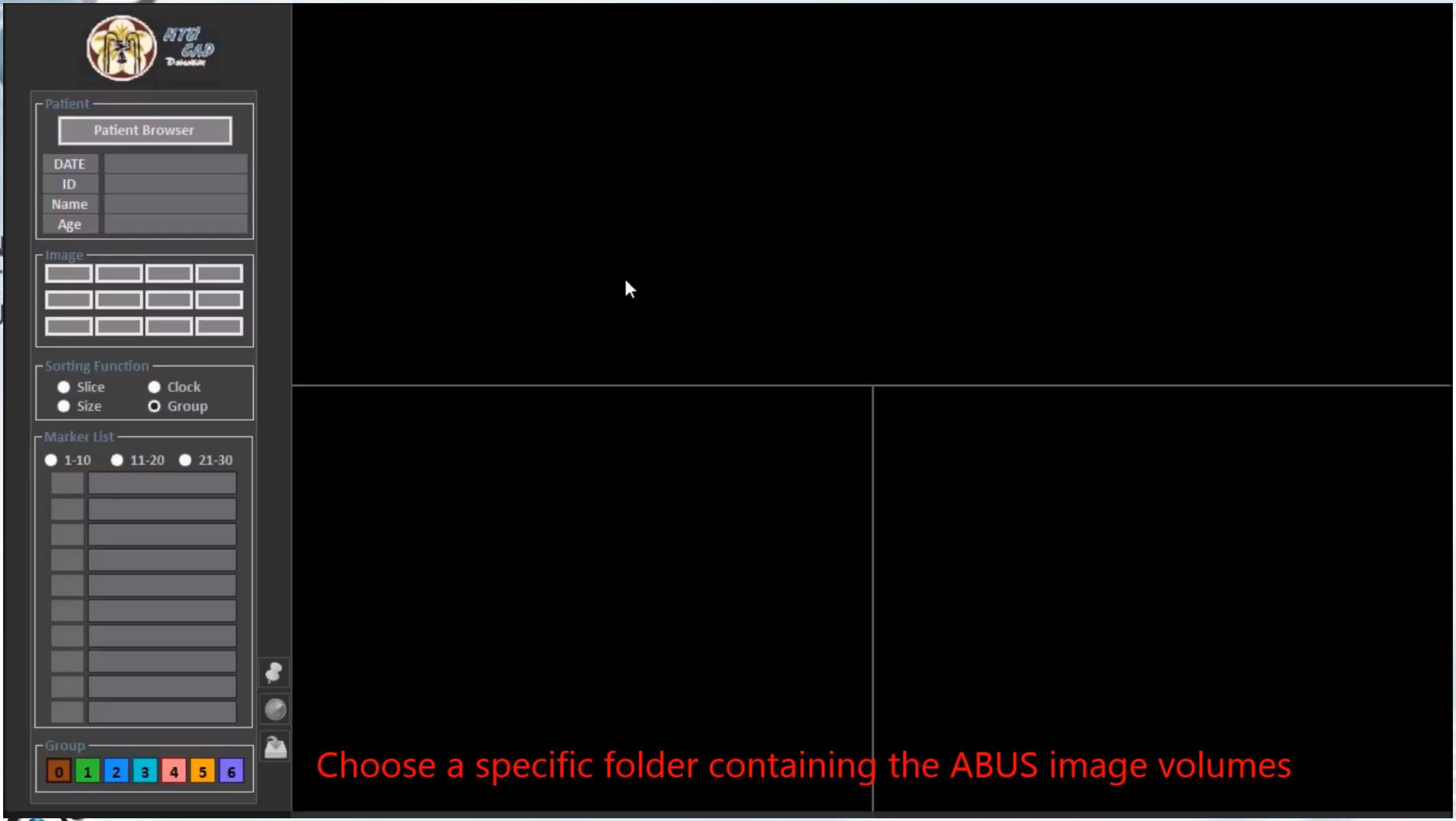
NTU CAD
Patient
Patient Browser
DATE
ID
Name
Age
Image
Sorting Function
Slice
Clock
Size
Group
Marker List
1-10
11-20
21-30
Group
0 1 2 3 4 5 6
Choose a specific folder containing the ABUS image volumes

DEMO

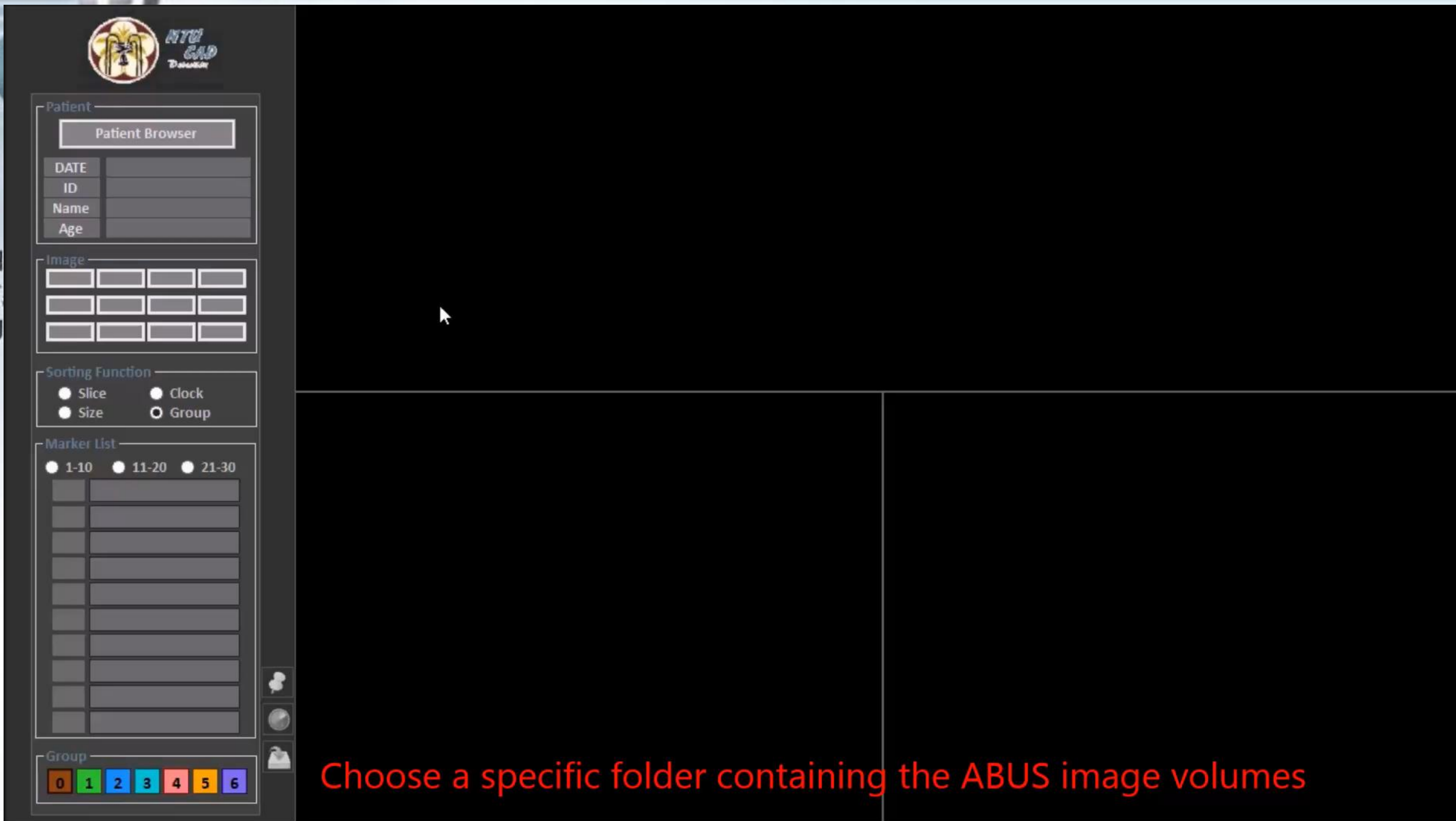
NTU CAD
Patient
Patient Browser
DATE
ID
Name
Age
Image
Sorting Function
Slice
Clock
Size
Group
Marker List
1-10
11-20
21-30
Group
0
1
2
3
4
5
6
Choose a specific folder containing the ABUS image volumes

Breast US GPS/Recoding System

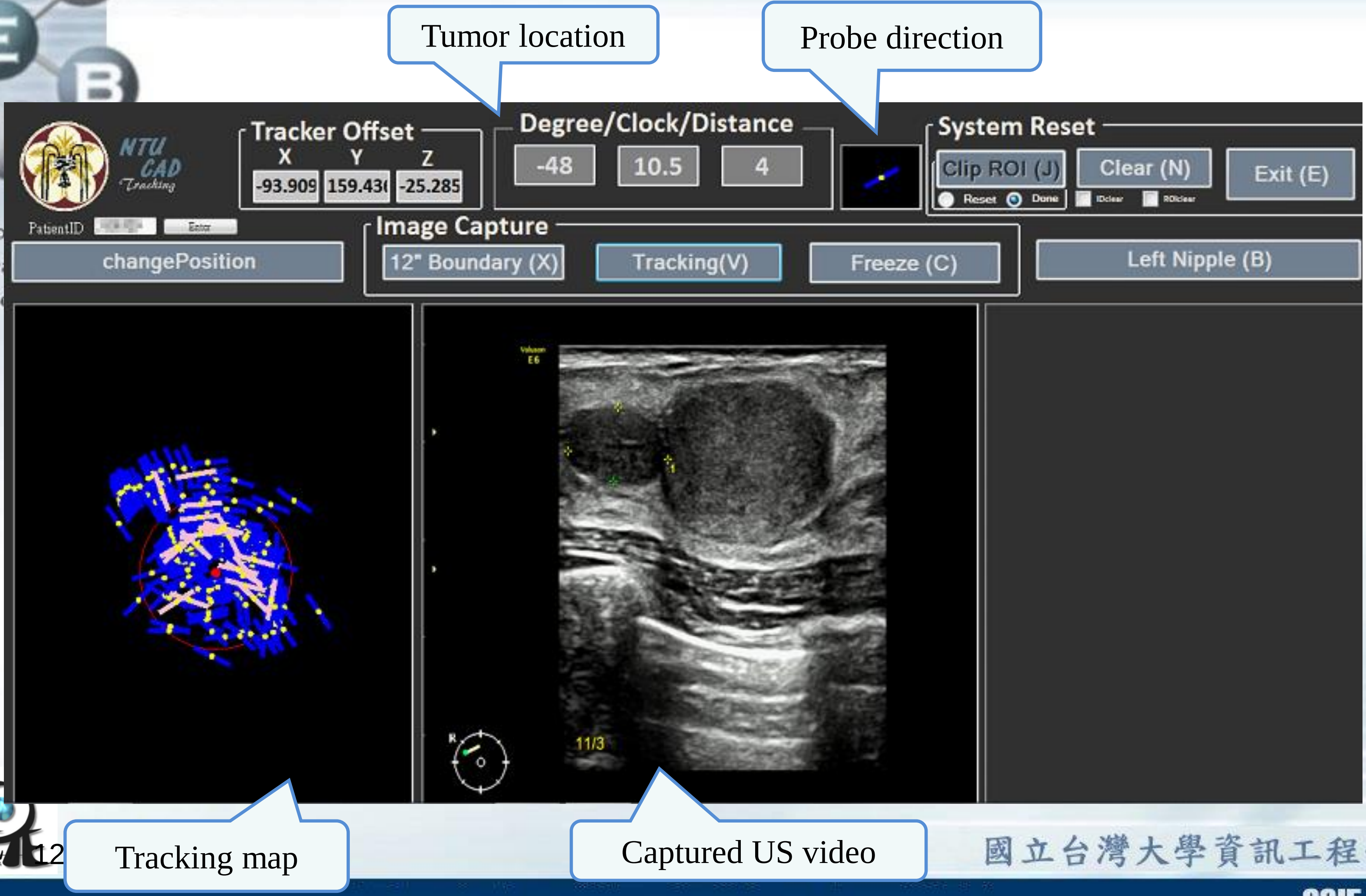

National Taiwan University

2-D BREAST US CAD

- ROBUST TEXTURE ANALYSIS

“Computer-aided Diagnosis Applied to US of Solid Breast Nodules by Using Neural Networks”, Radiology, vol. 213, no. 2, pp.407-412, 1999.

“Robust texture analysis using multi-resolution gray-scale invariant features for breast sonographic tumor diagnosis,” IEEE Transactions on Medical Imaging, vol. 32, no. 12, pp. 2262-2273, 2013.

“Computer-aided diagnosis for distinguishing between triple-negative breast cancer and fibroadenomas based on ultrasound texture features,” Medical Physics, vol. 42, no. 6, pp. 3024-3035, 2015.

2D US CAD

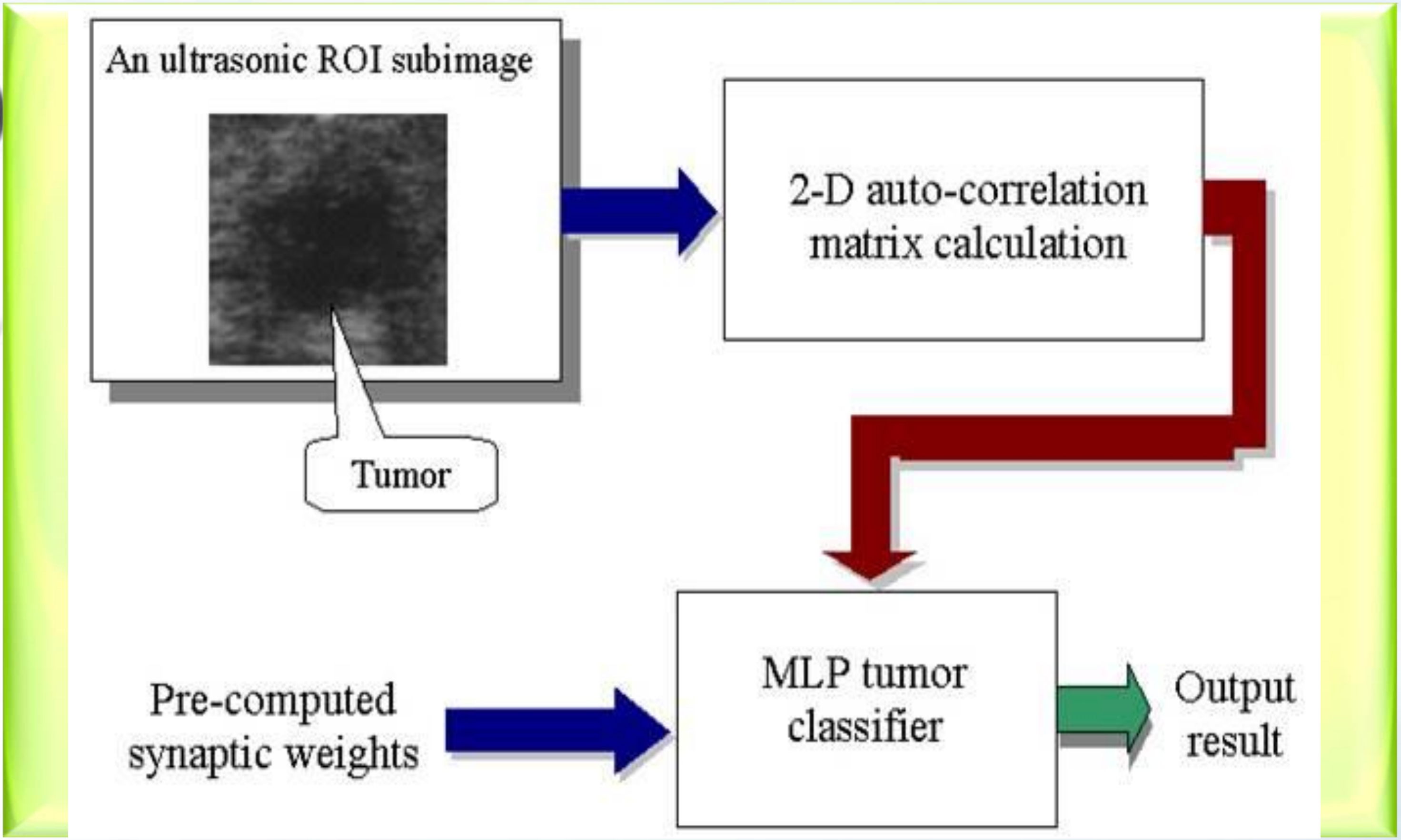

"Computer-aided Diagnosis Applied to US of Solid Breast Nodules by Using Neural Networks", Radiology, vol. 213, no. 2, pp.407-412, 1999.
Editorial: Georgia D. Tourassi, "Journey toward Computer-aided Diagnosis: Role of Image Texture Analysis," Radiology, vol. 213, no.2, pp.317-320, Nov. 1999.

Robust Texture Analysis

- Because the **parameters of ultrasonic machine** is adjustable, the images from the same machines may have different texture information.
- Moreover, the images from **different ultrasonic machines** have different texture information.
- Hence, the **ranklet transform** is proposed in this study to extract the **gray-scale invariant texture features** for tumor diagnosis.

"Robust texture analysis using multi-resolution gray-scale invariant features for breast sonographic tumor diagnosis," IEEE Transactions on Medical Imaging, vol. 32, no. 12, pp. 2262-2273, 2013

Ranklet Transform

- Similar to wavelet transform, the ranklet images can be derived from a family of **multi-resolution, orientation-selective** features
- Differently from wavelet transform, it deals with **ranks** of pixels rather than with their **gray-scale intensity** values

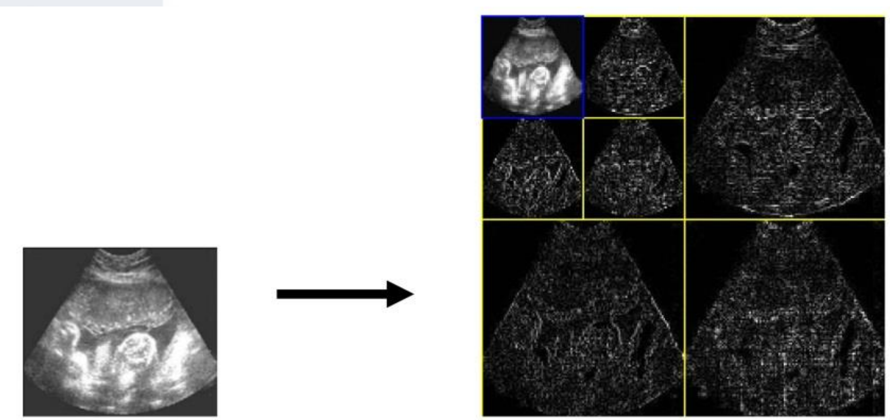

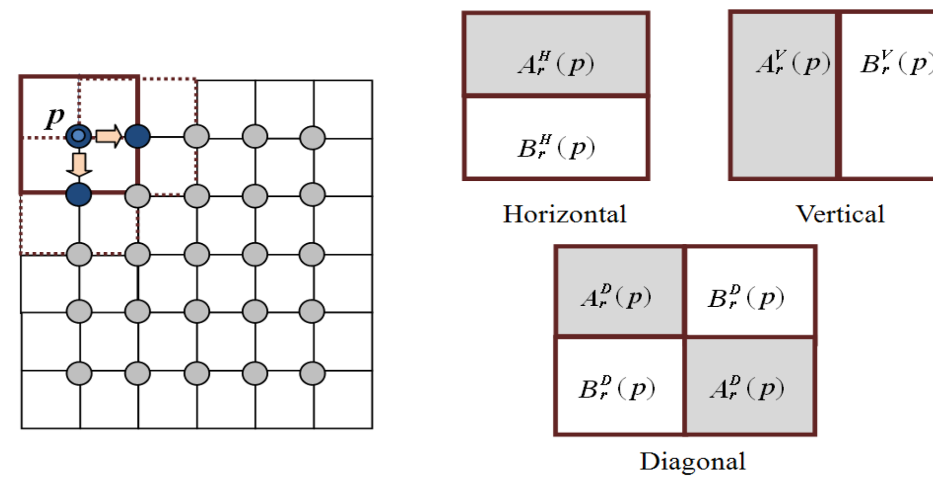

(a) (b)

HH (Diagonal subband, D)
HL (Horizontal subband, H)
LH (Vertical subband, V)

Ranklet Example

- The ranklet images from images with non-linear monotonic change filters (i.e., **gamma correlation**, **histogram equalization**) are nearly the same.

Origin	*Wavelets*			*Ranklets*		
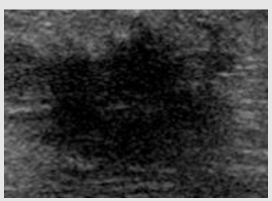	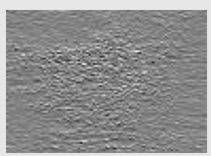	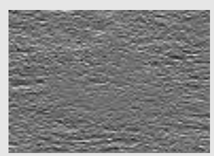		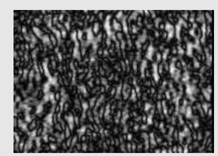	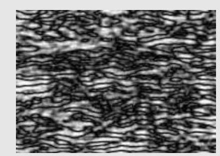	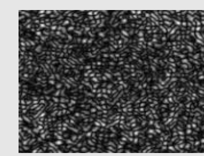
	W_{-1}^{V}	W_{-1}^{H}	W_{-1}^{D}	R_{8}^{V}	R_{8}^{H}	R_{8}^{D}
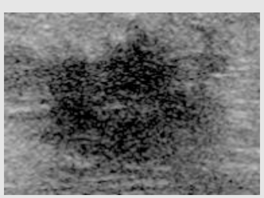	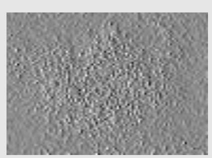		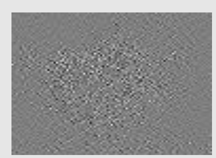	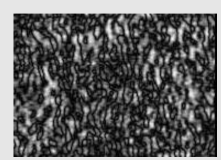	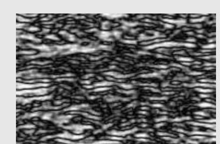	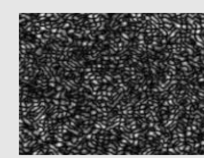
	W_{-1}^{V}	W_{-1}^{H}	W_{-1}^{D}	R_{8}^{V}	R_{8}^{H}	R_{8}^{D}

Proposed Robust Texture Analysis

- First, we decompose each BUS image from the test database into ranklets.
- Afterwards, the gray-scale invariant texture features based on GLCM can be calculated from each transformed image with regions of interest (ROIs).
- The SVM classifier is adopted to distinguish a benign tumor from a malignant one.

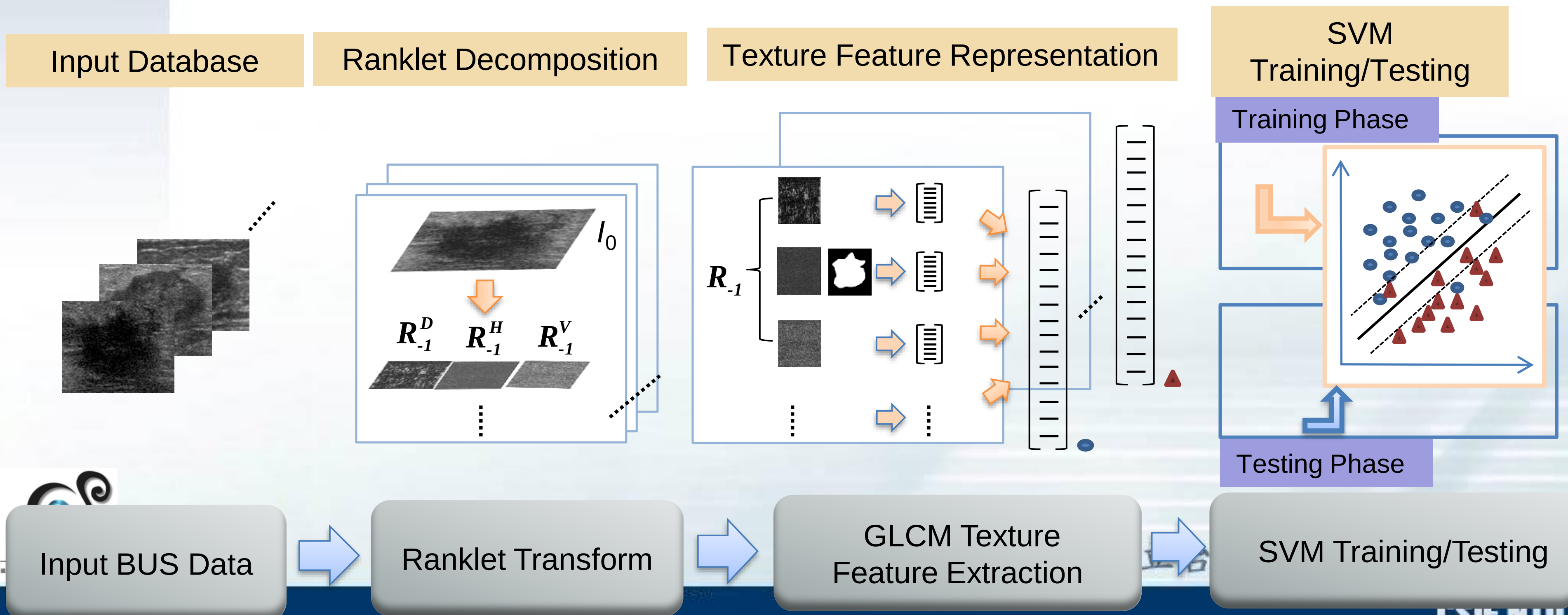

Three US Machines

- **Database A** includes 116 subjects (78 benign and 38 malignant cases) obtained with **Acuson Sequoia** machine.

- Database B includes 193 subjects (133 benign and 60 malignant cases) obtained with **GE LOGIQ 7** machine.

- Database C includes 161 subjects (104 benign and 57 malignant cases) obtained with **GE Voluson 730 expert** machine.

Experiments

- **The GLCM-based textural features are applied for original image (origin), multi-resolution wavelet images (wavelets) and multi-resolution ranklet images (ranklets).**

D.B.	Method	AUC	ACC (%)	SENS (%)	SPEC (%)
A	*Origin*	0.81±0.03	74.28±2.27	63.93±5.78	79.39±3.14
	Wavelets	0.84±0.03	79.45±1.73	**70.54±4.23**	83.76±2.39
	Ranklets	**0.90±0.02**	**81.68±1.69**	69.66±4.63	**87.55±2.15**
B	*Origin*	0.86±0.03	78.75±2.21	66.53±5.99	84.33±2.89
	Wavelets	0.92±0.02	84.23±1.71	74.99±4.74	88.38±2.12
	Ranklets	**0.94±0.02**	**86.35±1.64**	**79.56±4.44**	**89.35±2.11**
C	*Origin*	0.84±0.03	76.49±2.28	67.74±5.30	81.31±3.32
	Wavelets	0.85±0.02	77.14±1.74	69.27±3.87	81.48±2.51
	Ranklets	**0.92±0.02**	**84.58±1.70**	**81.50±3.66**	**86.19±2.44**

Cross-machine Experiments

- The AUC of cross-platform training and testing

Train Database	Method	Test Database		
A		B	C	B+C
	Origin (95% CI)	0.783 (0.717-0.846)	**0.823* (0.769-0.892)**	0.786 (0.739-0.835)
	Wavelets (95% CI)	**0.722† (0.6283-0.788)**	**0.752† (0.663-0.816)**	**0.729† (0.679-0.782)**
	Ranklets (95% CI)	**0.934* (0.896-0.965)**	0.877 (0.825-0.929)	**0.876* (0.837-0.909)**
B		A	C	A+C
	Origin (95% CI)	0.724 (0.633-0.816)	**0.807* (0.736-0.869)**	**0.764† (0.707-0.817)**
	Wavelets (95% CI)	**0.757† (0.643-0.828)**	**0.842* (0.784-0.906)**	**0.832* (0.779-0.879)**
	Ranklets (95% CI)	0.867 (0.792-0.929)	0.873 (0.817-0.922)	**0.875* (0.825-0.909)**
C		A	B	A+B
	Origin (95% CI)	**0.709† (0.614-0.806)**	0.789 (0.720-0.860)	**0.765† (0.708-0.821)**
	Wavelets (95% CI)	0.795 (0.677-0.864)	**0.785† (0.712-0.854)**	**0.808† (0.731-0.843)**
	Ranklets (95% CI)	0.859 (0.780-0.913)	**0.913* (0.871-0.949)**	**0.891* (0.855-0.925)**

TNBC vs. Fibroadenoma

- **Triple-negative breast cancer (TNBC)** is frequently misclassified as **fibroadenoma** due to benign morphologic features on breast ultrasound.
- The multi-resolution **ranklet features** are proposed to to discriminate between TNBC and benign fibroadenomas.

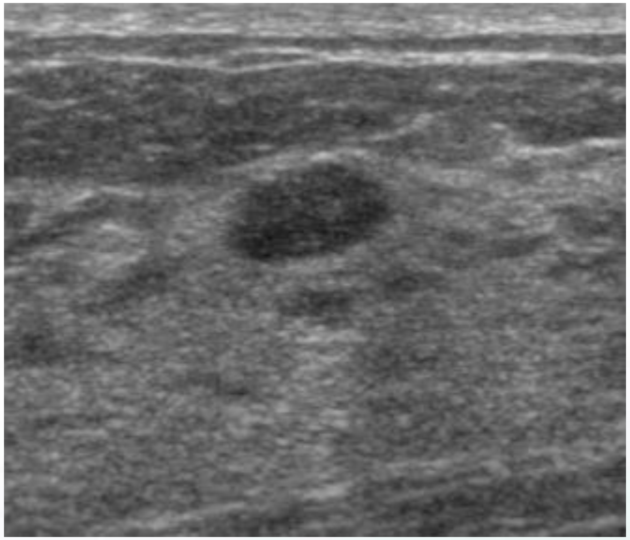

1*cm* benign fibroadenoma

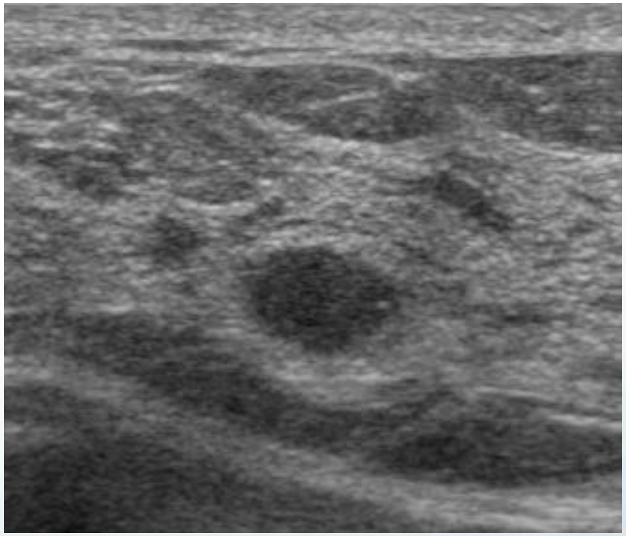

1*cm* triple-negative breast cancer

"Computer-aided diagnosis for distinguishing between triple-negative breast cancer and fibroadenomas based on ultrasound texture features," Medical Physics, vol. 42, no. 6, pp. 3024-3035, 2015.

Experiments

- 169 tumors, including **84 benign fibroadenomas** and **85 TNBCs**, are used in this study

	Accuracy (%)	Sensitivity (%)	Specificity (%)	PPV (%)	NPV (%)	Az
Morphology	76.92* (130/169)	78.82* (67/85)	75.00* (63/84)	76.13* (67/88)	77.78* (63/81)	0.8470*
Conventional Texture (GLCM)	79.29* (134/169)	81.18* (69/85)	77.38* (65/84)	78.41* (69/88)	80.25* (65/81)	0.8542*
Invariant Ranklet texture	**87.57** (148/169)	**89.41** (76/85)	**85.71** (72/84)	86.36 (76/88)	88.89 (72/81)	**0.9695**
Combined	**93.49** (158/169)	**94.12** (80/85)	**92.86** (78/84)	93.02 (80/86)	93.98 (78/83)	**0.9702**

ROC Curves

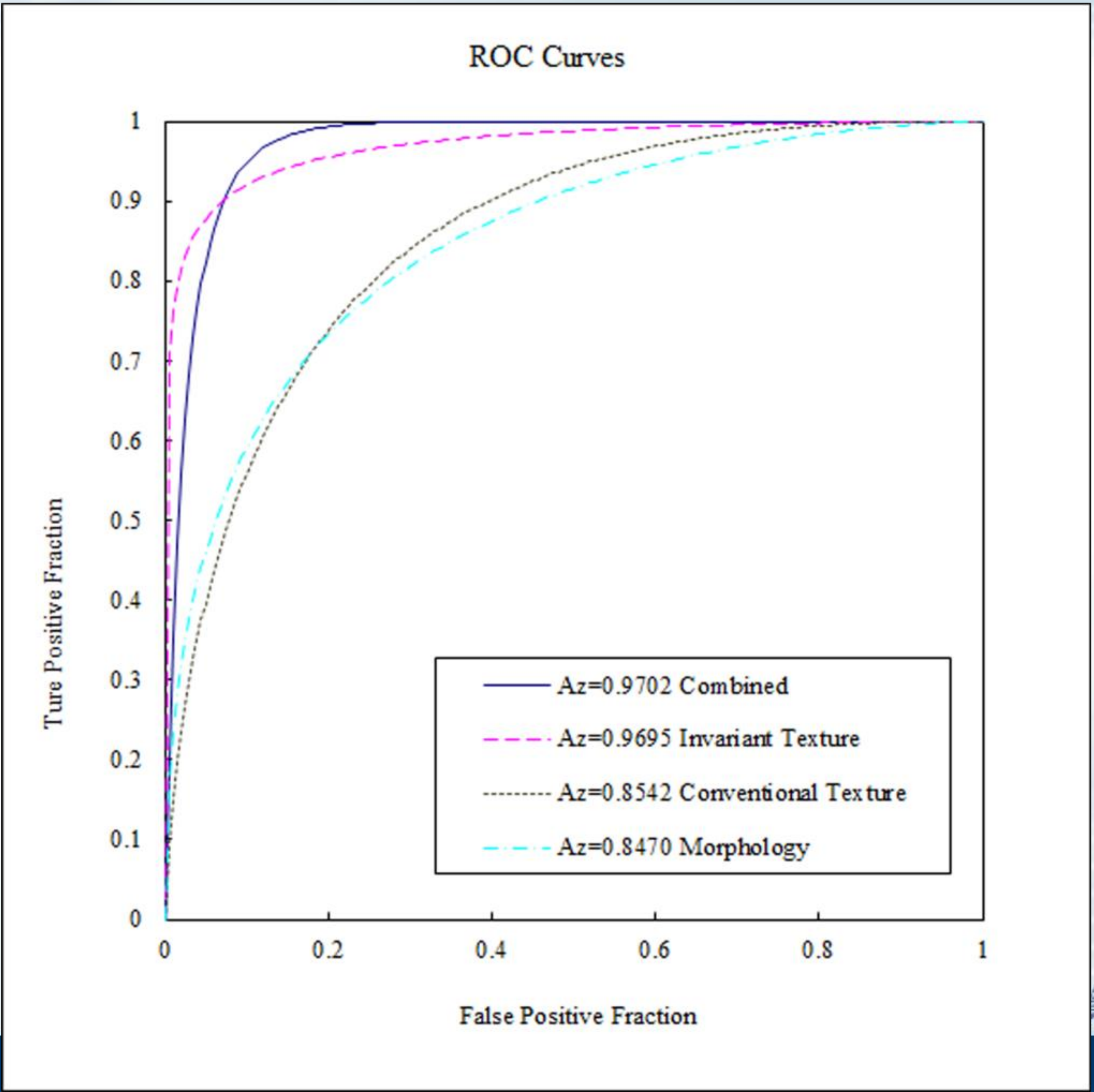
ROC Curves
Ture Positive Fraction
False Positive Fraction
0
0.1
0.2
0.3
0.4
0.5
0.6
0.7
0.8
0.9
1
0
0.2
0.4
0.6
0.8
1
Az=0.9702 Combined
Az=0.9695 Invariant Texture
Az=0.8542 Conventional Texture
Az=0.8470 Morphology

Elastography CADx

- SHEAR-WAVE ELASTOGRAPHY

“Analysis of elastographic and B-mode features at sonoelastography for breast tumor classification”, Ultrasound in Medicine and Biology, vol. 35, no. 11, pp. 1794–1802, 2009.

“Automatic selection of representative slice from cine-loops of real-time sonoelastography for classifying solid breast masses”, Ultrasound in Medicine and Biology, vol. 37, no. 5, pp. 709-718, 2011.

“Breast Tumor Classification Using Fuzzy Clustering for Breast Elastography”, Ultrasound in Medicine and Biology, vol. 37, no. 5, pp. 700-708, 2011.

“Classification of breast tumors using elastographic and B-mode features: Comparison of automatic selection of representative slice and physician-selected slice of images”, Ultrasound in Medicine and Biology, vol. 39, no. 7, pp. 1147-1157, 2013.

Dynamic Stain Elastography

- A lot of elastography slices are obtained during the operator to compress a tumor.
  - That is, the stain elastography image is **dynamic**.

Benign

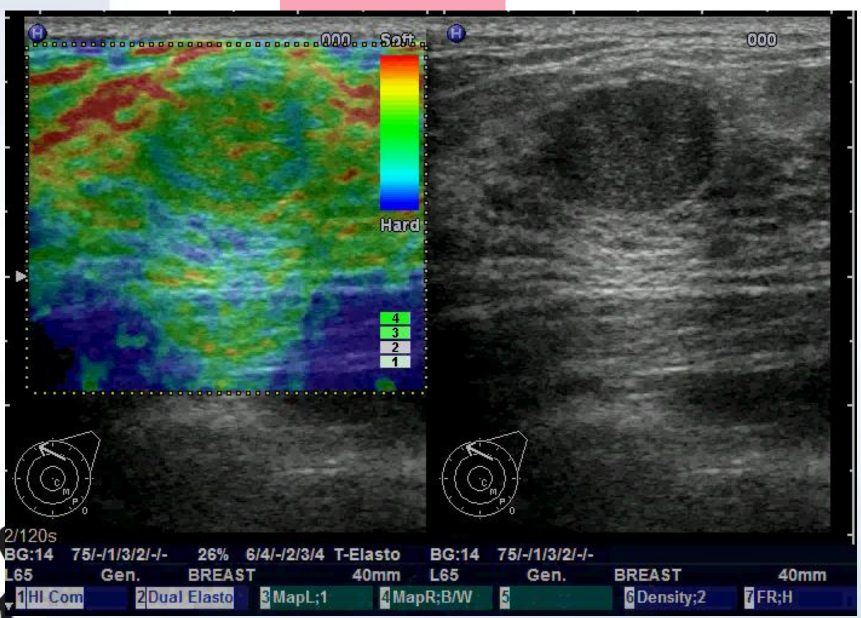

Malignant

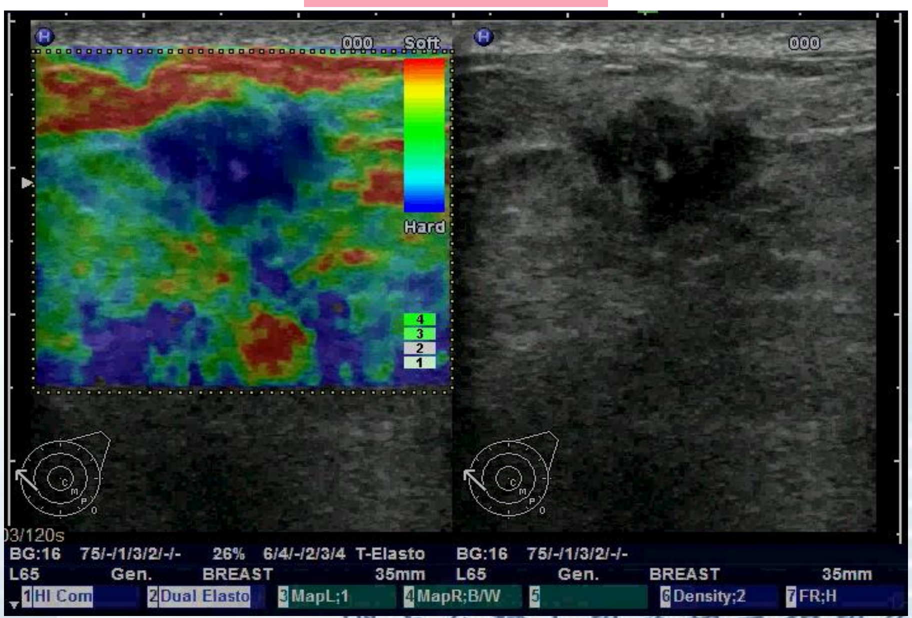

Elastography CAD

- A **representative slice** of the **dynamic elastography** image needs to be selected.
- The **B-mode** image could be used to **segment** the tumor and the tumor contour could be applied to the corresponding elastography image.
- Both the **elastography features** and **B-mode features** could be used to diagnose the tumor.

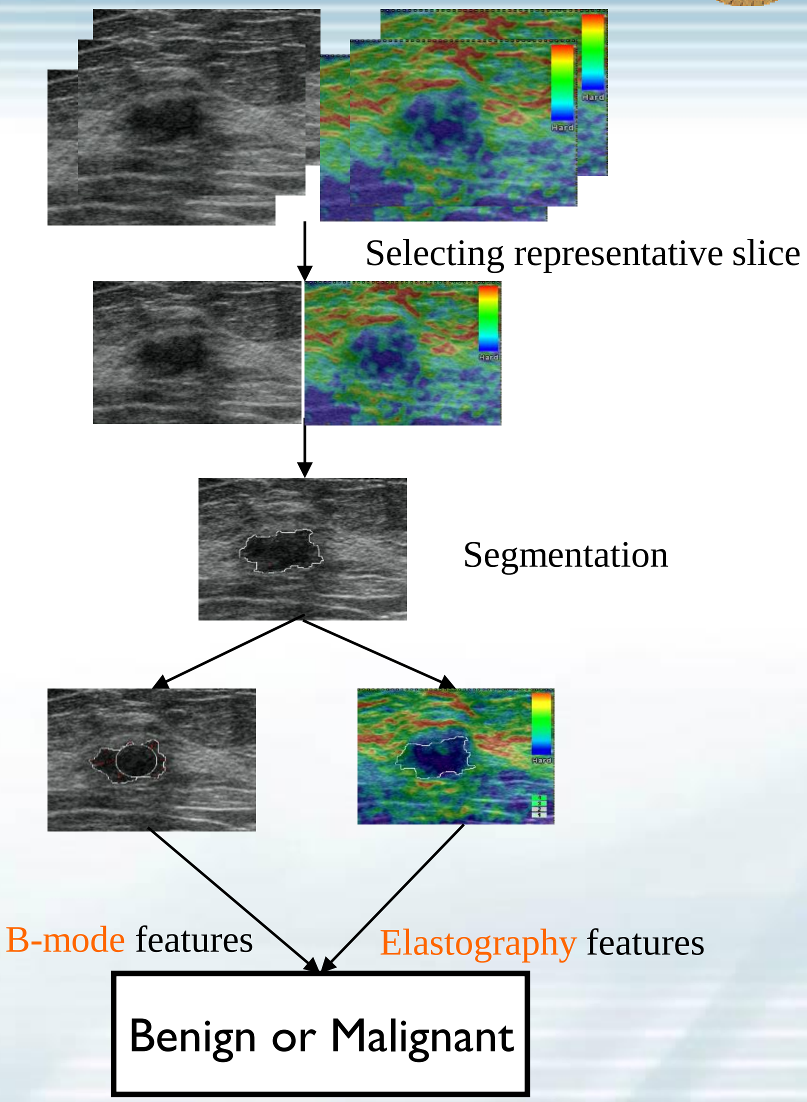

"Analysis of elastographic and B-mode features at sonoelastography for breast tumor classification", Ultrasound in Med. & Biol., Vol. 35, No. 11, pp. 1794–1802, 2009.

Image Quality Quantification

- Signal to Noise Ratio (SNR) and Contrast to Noise Ratio (CNR) are used to quantify the elastography image quality.
  - The middle block in the tumor is used to calculate the SNR.

$$SNR = \frac{mean}{standard\_deviation}$$

Low SNR

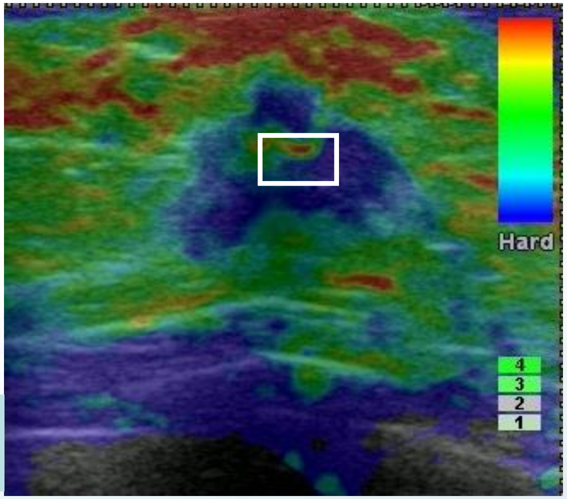

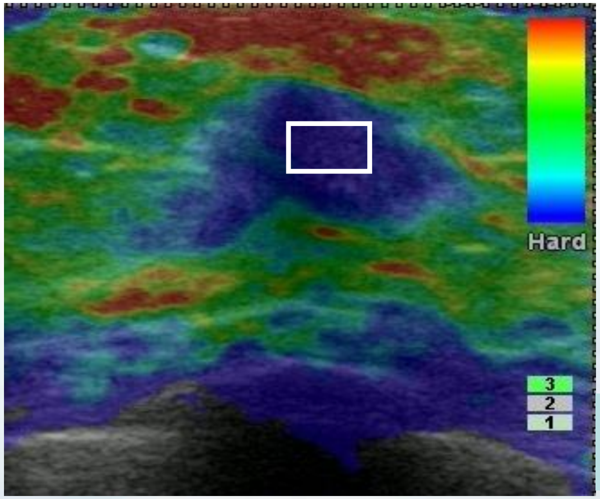

High SNR

"Automatic selection of representative slice from cine-loops of real-time sonoelastography for classifying solid breast masses", Ultrasound in Med. & Biol., Vol. 37, No. 5, pp. 709-718, 2011.

Image Quality Quantification

- In the CNR method, not only **the middle block** but also **two outside blocks** are used.

$$CNR = \frac{(middle\_mean - outside\_mean)^2}{middle\_SD^2 + outside\_SD^2}$$

Over-compressed

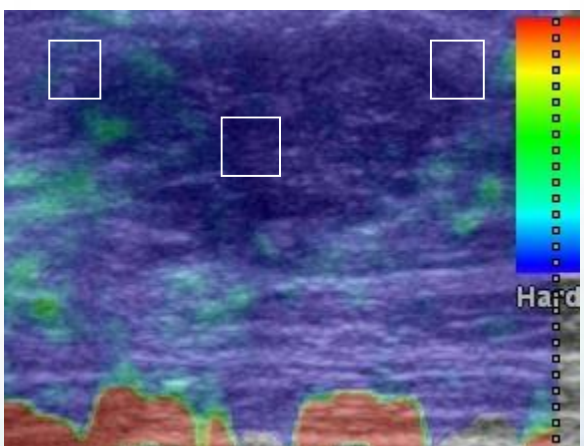

Low CNR

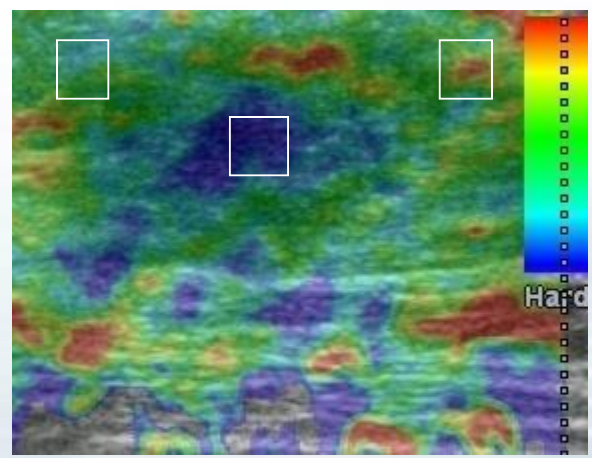

High CNR

The Strain Curve

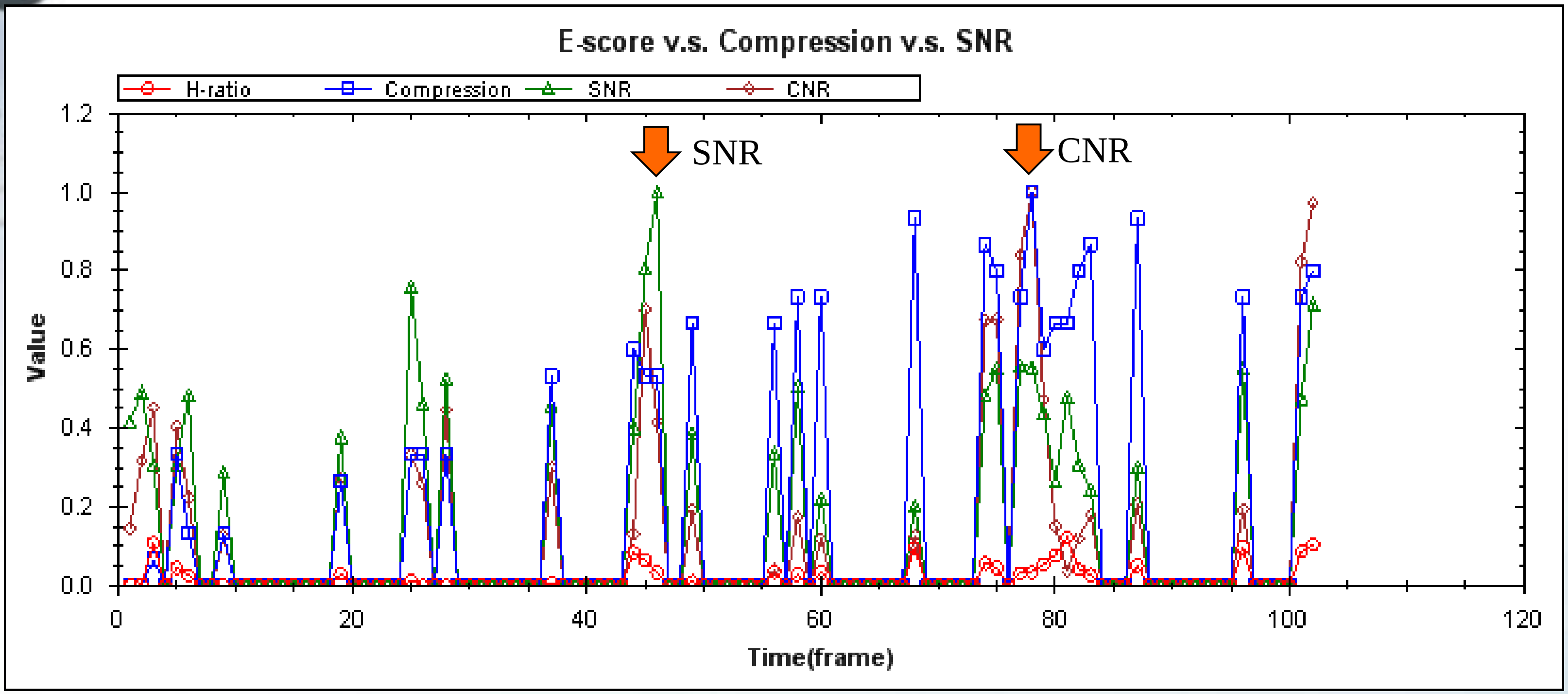

Tumor Segmentation

- The **contrast-enhanced gradient** image is used to segment the tumor using the **level set** method.

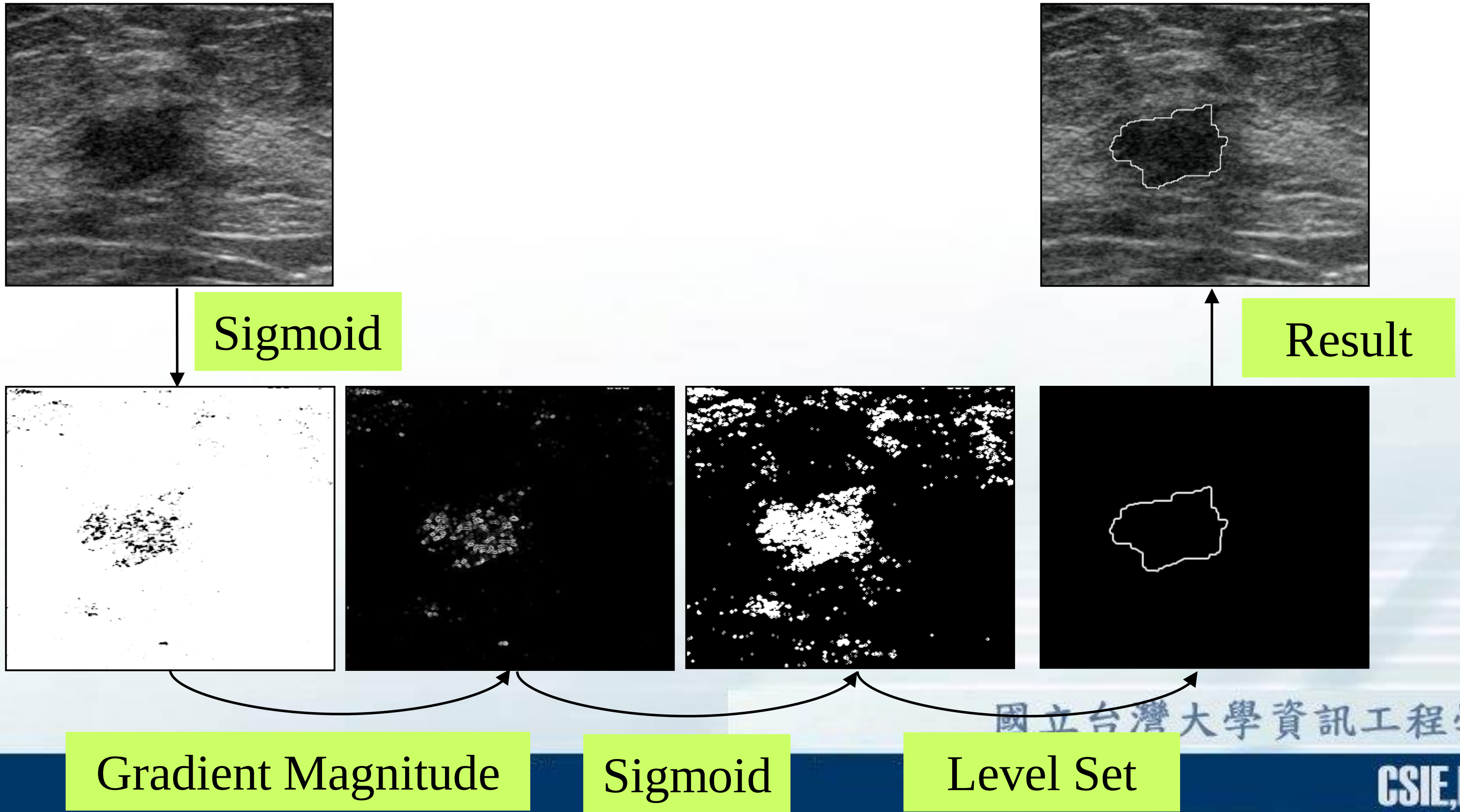

BI-RADS Features

- Shape
  - Oval, Round, Irregular
- Orientation
  - Parallel, Not parallel
- Margin
  - Circumscribed
  - Not circumscribed
    - Indistinct, Angular, Microlobulated, Spiculated
- Lesion boundary
  - Abrupt interface, Echogenic halo
- Echo pattern
  - Anechoic, Hyperechoic, Complex, Hypoechoic, Isoechoic
- Posterior shadowing
  - No posterior acoustic features, Enhancement, Shadowing, Combined patter

BI-RADS Atlas

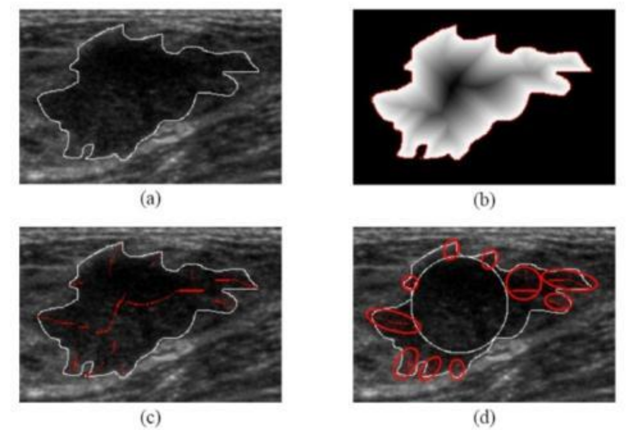

Elastography Features

- Stiffness Ratio
- Elasticity mean
- Lesion boundary elasticity

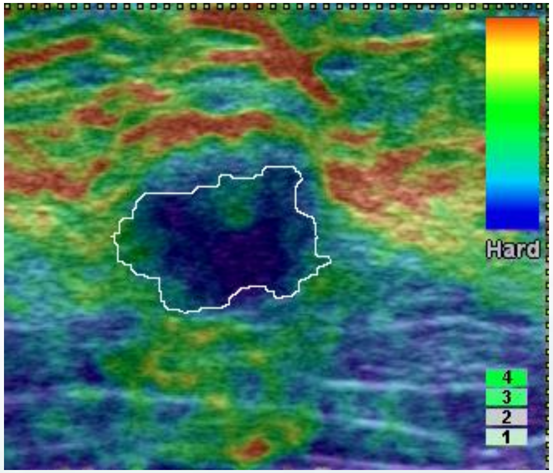

Experimental Results

- The data consisted of 151 biopsy-proved lesions (89 benign and 62 malignant lesions) from Dr. Moon.
- For CNR, elastography (82.12%) is better than B-mode (80.79%).
  For SNR and Physician-selected, B-mode (87.42%, 84.11%) is better than elastography (82.12%, 82.78%).
- SNR (90.07%) is better than CNR (86.09%) .
  SNR (90.07%) is similar to Physician-selected (89.40%) .

Features		Accuracy	Sensitivity	Specificity	PPV	NPV
CNR	B-mode	80.79%	70.97%	87.64%	80.00%	81.25%
	Elastography	82.12%	74.19%	87.64%	80.70%	82.98%
	All Features	86.09%	82.26%	88.76%	83.61%	87.78%
SNR	B-mode	87.42%	83.87%	89.89%	85.25%	88.89%
	Elastography	82.12%	79.03%	84.27%	77.78%	85.23%
	All Features	90.07%	90.32%	89.89%	86.15%	93.02%
Physician selected	B-mode	84.11%	77.42%	88.76%	82.76%	84.95%
	Elastography	82.78%	74.19%	88.76%	82.14%	83.16%
	All Features	89.40%	85.48%	92.13%	88.33%	90.11%

"Classification of breast tumors using elastographic and B-mode features: Comparison of automatic selection of representative slice and physician-selected slice of images", Ultrasound in Medicine and Biology, vol. 39, no. 7, pp. 1147-1157, 2013

ROC curves for SNR Representative Slice

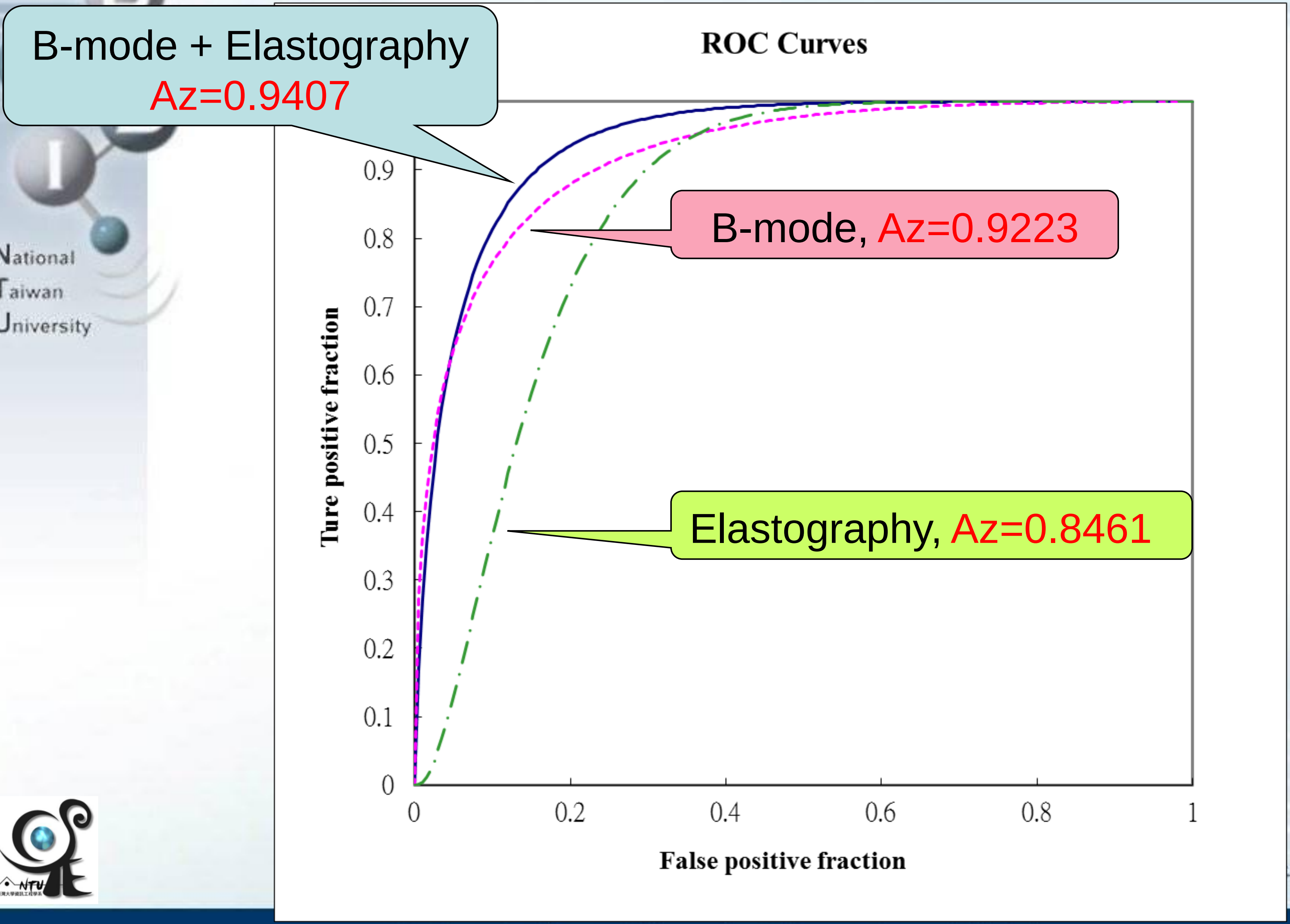

True Negative Case

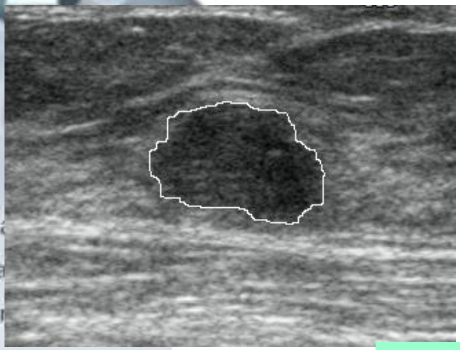

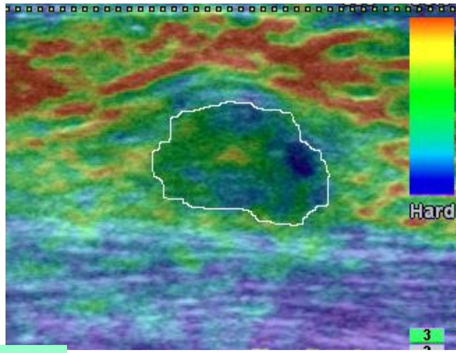

CNR

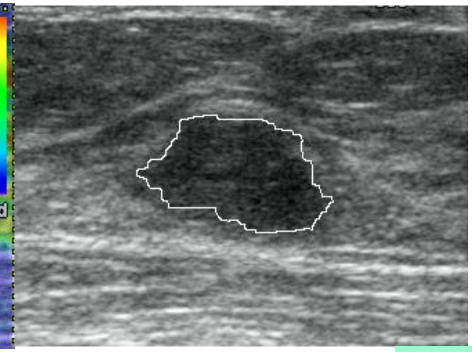

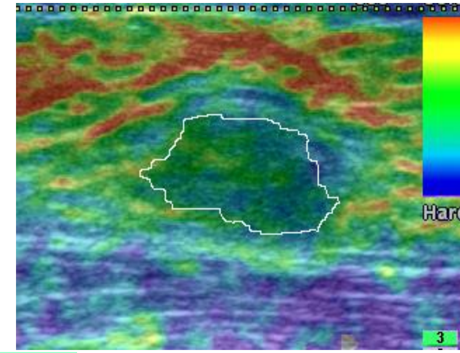

SNR

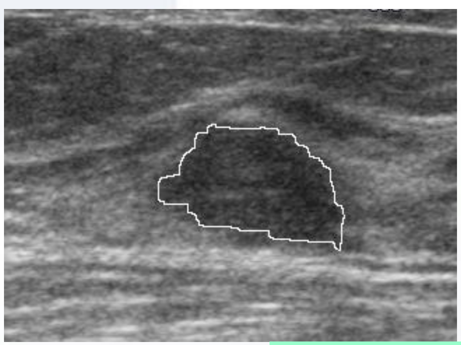

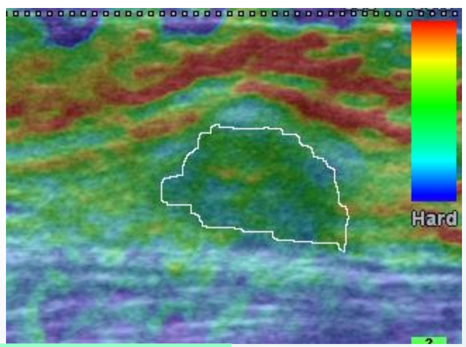

Physician-selected

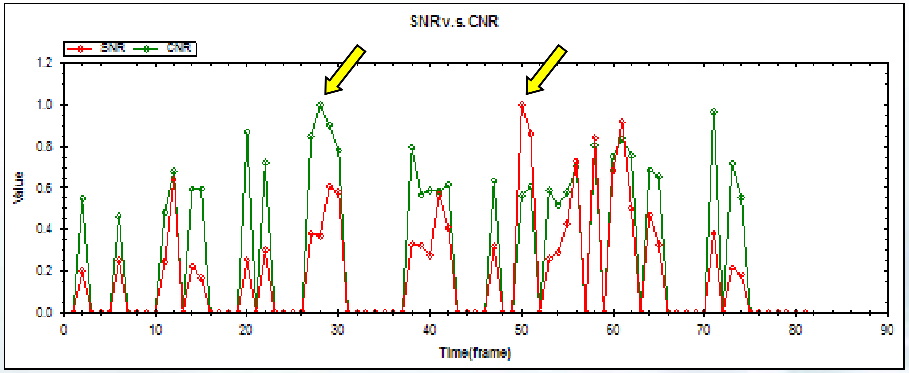

Fibroadenomas

True Positive Case

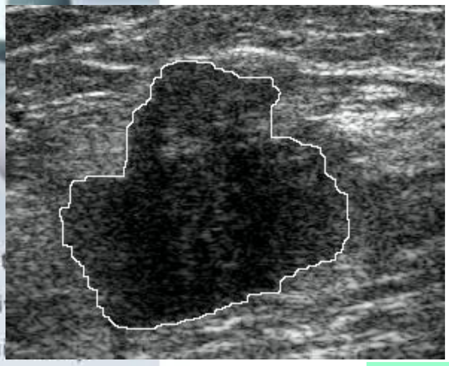

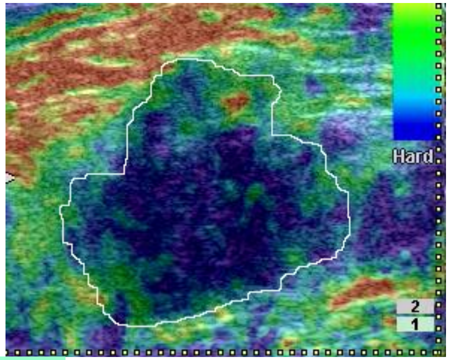

CNR

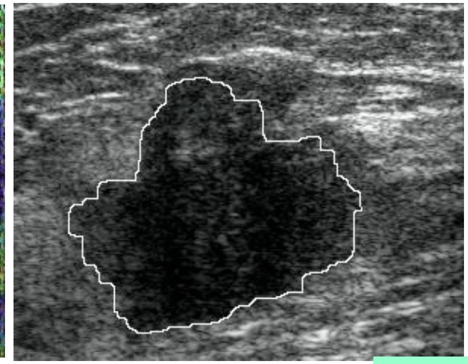

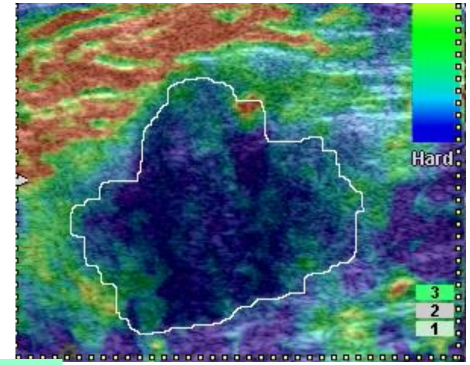

SNR

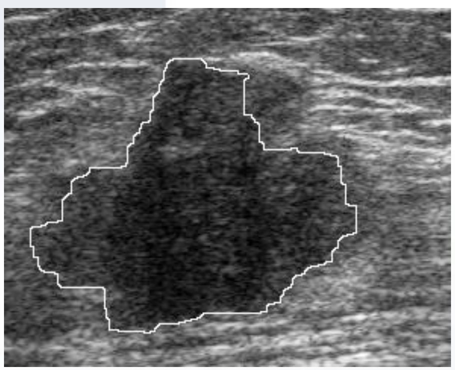

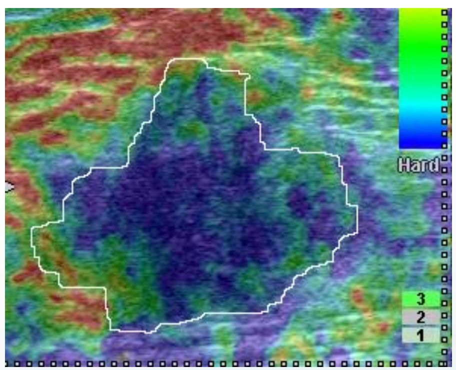

Physician-selected

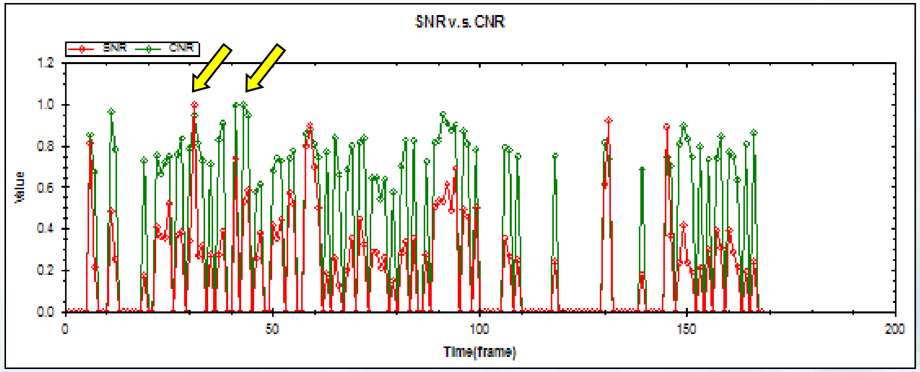

Infiltrating carcinomas

Summary

- The performance of B-mode features is better than that of elastography features in this study.
- Combining the B-mode and elastography features could improve the diagnosis performance.
- The proposed image quantification methods could have similar performances with the physician.
  - The proposed selection of representative slice is robust and reliable.

Shear-wave Elastography

- Stain elastography requires manual tissue compression which is operator dependent.
- Shear-wave elastography (SWE) is a new method to permit absolute quantification of tissue stiffness.
- Using acoustic radiation to stimulate tissues

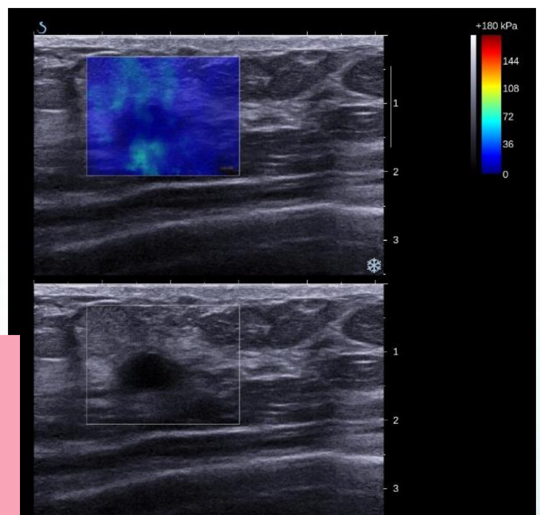

Benign
Softer
(low kPa)

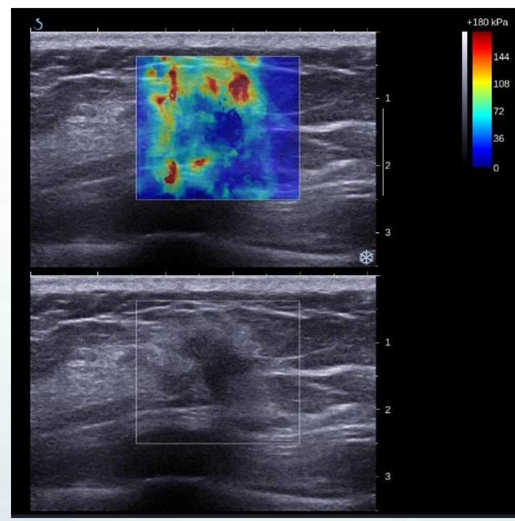

Malignant
Harder
(high kPa)

Shear-wave CAD

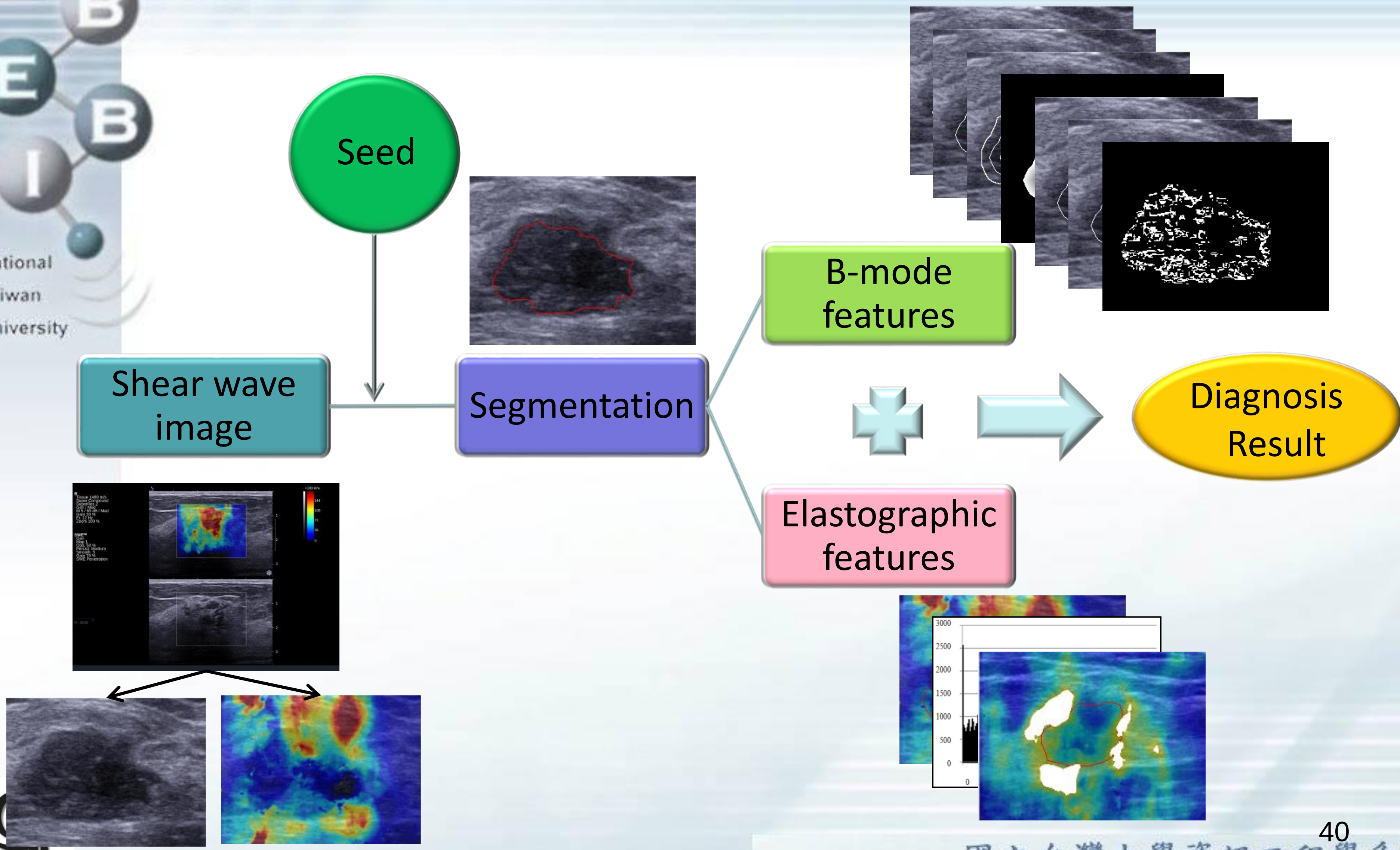

Experimental Results

- SuperSonic Imagine Aixplorer US
- 109 breast tumors
  - 57 benign and 52 malignant

109 cases: 57 benign and 52 malignant						
	Accuracy (%)	Sensitivity (%)	Specificity (%)	PPV (%)	NPV (%)	Az
B-mode	87.16 (95)	86.54 (45)	87.72 (50)	86.54 (45/52)	87.72 (50/57)	0.8312
Elastography	89.91 (98)	86.54 (45)	92.98 (53)	91.84 (45/49)	88.33 (53/60)	0.9511
Combined	94.50 (103)	92.31 (48)	96.49 (55)	96.00 (48/50)	93.22 (55/59)	0.9705

ROC Curves

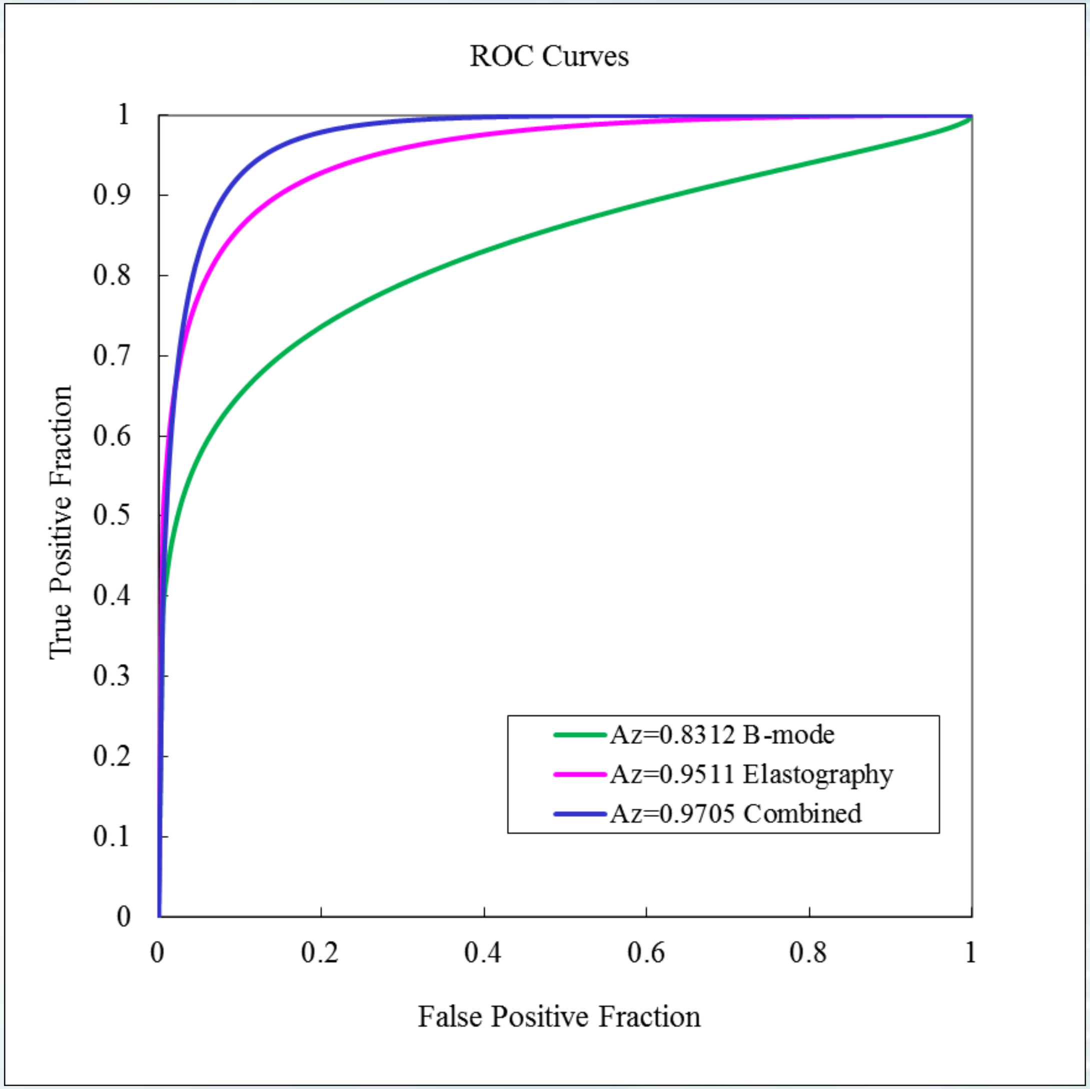
ROC Curves
True Positive Fraction
False Positive Fraction
1
0.9
0.8
0.7
0.6
0.5
0.4
0.3
0.2
0.1
0
0
0.2
0.4
0.6
0.8
1
Az=0.8312 B-mode
Az=0.9511 Elastography
Az=0.9705 Combined

3D/4D Elastography

- **The new CAD systems could be further developed for the 3D/4D elastography to provide more robust diagnosis.**

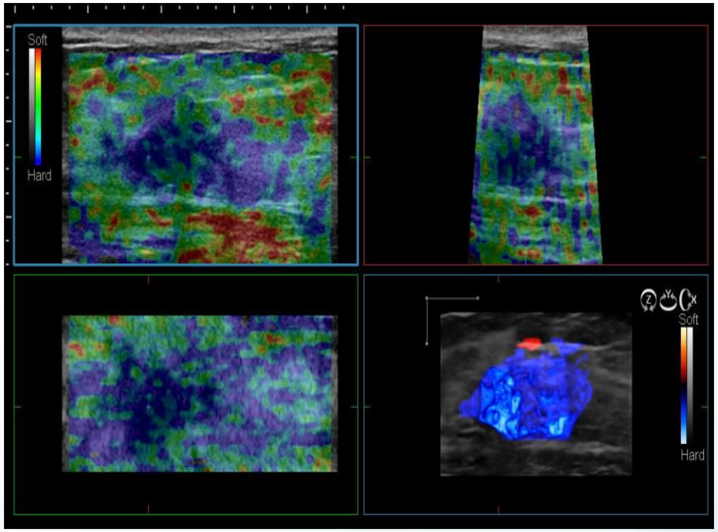

From Dr. Takada

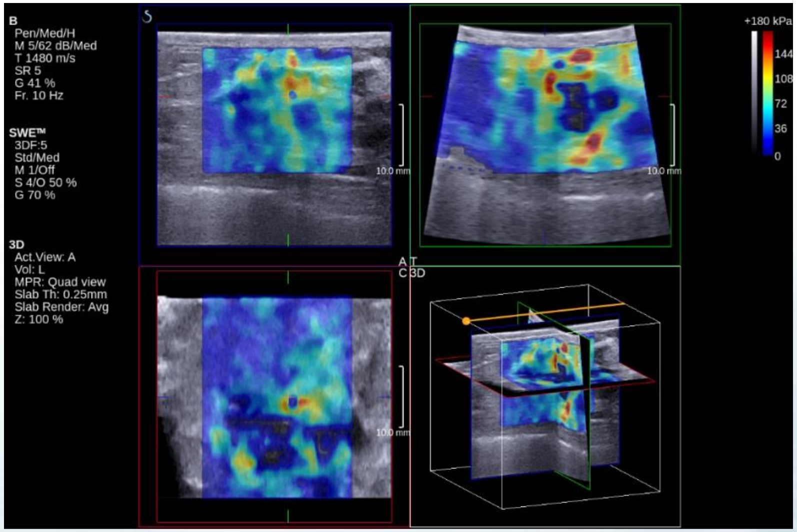

From Dr. Moon and Dr. Chou

3-D BREAST US/ABUS CADX

“Characterization of Spiculation on Ultrasound Lesions”, **IEEE Transactions on Medical Imaging**, vol. 23, no. 1, pp. 111-121, 2004.

“Solid Breast Masses: Neural Network Analysis of 3-D Power Doppler Ultrasound Image Features for Classification as Benign or Malignant”, **Radiology**, vol. 243, no. 1, pp. 56-62, 2007.

“Analysis of Tumor Vascularity Using Three-Dimensional Power Doppler Ultrasound Images,” **IEEE Transactions on Medical Imaging**, vol. 27, no. 3, pp. 320-330, 2008.

“Vascular Morphology and Tortuosity Analysis of Breast Tumor Inside and Outside Contour by 3-D Power Doppler Ultrasound”, **Ultrasound in Med. & Biol.**, vol. 38, no. 11, pp. 1859-1869, 2012.

“Computer-aided diagnosis for the classification of breast masses in automated whole breast ultrasound images,” **Ultrasound in Medicine and Biology**, vol. 37, no. 4, pp. 539-548, 2011.

3D US Spiculation

- A kind of stellate distortion caused by the intrusion of the breast cancer.
- The spiculation displayed only on the C-view of 3D US.
  - The conventional 2D US cannot see the spiculation.

Spiculation

Tumor

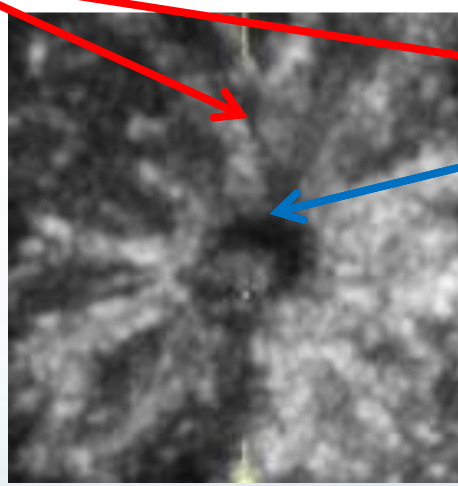

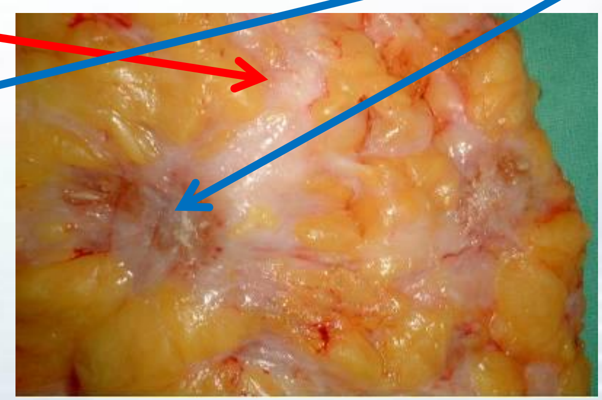

*IEEE Transactions on Medical Imaging, vol. 23, no. 1, pp. 111-121, Jan. 2004.

Experimental Result

- Spiculations are more easily seen in malignant tumors.
- Spiculations are more likely to appear in the coronal view.

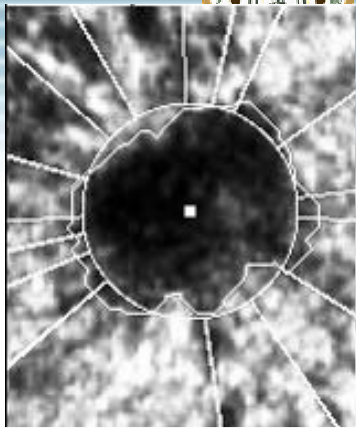

120 benign 3D datasets

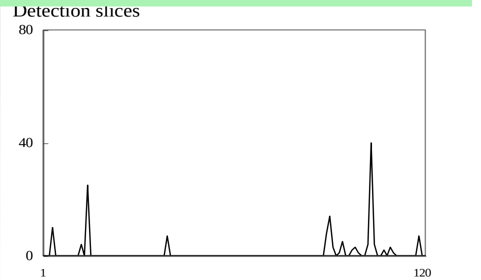

Coronal view

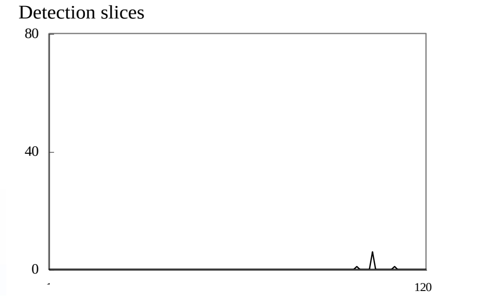

Transverse view

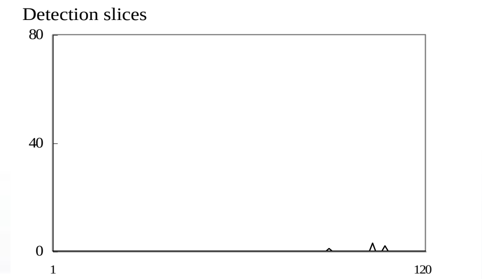

Longitudinal view

105 malignant 3D datasets

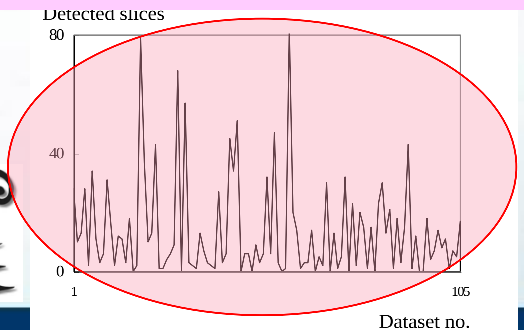

(a)

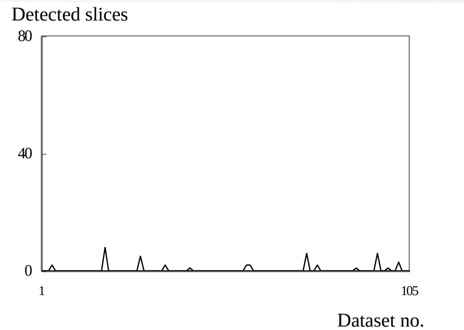

(b)

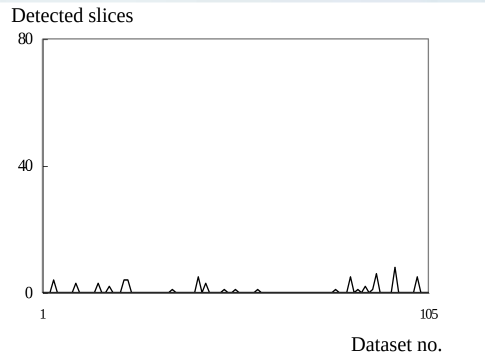

3D Power Doppler US

- A useful tool to detect the vessels.
  - 2D Doppler US can not obtain the entire 3-D vessels.
- The blood supply and vessel distribution are the important features to diagnose an tumor.

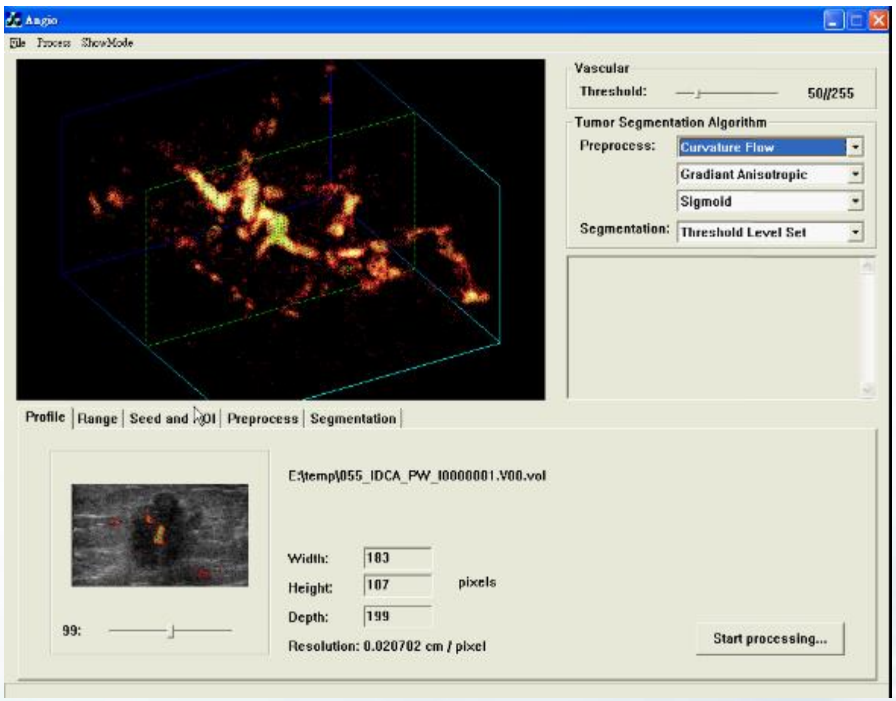

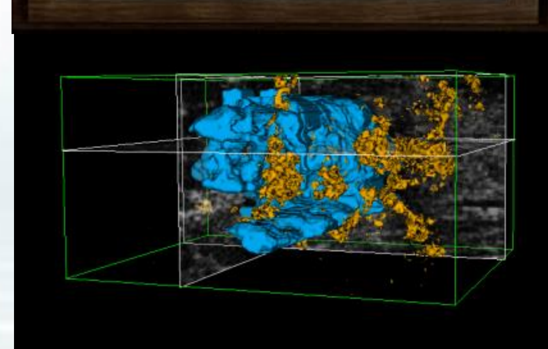

"Solid Breast Masses: Neural Network Analysis of 3-D Power Doppler Ultrasound Image Features for Classification as Benign or Malignant", Radiology, vol. 243, no. 1, pp. 56-62, 2007.

System Overview

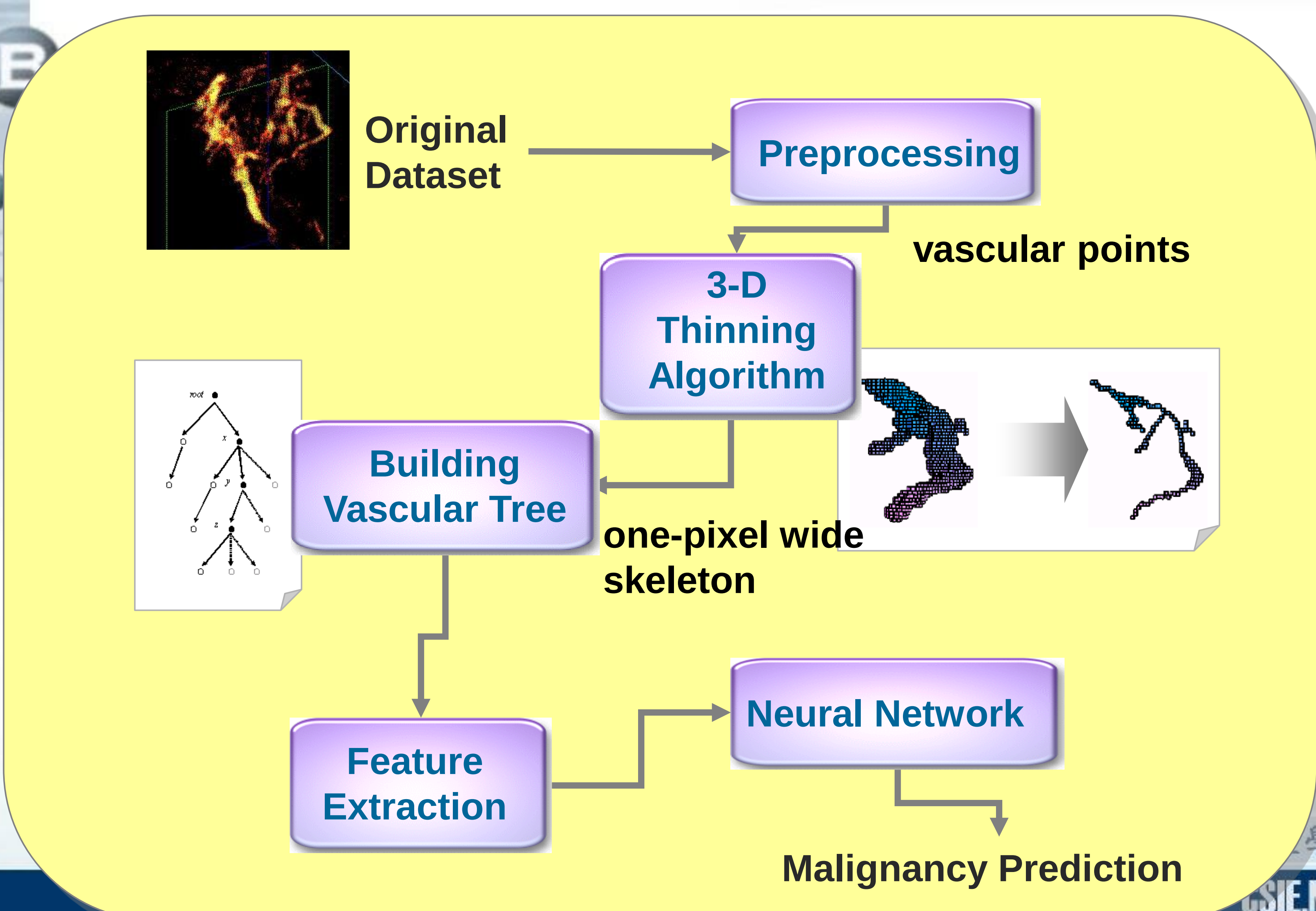

Thinning Result

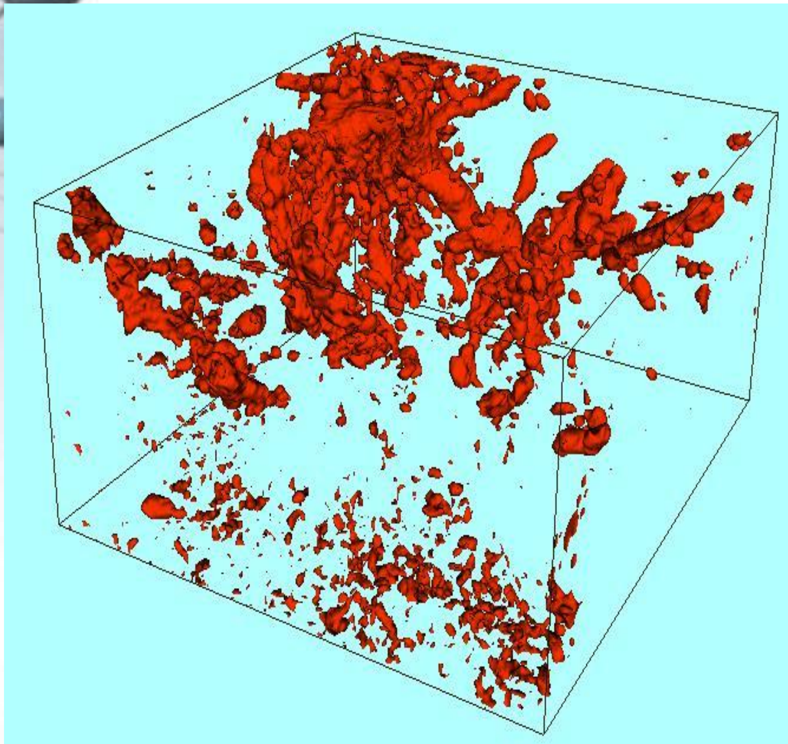

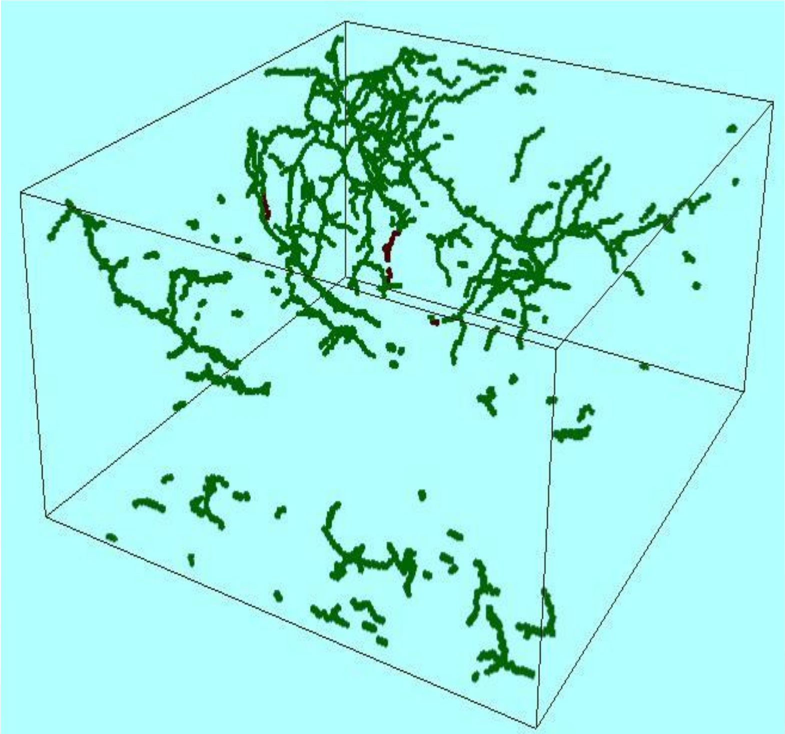

Vascular Tree Construction

- To generate a skeleton representation, the thinning result was converted into tree structure using breadth first search (BFS) algorithm.

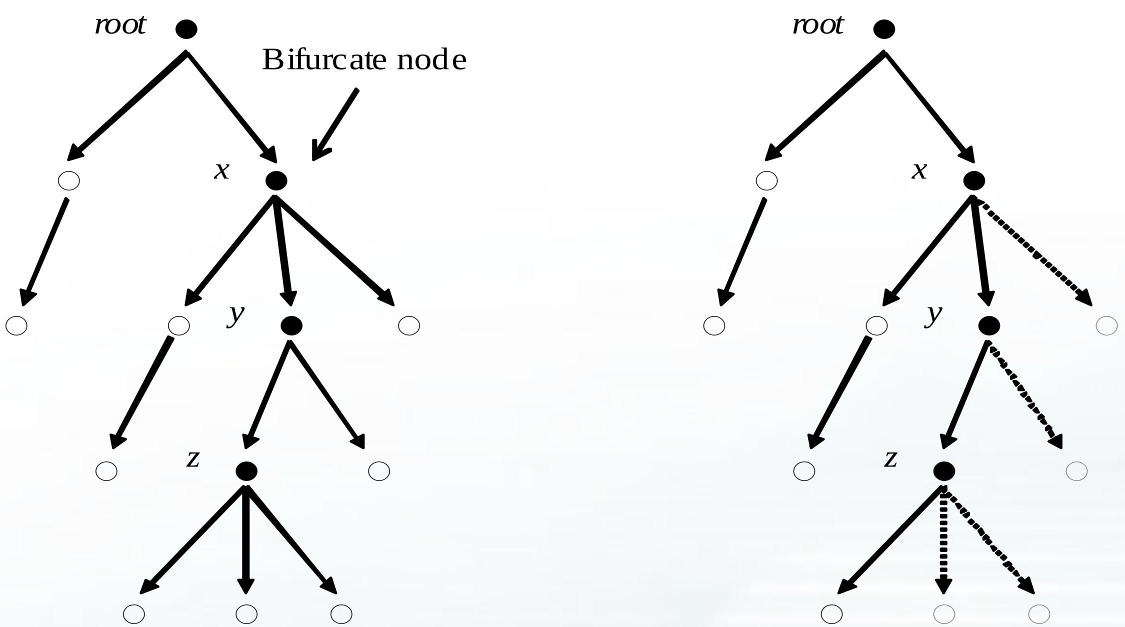

Feature Extraction

- Ten features are used for the vessel tree.
  - Vessel-to-Volume Ratio (R_v)
  - Number of Vascular Trees (N_v)
  - Measurement of Length
    - Total length (L_1)
    - Length of the longest path (L_2)
  - Bifurcation (*Bn*)
  - Diameter (D_v)
  - Number of cycles (NC)
  - Tortuosity measures (DM, ICM, SOAM)

Benign Case

Original

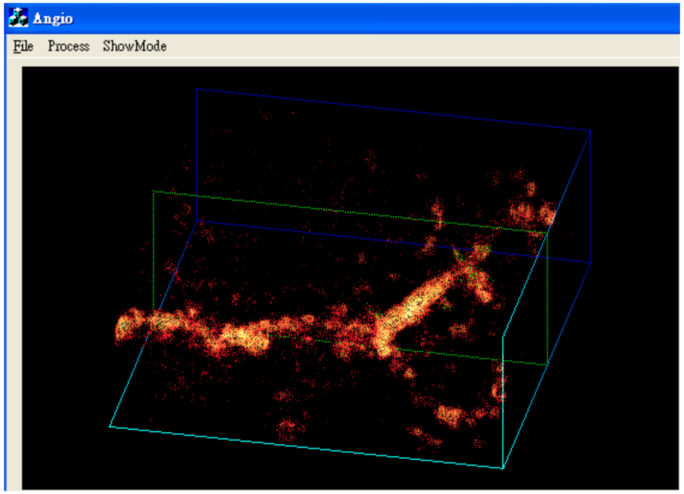

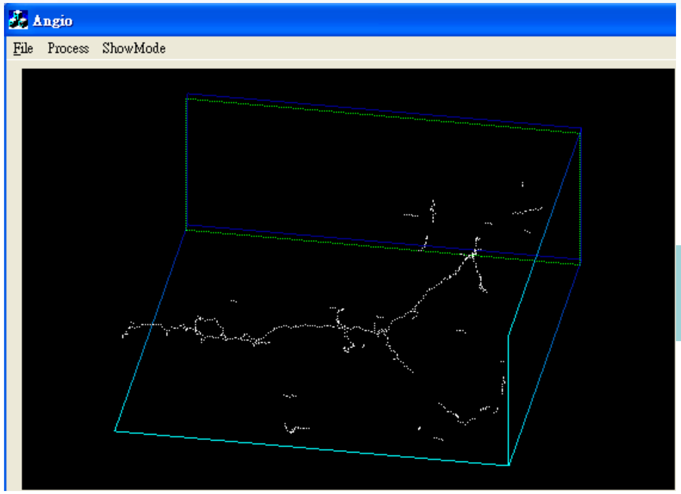

Thinning

All Vessels

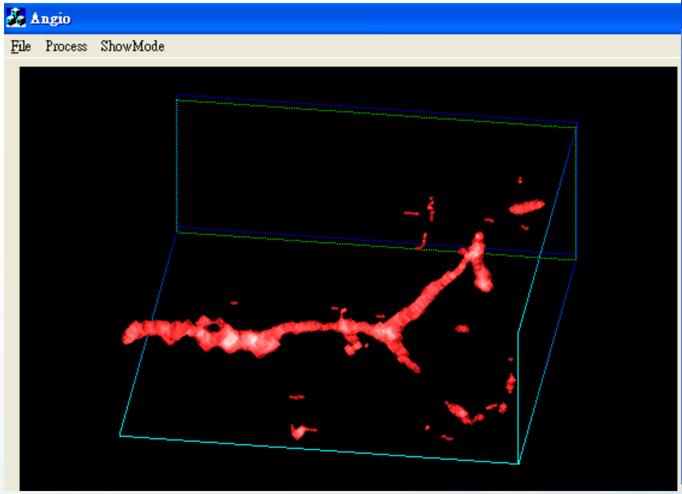

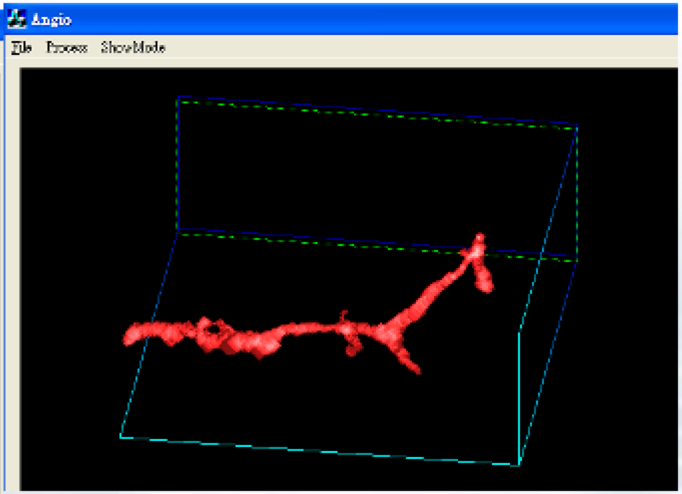

Longest Vessel

Malignant Case

Original

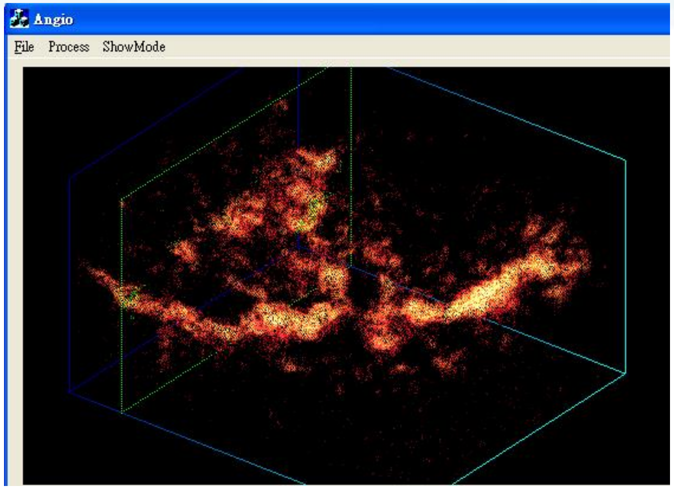

Thinning

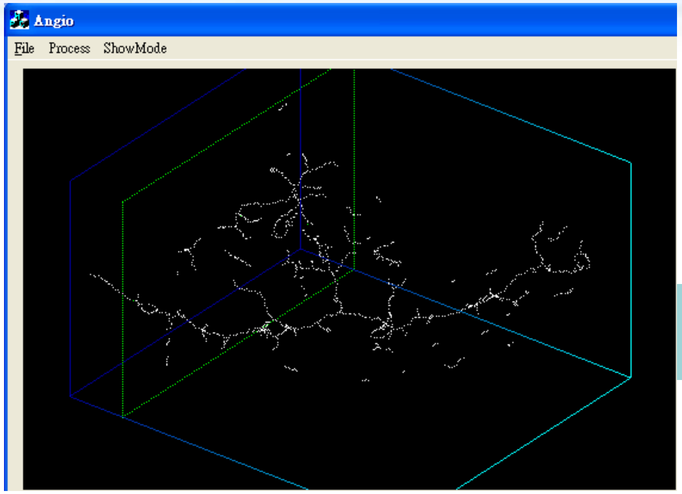

All Vessels

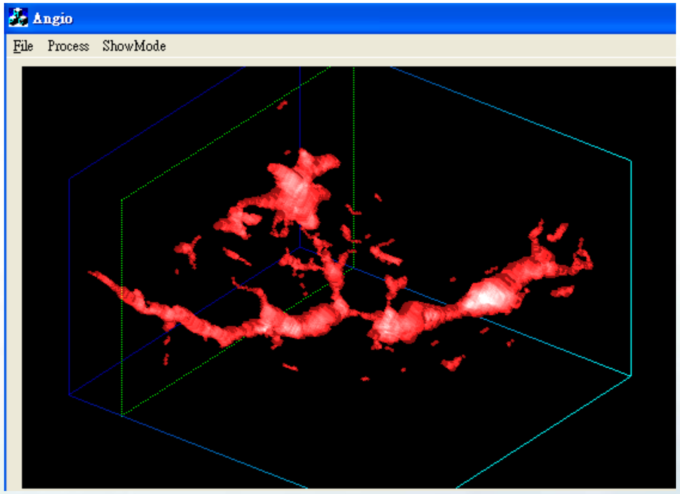

Longest Vessel

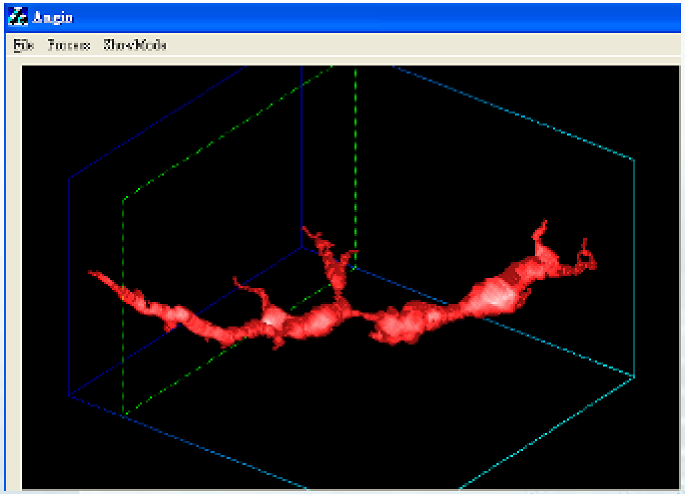

Benign vs. Malignant

- The bottom images are the longest vessel.
- The longest vessel of malignance has more curvature.

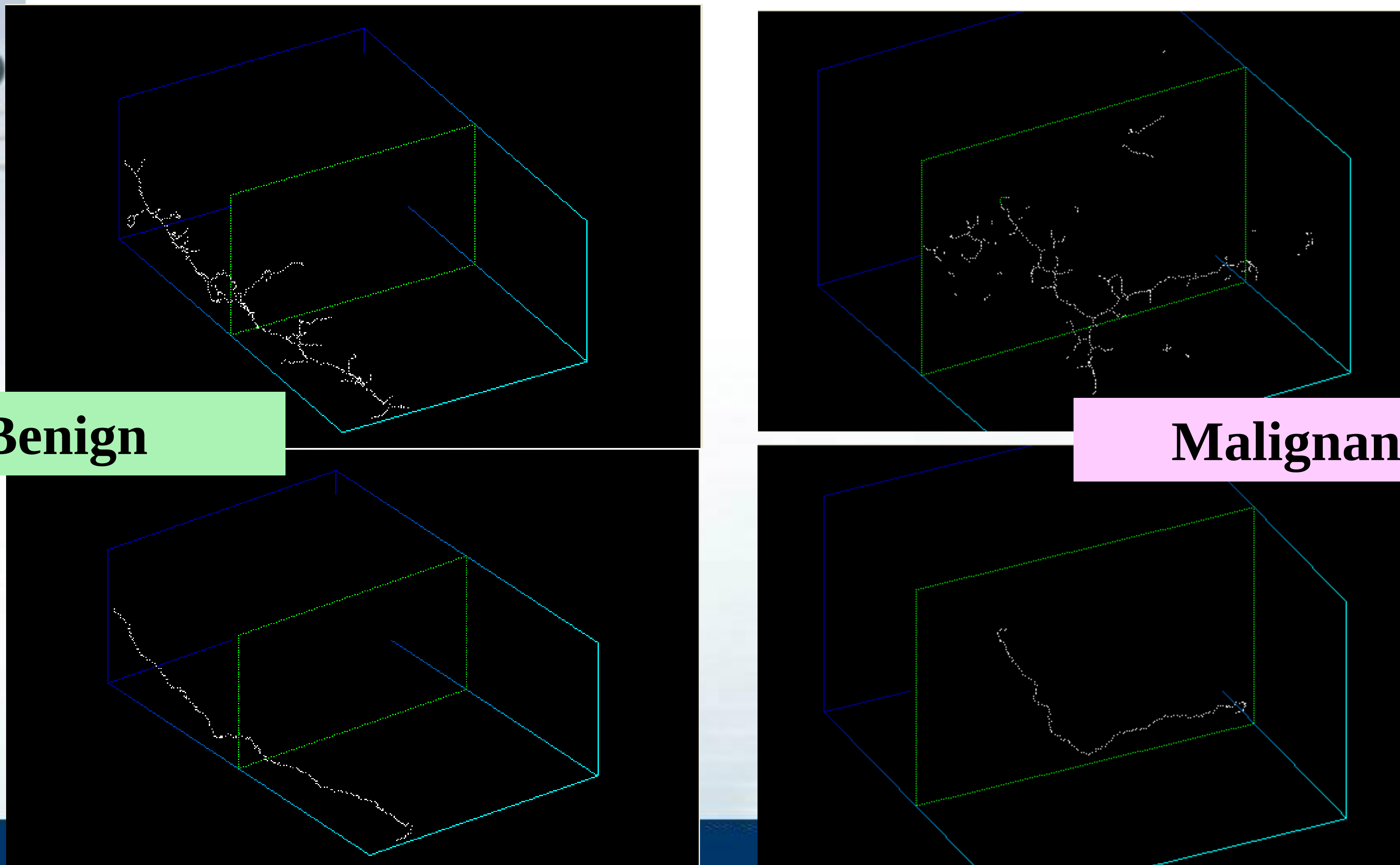

Vascular Analysis Inside/outside Tumor

- To evaluate morphologic and tortuous features of vessels **inside and outside the tumor region** on 3-D power Doppler US

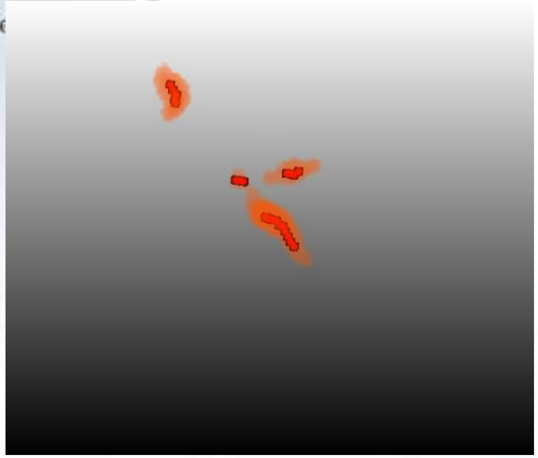

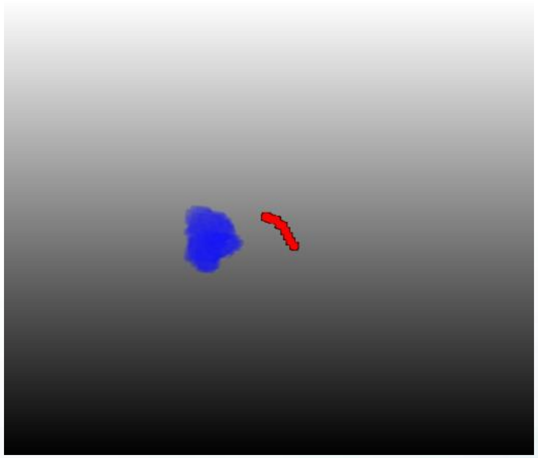

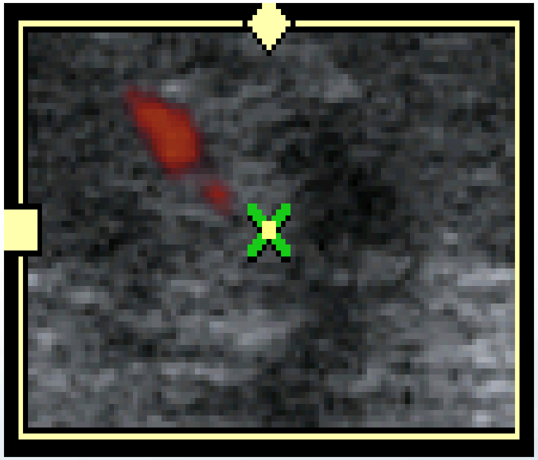

Benign

"Vascular Morphology and Tortuosity Analysis of Breast Tumor Inside and Outside Contour by 3-D Power Doppler Ultrasound", Ultrasound in Med. & Biol., vol. 38, no. 11, pp. 1859-1869, 2012

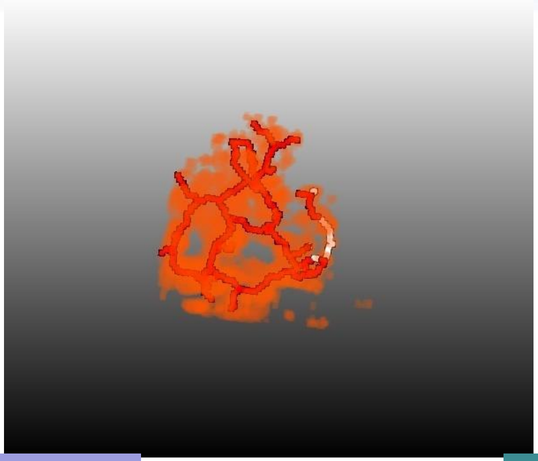

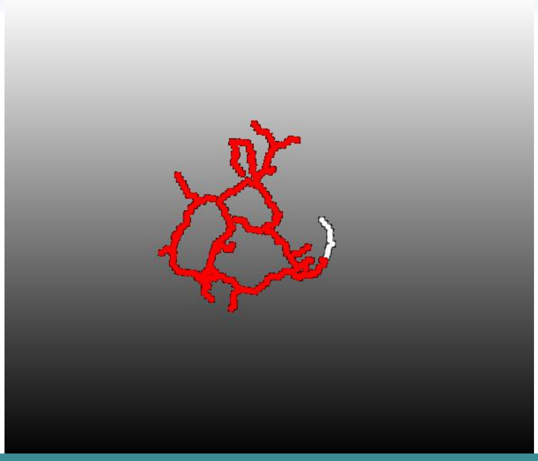

Vessels (orange) and skeletons (red and white)

The significant vessel trees outside (red) and inside (white) tumor.

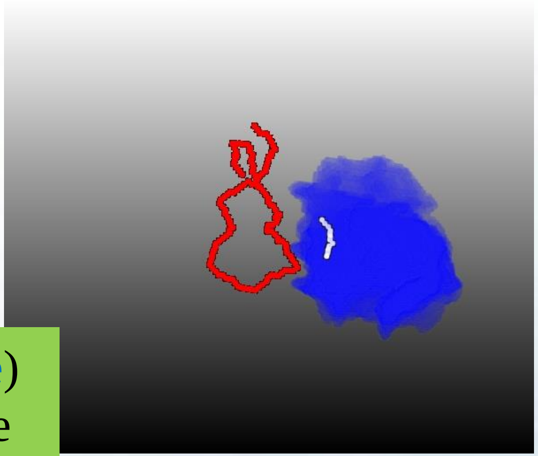

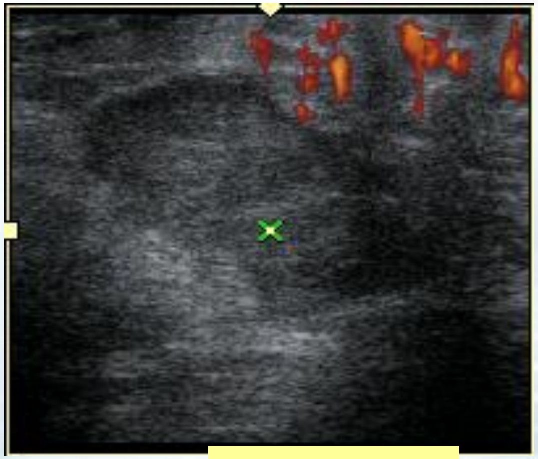

The tumor contour (blue) and primary path outside tumor (red) and inside tumor (white)

2-D PDUS

Malignant

ROC Curves

- There were 113 solid breast masses (60 benign, 53 malignant).

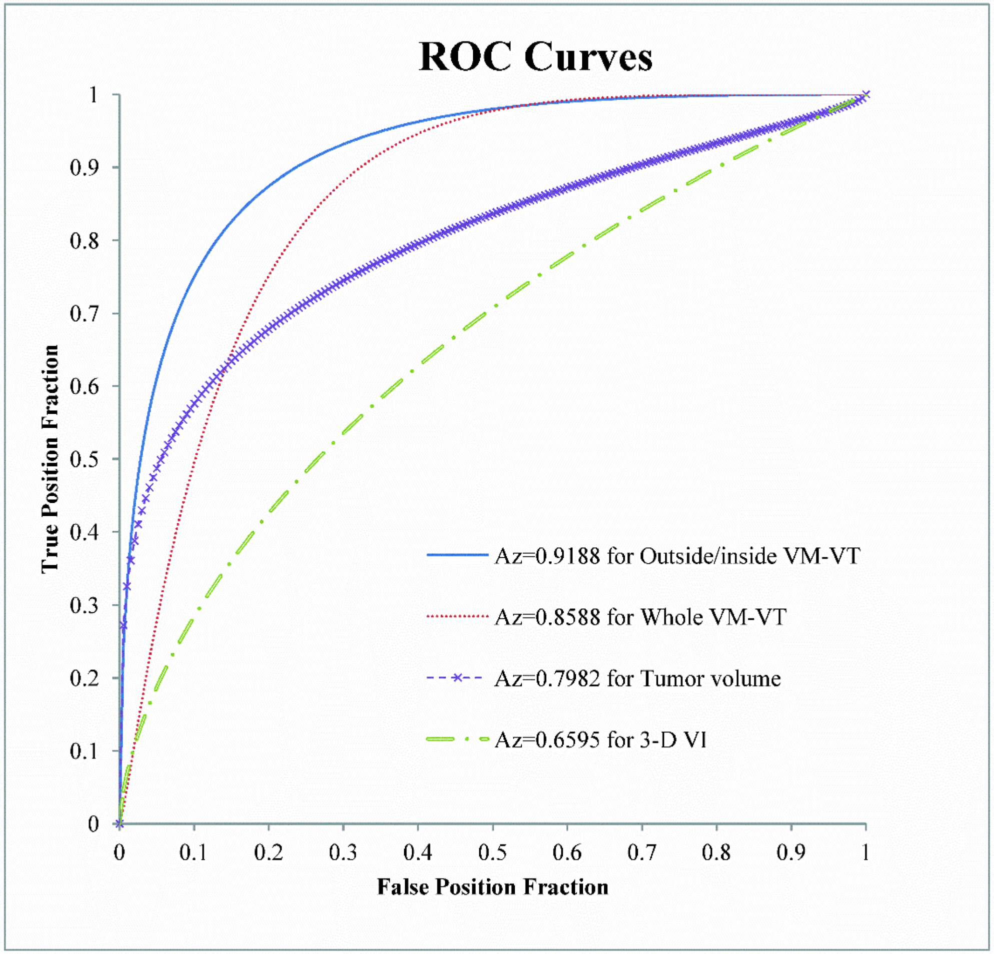

ABUS CADx

- 2D/3D CADx could be applied for ABUS.

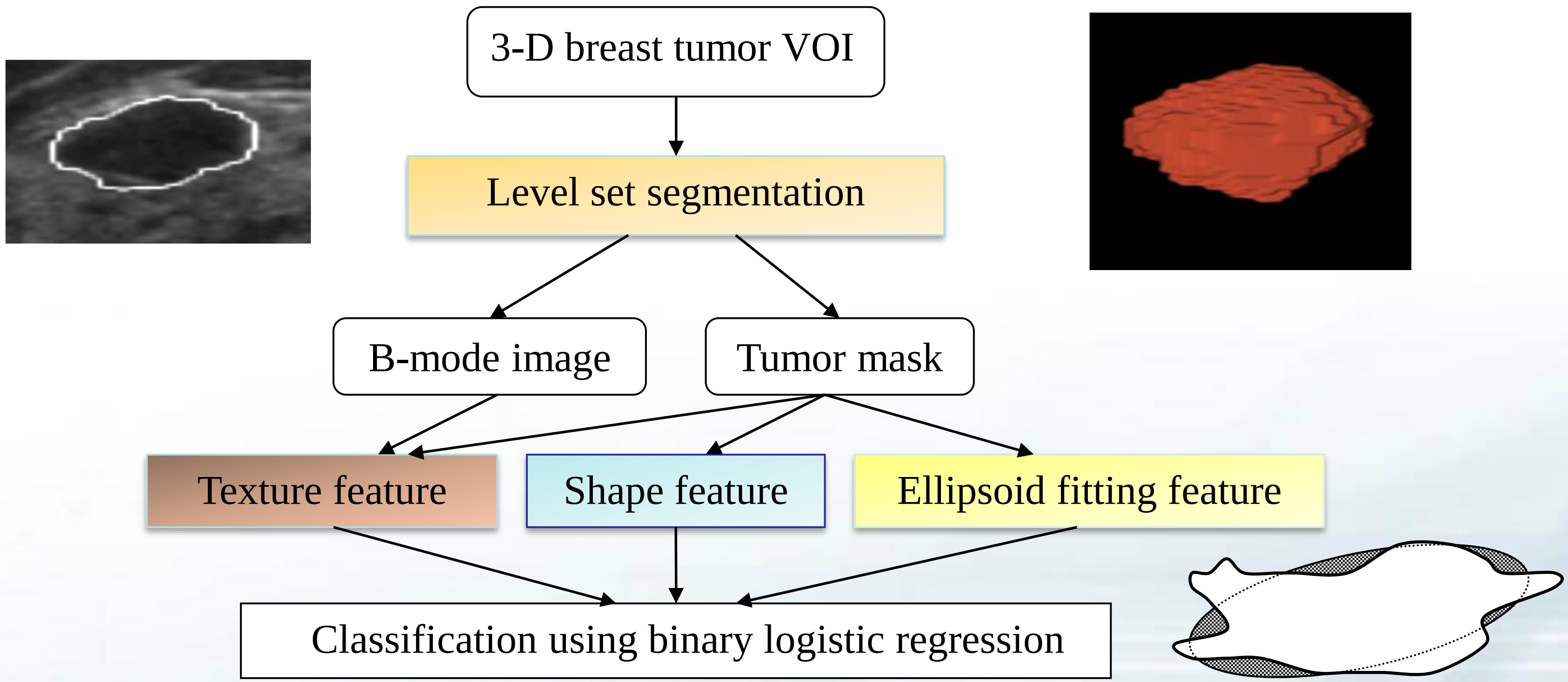

"Computer-aided diagnosis for the classification of breast masses in automated whole breast ultrasound images," Ultrasound in Medicine and Biology, vol. 37, no. 4, pp. 539-548, 2011.

3D Tumor Segmentation

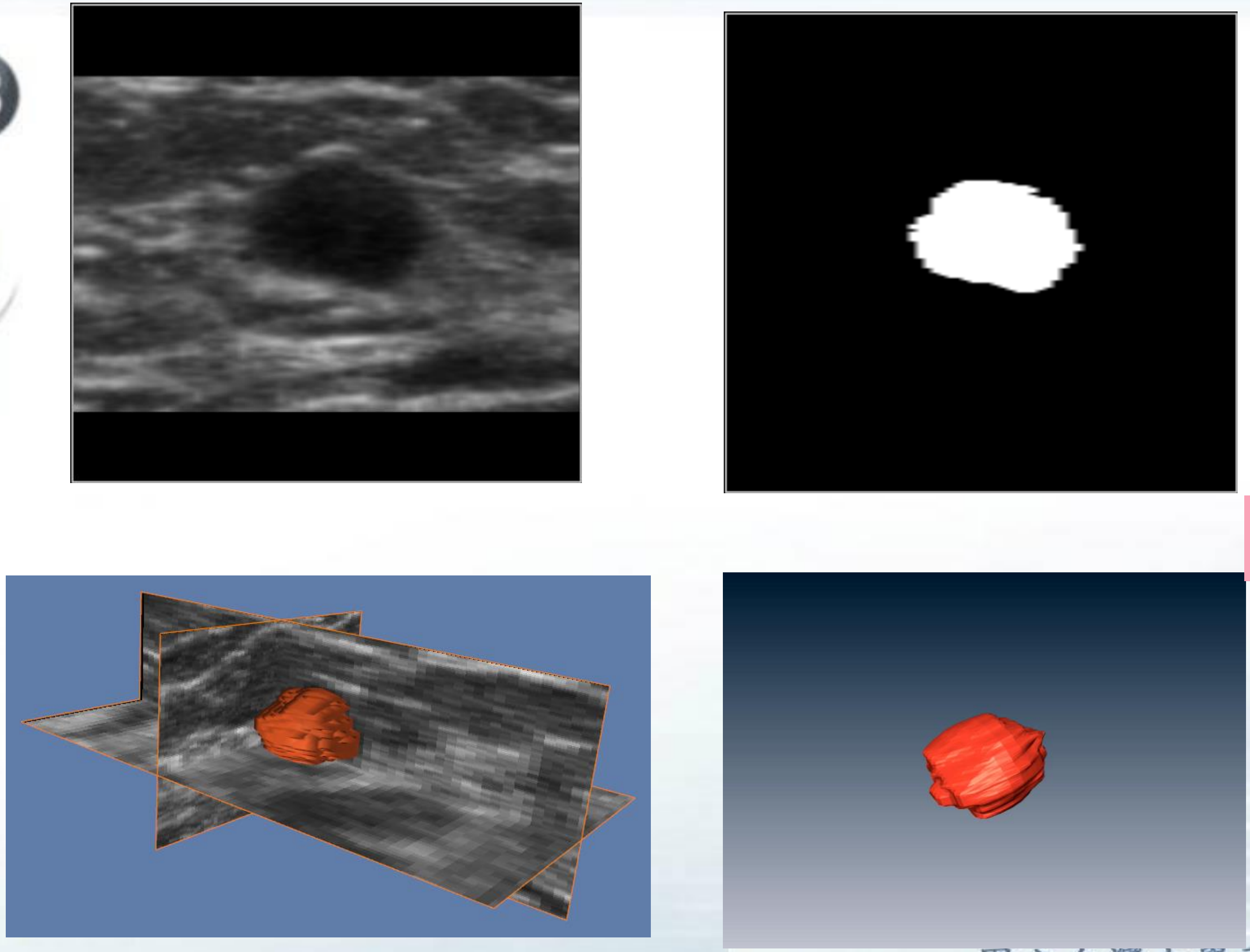

Benign

國立台灣大學資訊工程學系

CSIE,NTU

Malignant Example

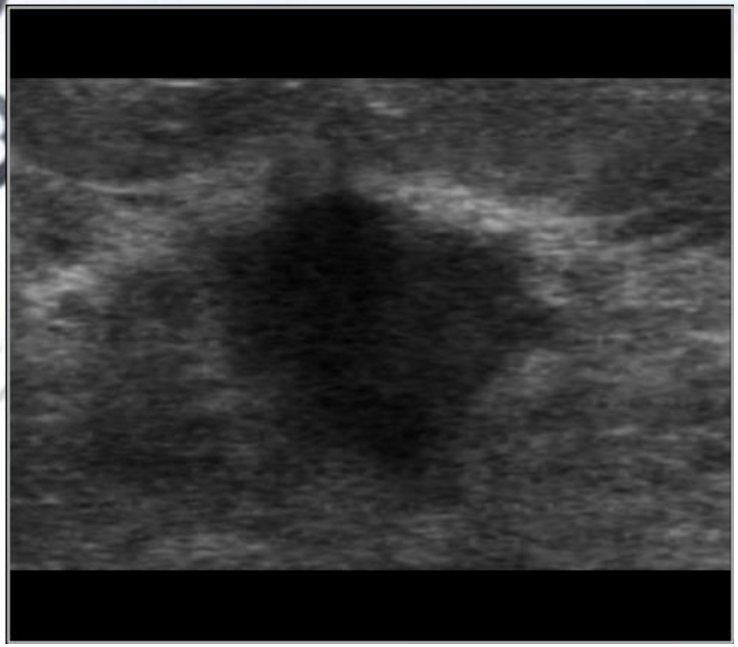

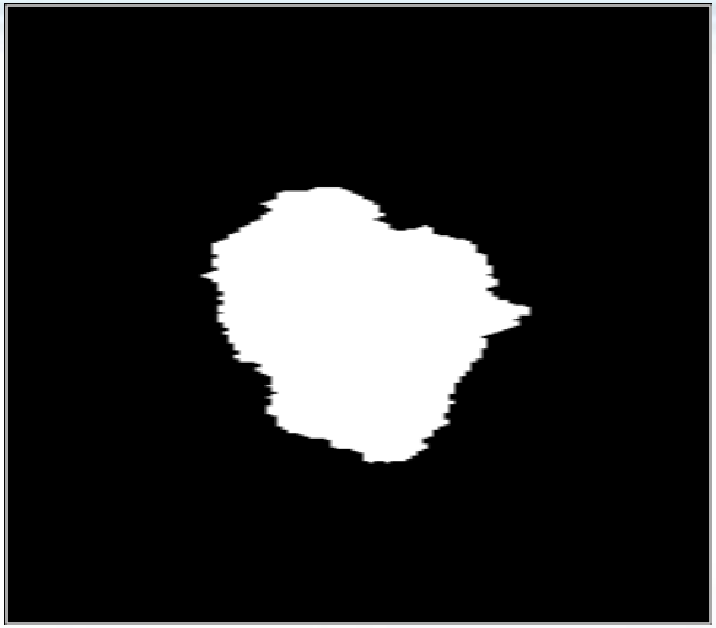

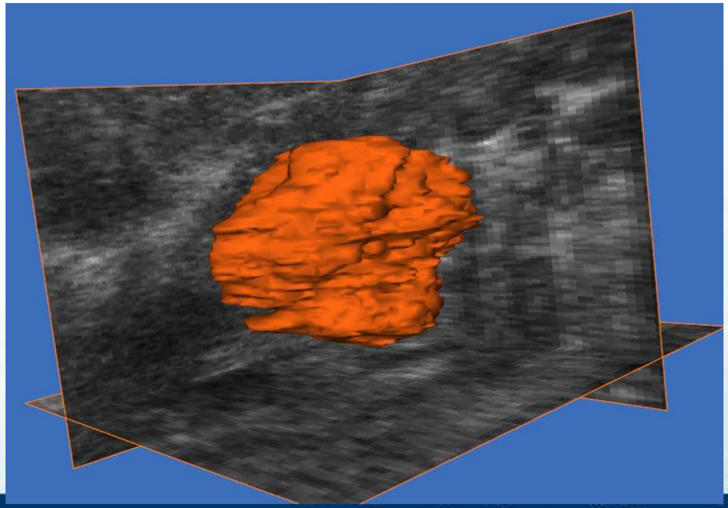

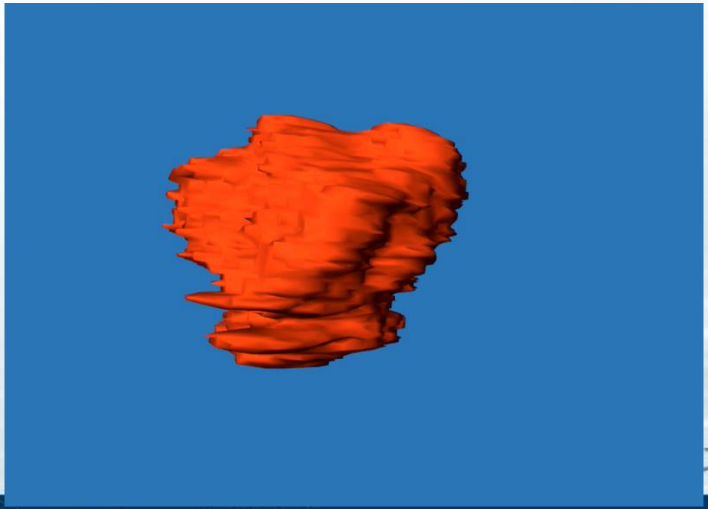

- 147 cases (76 benign and 71 malignant breast masses) were obtained by U-systems ABUS.

	GLCM	Shape	Ellipsoid fitting	GLCM and shape	GLCM and ellipsoid fitting	Shape and ellipsoid fitting	ALL
Accuracy (%)	75.51 (111/147)	82.31 (121/147)	79.59 (117/147)	80.27 (118/147)	81.63 (120/147)	85.03 (125/147)	82.31 (121/147)
Sensitivity (%)	81.69 (58/71)	84.51 (60/71)	76.06 (54/71)	83.10 (59/71)	84.51 (60/71)	84.51 (60/71)	83.10 (59/71)
Specificity (%)	69.74 (53/76)	80.26 (61/76)	82.89 (63/76)	77.63 (59/76)	78.95 (60/76)	85.53 (65/76)	81.58 (62/76)
PPV (%)	71.60 (58/81)	80.00 (60/75)	80.60 (54/67)	77.63 (59/76)	78.95 (60/76)	84.51 (60/71)	80.82 (59/73)
NPV (%)	80.30 (53/66)	84.72 (61/72)	78.75 (63/80)	83.10 (59/71)	84.51 (60/71)	85.53 (65/76)	83.78 (62/74)
Az	0.8603	0.9138	0.8496	0.9153	0.8195	0.9466	0.9388

ABVS CADe

- TUMOR DETECTION
- TUMOR MAPPING

"Computer-Aided Tumor Detection Based on Multi-Scale Blob Detection Algorithm in Automated Breast Ultrasound Images", IEEE Transactions on Medical Imaging, vol. 32, no. 7, pp. 1191-1200, July 2013.

"Tumor detection in automated breast ultrasound images using quantitative tissue clustering", Medical Physics, vol. 41, no. 4, pp. 042901-1-8, April 2014.

"Multi-dimensional tumor detection in automated whole breast ultrasound using topographic watershed," IEEE Transactions on Medical Imaging, vol. 33, no. 7, pp. 1503-1511, July 2014.

"Feasibility Testing: Three-dimensional Tumor Mapping in Different Orientations of Automated Breast Ultrasound," Ultrasound in Medicine and Biology, vol. 42, no.5, pp. 1201-1210, 2016.

Automated Whole Breast US

- **Aloka**, **U-systems** (acquired by **GE**), and **Siemens**, **SonoCiné** (distribution agreement with **Philips**), and **iVu** have developed the automated whole breast ultrasound (ABUS) systems.


U-systems


U-systems, 2006.09


iVu

Aloka


Aloka, 2006.07


Siemens


SonoCiné

Siemens ABVS

- ACUSON S2000 Automated Breast Volume Scanner (ABVS)

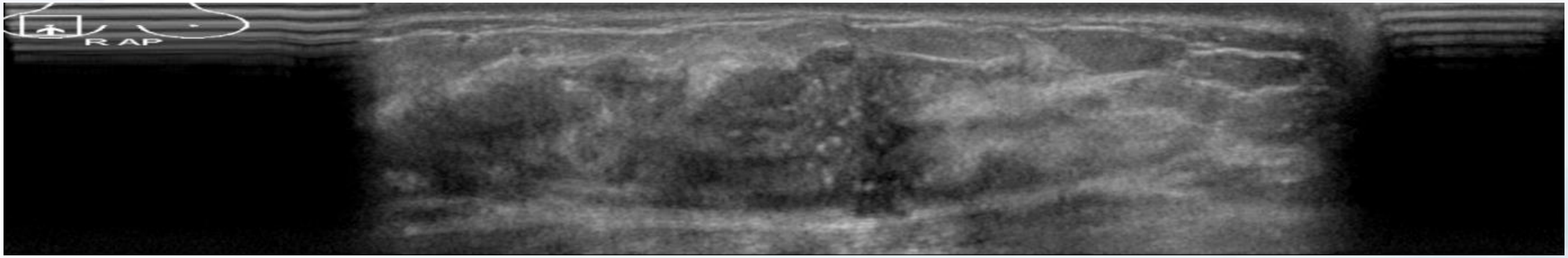

- Siemens: 736×481×318 = 0.208mm×0.052mm×0.526mm

ABVS Viewer

- Our ABVS view system has been transferred to TaiHao Medical Inc, Taiwan.
  - BR-ABVS Viewer 1.0
  - FDA cleared, 2016.01
  - http://taihaomed.com/

105年3月3日／星期四 健康照護 A19 工商時報

太豪生醫 研發3D自動掃描全乳超音波

■李水蓮

太豪生醫研發出台灣第1套可用於3D自動掃描全乳超音波閱片系統BR-ABVSViewer，頃獲美國FDA產品上市許可，這也是全世界第1套可安裝於一般PC環境並適用於3D自動掃描全乳超音波的高階醫材系統。其技術由台灣大學資訊工程學系張瑞峰教授及台大醫院乳醫中心黃俊升教授率領的團隊研發，再經由太豪生醫兩年多的努力，將台大技轉之經濟部學界開發產業技術計畫「多功能乳房超音波電腦輔助診斷系統」學術成果商品化成功，亦為我國產學合作的最佳典範。

●3D自動掃描全乳超音波掃描方式類似影印機，可自動掃瞄整個乳房區域，不僅可節省掃瞄時間，非常適用於乳房腫瘤篩檢。 圖／太豪生醫提供

波掃描方式類似影印機，可自動掃瞄整個乳房區域，不僅可節省掃瞄時間，並可去除人為操作結果不一的情況，故3D自動掃描全乳超音波非常適用於乳房腫瘤篩檢。

，並能當場提供數位化報告，以提升臨床診斷品質，降低醫療支出。

這項軟體系統取得美國FDA產品上市許可後，即可在美國銷售及與國際超音波醫療儀器

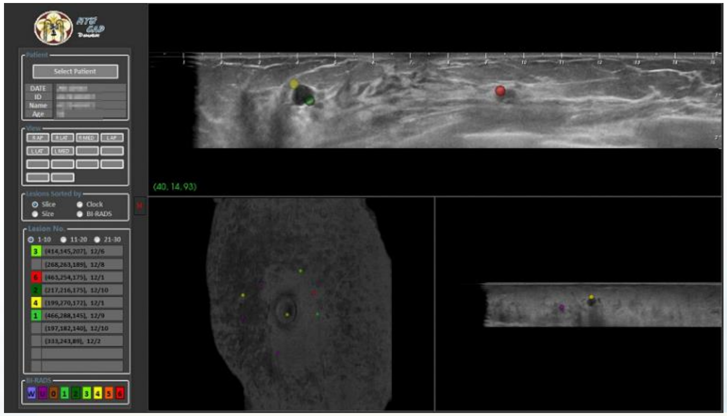

DEPARTMENT OF HEALTH & HUMAN SERVICES

Public Health Service

Food and Drug Administration
10903 New Hampshire Avenue
Document Control Center – WO66-G609
Silver Spring, MD 20993-0002

TaiHao Medical, Inc.
% Chiu S. Lin, Ph.D.
President
LIN & ASSOCIATES, LLC
9223 Cambridge Manor Court
POTOMAC MD 20854

January 15, 2016

Re: K151075
Trade/Device Name: BR-ABVS Viewer 1.0
Regulation Number: 21 CFR 892.2050
Regulation Name: Picture archiving and communications system
Regulatory Class: II
Product Code: LLZ
Dated: December 15, 2015
Received: December 15, 2015

Dear Dr. Lin:

Device Classification Name	System, Image Processing, Radiological
510(K) Number	K151075
Device Name	BR-ABVS Viewer 1.0
Applicant	TAIHAO MEDICAL INC. 7f., No.410, Sec.5m Zhongxiao E. Rd., Xinyi Dist. Taipei, TW

ABVS Viewer (2)

- Our ABVS view system is applied for a ABUS system from a Taiwan company.
  - The probe is rotated to obtain a whole breast image in only one scanning.
  - Begin clinical trials in NTUH and other hospitals

- Cooperation with China company for CFDA

Supine/Prone ABUS

- Supine ABUS
  - Same position with surgery
  - At least three passes for a breast
- Prone ABUS
  - Same position with MRI
  - One pass for a breast

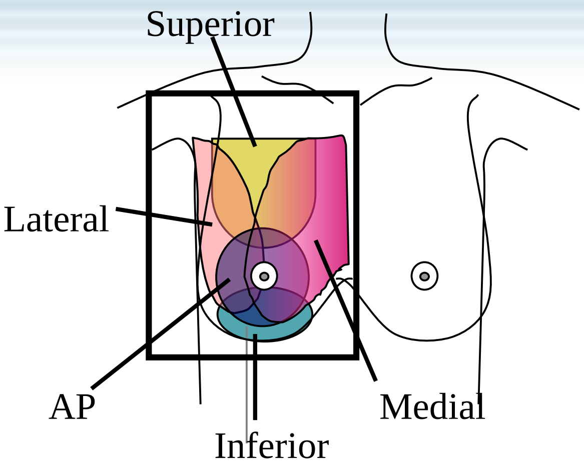

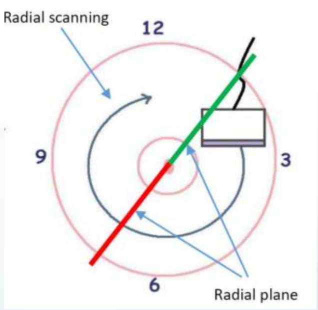

- Reconstruction of rotated prone ABUS (iABUS/iVu)

iABUS Viewer

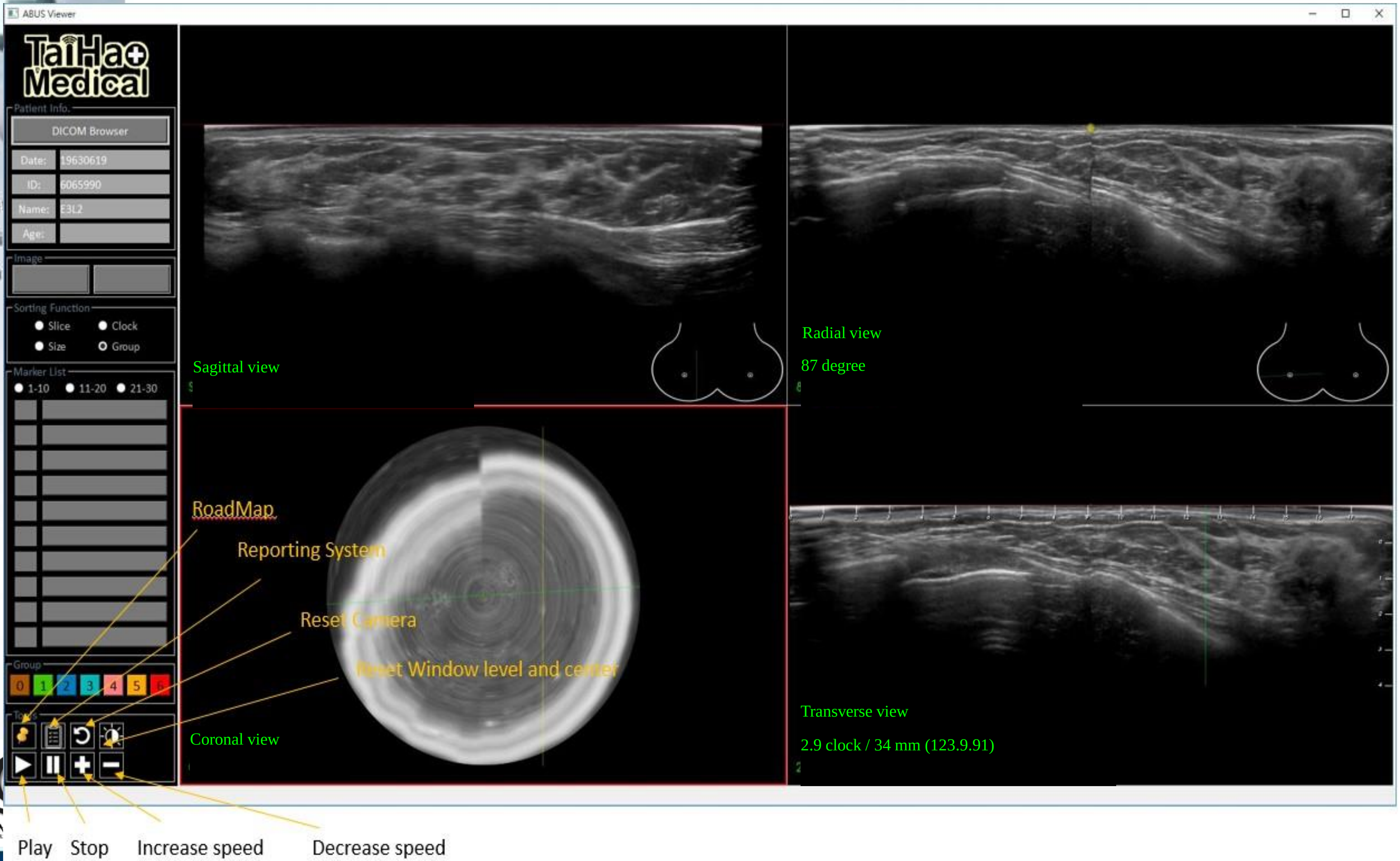

Dual-modality ABUS System

- Combines an FFDM **X-ray machine** with automated breast ultrasound (**ABUS**) technology
  - CapeRay Medical Ltd.
  - A long probe is scanned under the plate.

ABUS/MAMMO Viewer

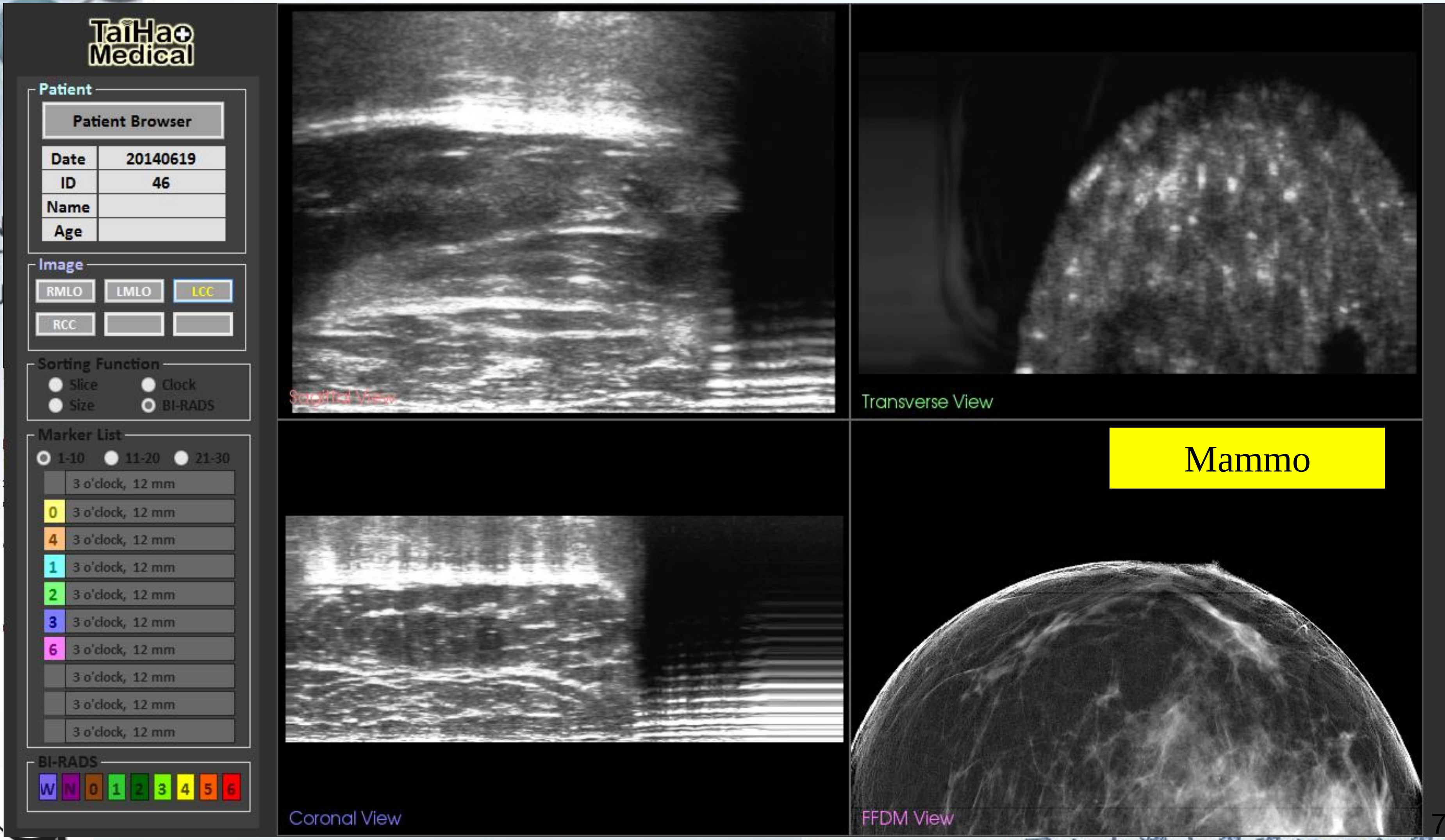

Watershed Tumor Detection

- Our ABUS CADe is based on a **watershed transform** method.
  - The watershed transform was applied to gather similar tissues around local minima to be **homogeneous regions**.
- This method detects every tumor, but some non-tumors (false positive, FP) are also detected.
  - Hence, the **likelihoods of being tumors** of the regions were estimated using the quantitative **morphology**, **intensity**, and **texture** features in the 2-D/3-D false positive reduction (FPR).

"Multi-dimensional tumor detection in automated whole breast ultrasound using topographic watershed," IEEE Transactions on Medical Imaging, vol. 33, no. 7, pp. 1503-1511, July 2014.

Proposed System

Slice by slice processing

ABUS image

↓

Resolution reduction & image enhancement

↓

Watershed transform for tissue segmentation

↓

Suspicious abnormality extraction

↓

2-D/3-D false positive reduction

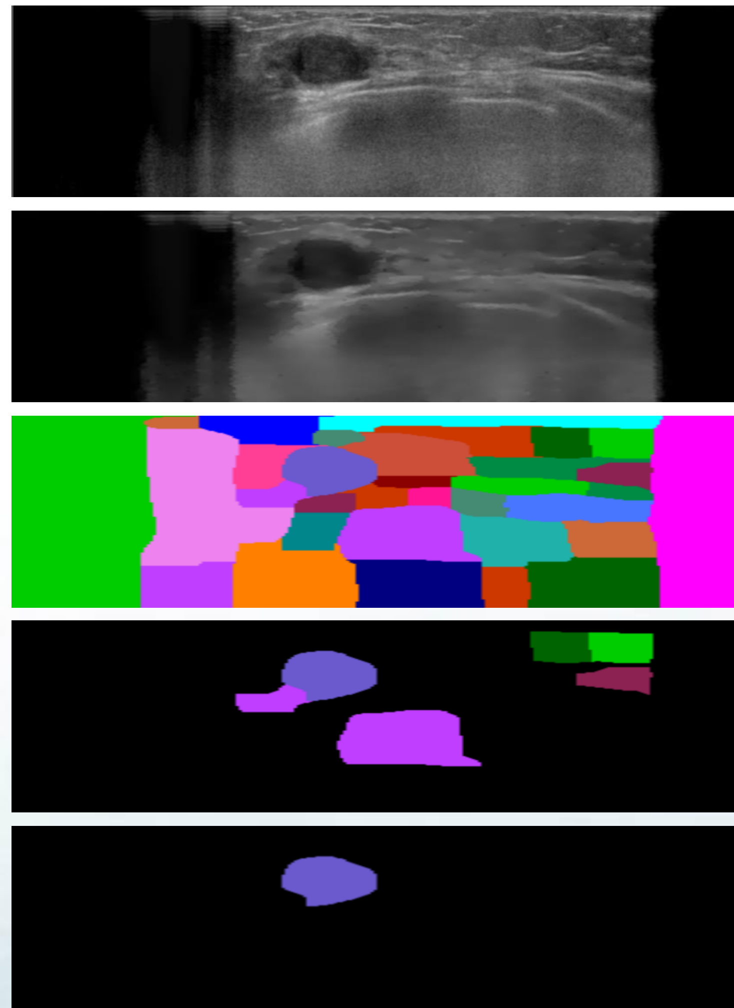

False Positive Reduction (FPR)

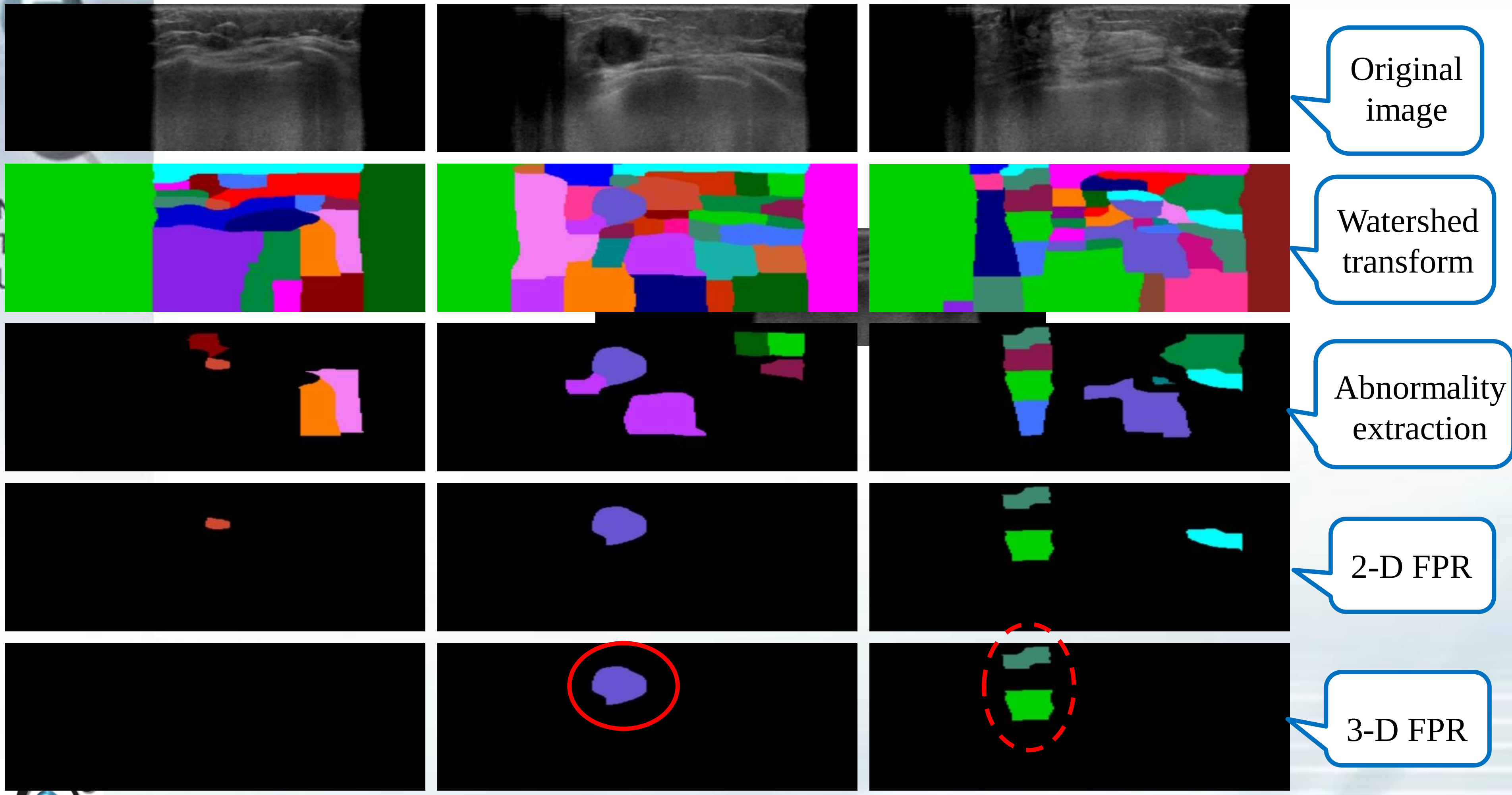

Experiments

- ABUS SomoVu ScanStation
  - 138 cases (104 abnormal and 34 normal)
  - 104 breast lesions of 104 patients
    - 68 benign lesions
    - 65 malignant lesions
    - Lesion size : 1.75±1.13 cm
- 10-fold cross validation (10F-CV) is used.
- **FROC curves** and the jackknife alternative of FROC-1 (JAFROC) **figure of merit (FOM)** were performed to evaluate the performance of the CADe system

FPs/pass after applying 2-D/3-D FPR

- Before FPR, the average number of suspicious abnormalities was 291.6.

Sensitivity (%)	FPs/pass	
	After 2-D FPR	After 3-D FPR
60	1.48	1.58
70	2.32	2.14
80	4.64	3.33
90	9.31	5.42
100	18.19	9.44

Reduce 94%

Reduce 48%

FROC Curves

- The **FROC curves** and the corresponding JAFROC-1 **figure of merit (FOM)** for each feature set.

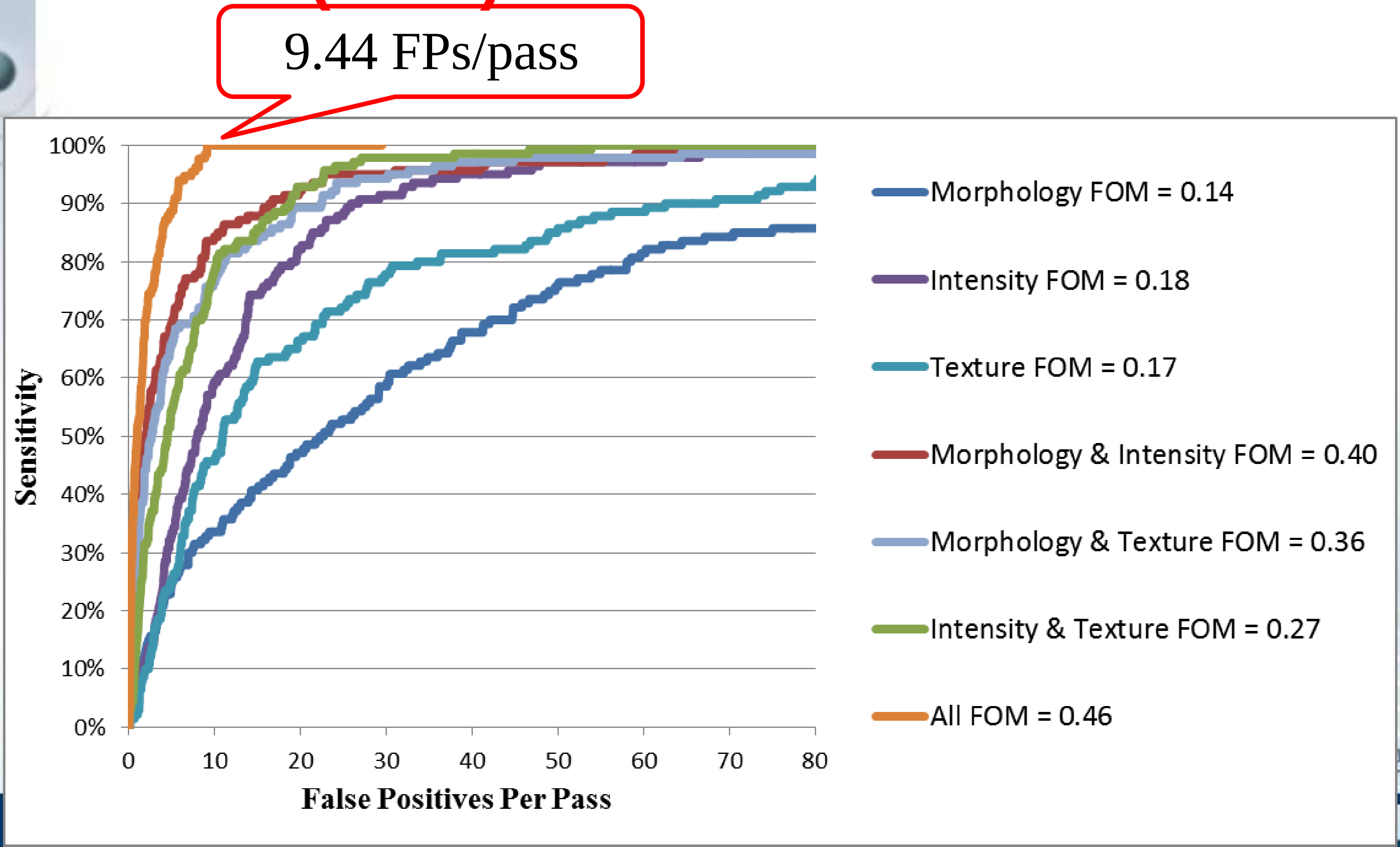

Detected Results

- A true positive case of 1.51 cm fibroadenomas

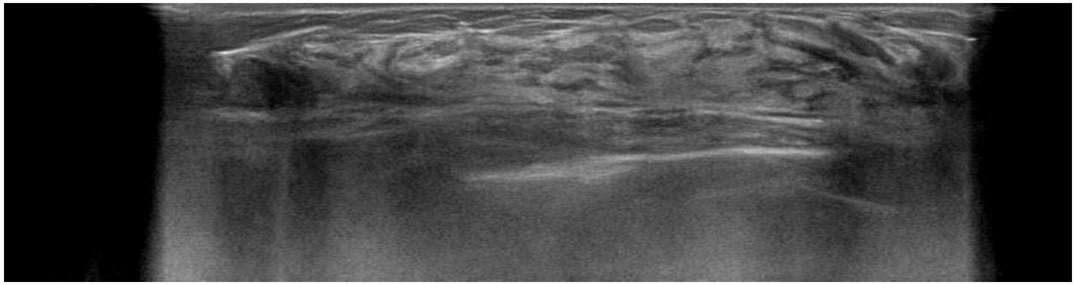

The original ABUS image

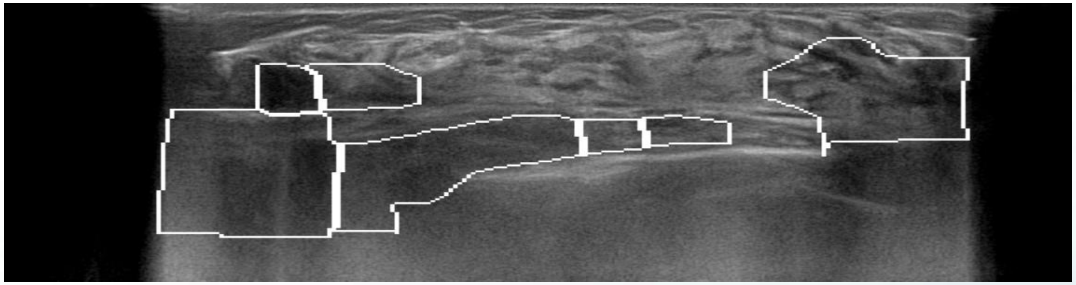

The potential tumor regions delineated by watershed segmentation.

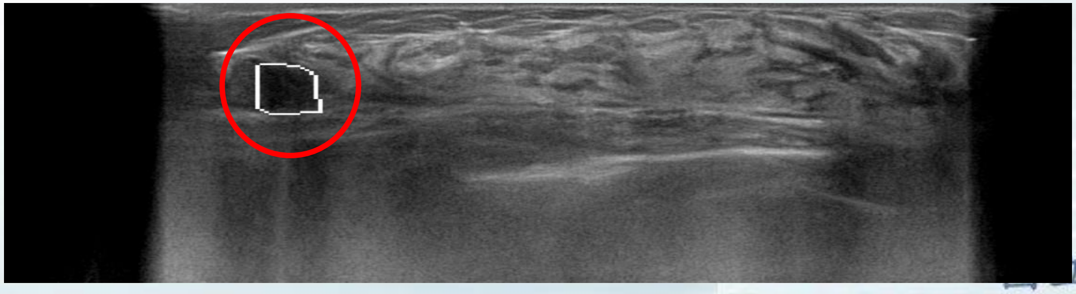

CAD

Detected Results

- A true positive case of 4.46 cm ductal carcinoma in situ

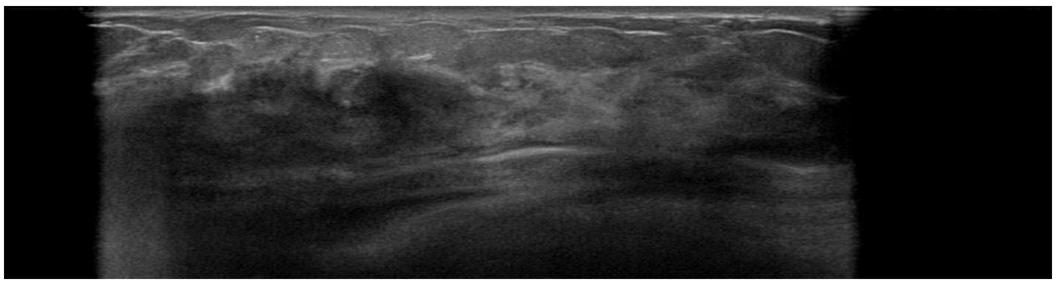

The original ABUS image

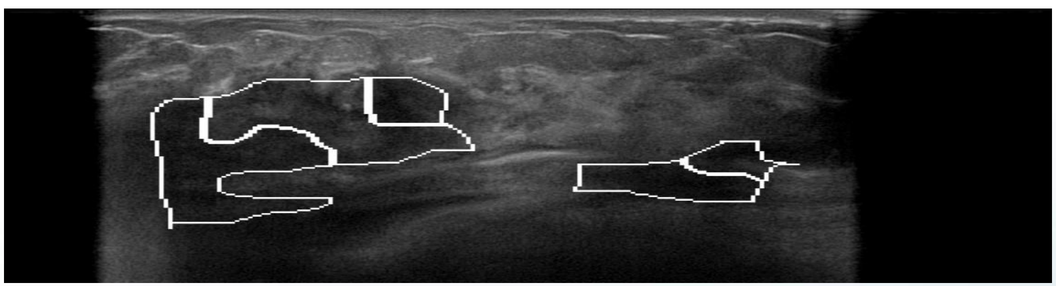

The potential tumor regions delineated by watershed segmentation.

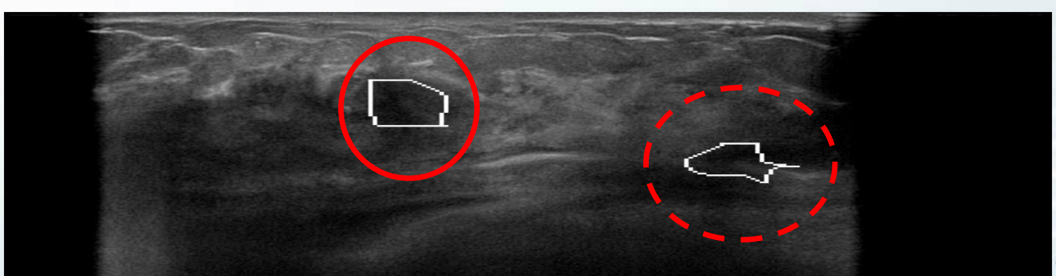

CAD
The dot circle indicates the false positive.

Detected Results

- A false positive case

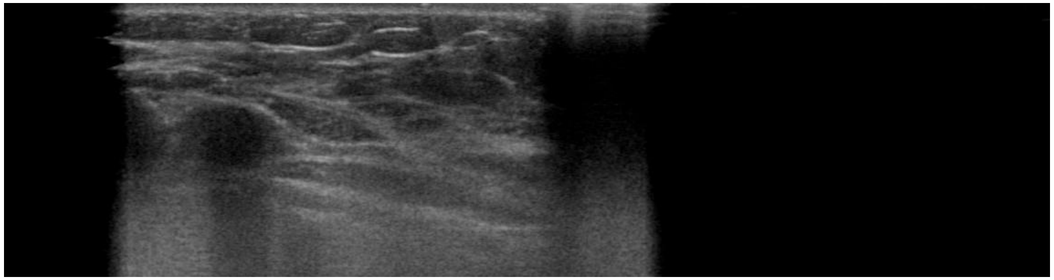

The original ABUS image

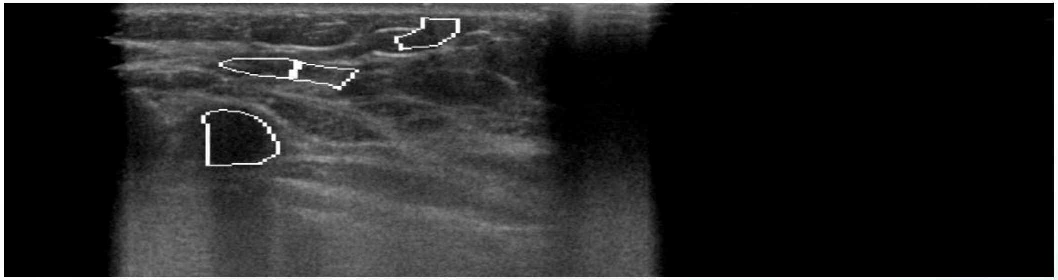

The potential tumor regions delineated by watershed segmentation.

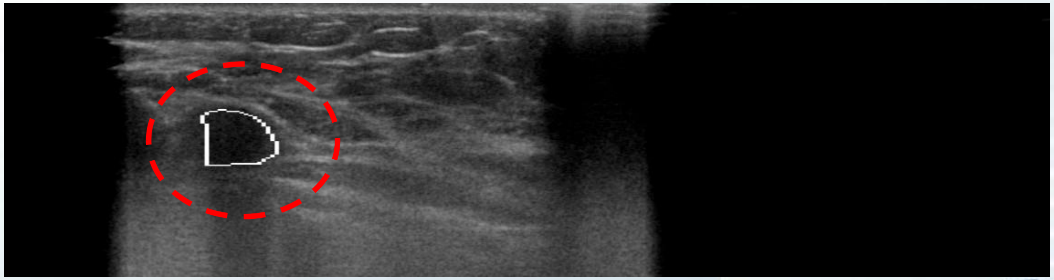

CAD
The dot circle indicates the false positive.

Discussion

- We also applied the **multi-scale Hessian analysis** (published in IEEE TMI) to **the same dataset** used in this study to provide a performance comparison.
  - "Computer-Aided Tumor Detection Based on Multi-Scale Blob Detection Algorithm in Automated Breast Ultrasound Images," **IEEE Transactions on Medical Imaging**, vol. 32, no.7, pp.1191-1200, 2013.
- The proposed watershed method has **better performance** and **short running time**.

Detection rates	100%	90%	70%	Running time
Hessian	18.0	9.1	4.3	13 minutes
Watershed	9.4	5.4	2.1	74.3 seconds

Summary

- A fully automatic CADe system was proposed based on topographic watershed for analyzing ABUS image.
- The proposed CADe system showed sensitivities of 100% with 9.44 FPs/pass.
- Rib and shadow regions were misclassified
  - Further reduce the FPs.

Tumor Mapping

- For ABUS, there are three views for a breast and a tumor will be demonstrated in multiple views.

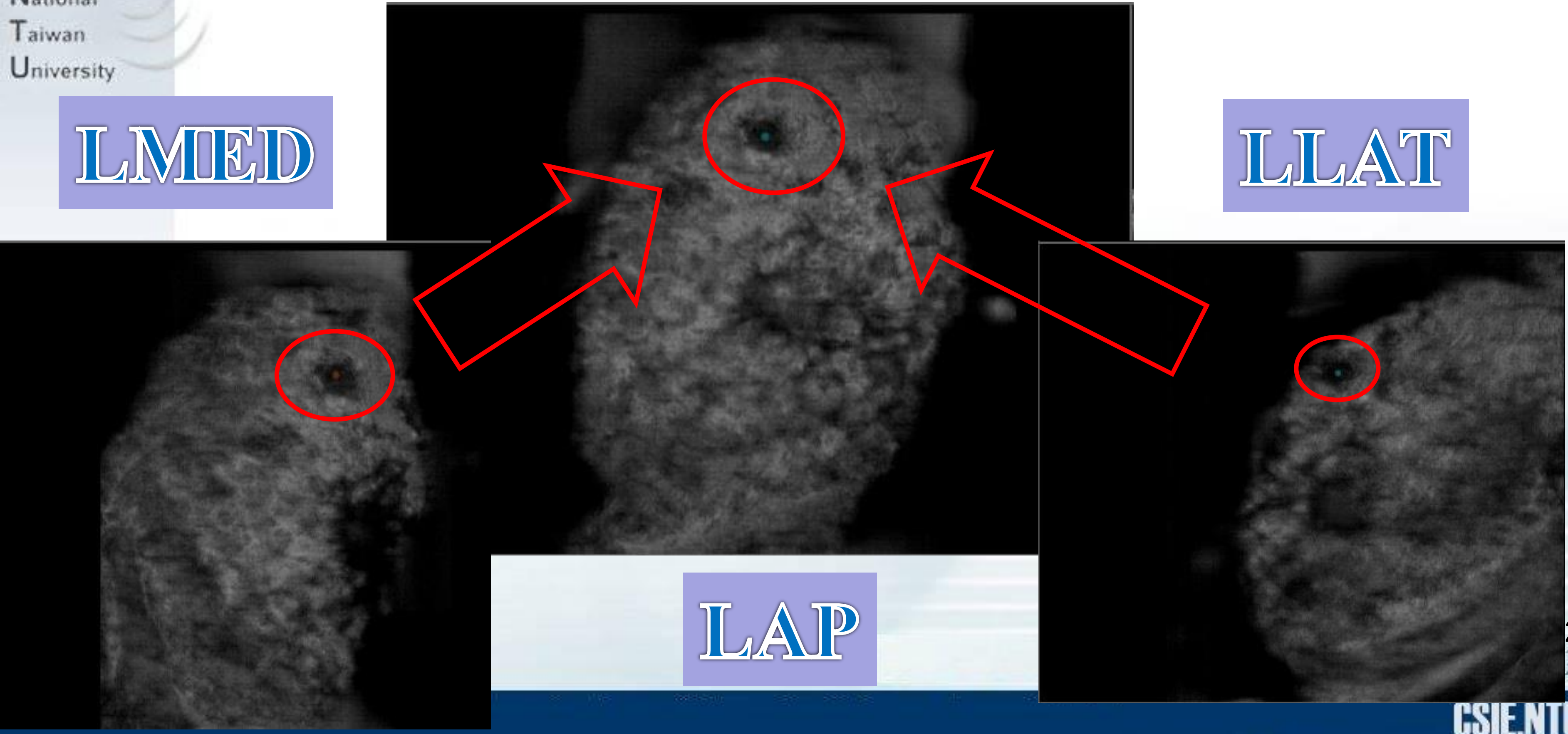

Experiment

- A total of 53 abnormal passes with 41 biopsy-proven tumors and 13 normal passes were collected.
- After CAD detection, a mapping pair was composed of a detected region in one pass and another region in another pass.
  - Location criteria, including the radial position, relative distance and distance to nipple, were used to extract mapping pairs with close regions.
- Quantitative intensity, morphology, texture and location features were then combined in a classifier for further classification.
- The performance of the classifier achieved a mapping rate of 80.39% (41/51), with an error rate of 5.97% (4/67).

"Feasibility Testing: Three-dimensional Tumor Mapping in Different Orientations of Automated Breast Ultrasound," Ultrasound in Medicine and Biology, vol. 42, no.5, pp. 1201-1210, 2016.

Mapping Case

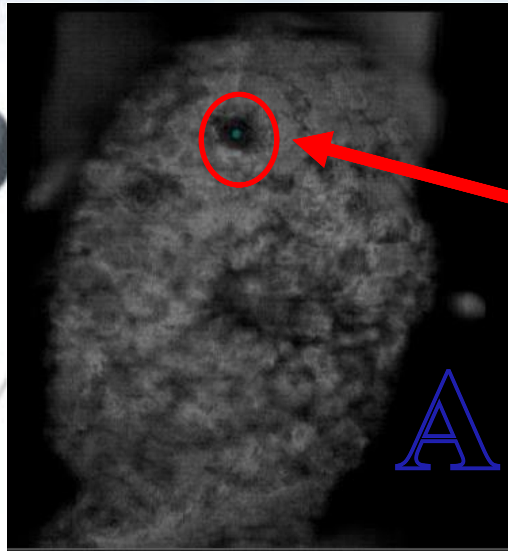

Benign fibroadenoma

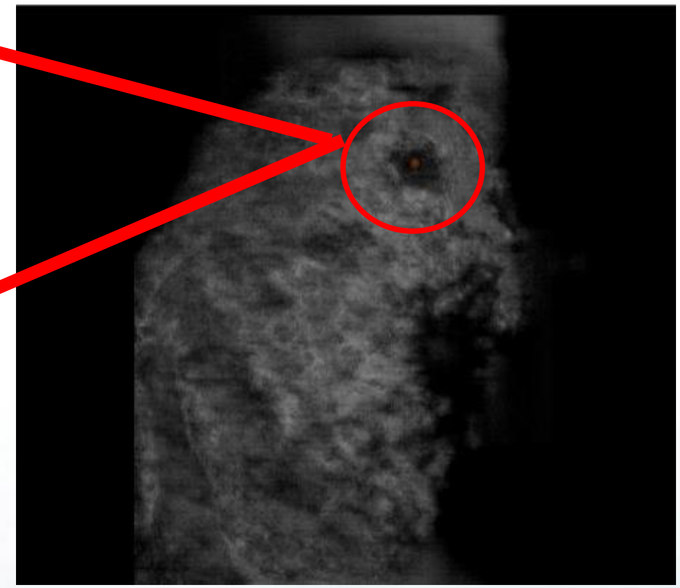

L AP

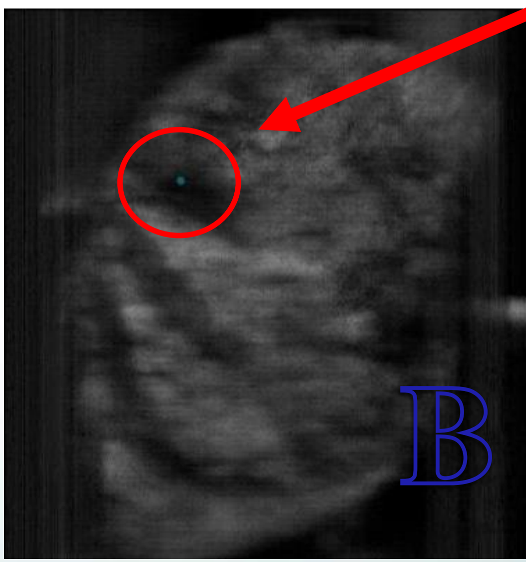

L MED

ABUS/Mammo Mapping

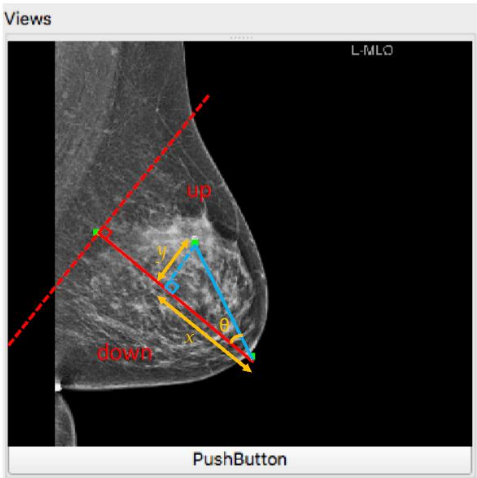

Sagittal view

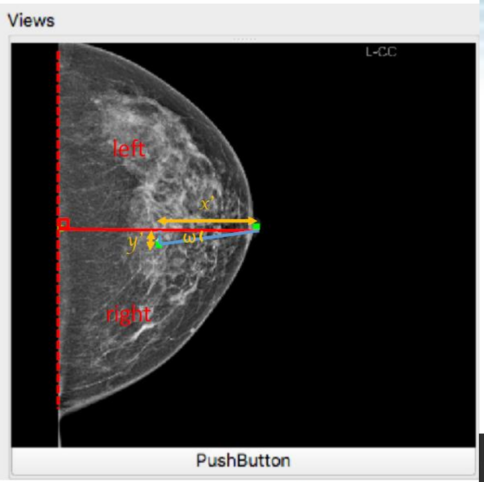

Transverse view

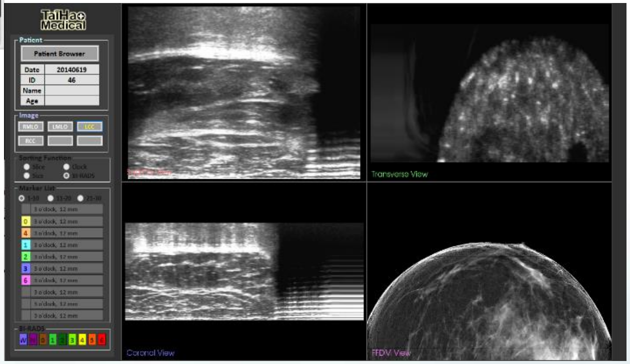

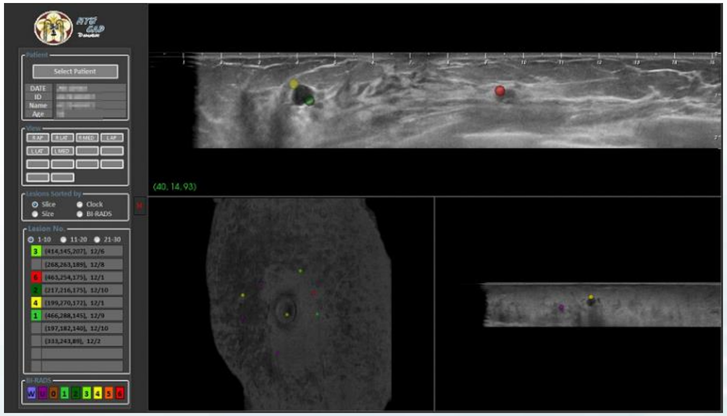

Preliminary Clinical Result

- Three readers: radiologist, surgeon, sonographer
  - 168 ABUS views from 28 patients
  - With CADe, more tumors could be found
- Study design
  - Step 1: Reader reviews the cases **without CAD**
  - Step 2: Reader reviews the **missed CAD markers at step 1**
    - Only the CAD marked missed at step 1 will be presented to reader.
    - The **missed CAD markers** are decided by the **distance of their nearest markers at step 1**.

Step 1
Review without CAD

→

Step 2
Review the **missed** CAD markers

Results

	CADe	Reader A	Reader A with CAD	Reader B	Reader B with CAD	Reader C	Reader C with CAD
#TP	101	99	103	77	79	113	115
#FP	968	186	203	60	62	237	257
#FN	14	16	12	38	36	2	0
SEN	87.83	86.09	89.57	66.96	68.69	98.26	100
FP per Pass	5.76	1.11	1.21	0.36	0.37	1.41	1.53

- The **missed CAD markers** and their **BI-RADS scores** were re-evaluated by reader at step 2.

BI-RADS	3	4a	4b	4c	5	Total
Reader A	7	2	3	2	1	15
Reader B	2	1	0	0	1	4
Reader C	23	0	0	0	0	23

- Reviewing times of step 1 and step 2

Time per View	Step 1	Step 2 (CAD)	Total	CAD Markers	Time per Marker
Reader A	57.7	34.1	91.8	6.0	5.7
Reader B	26.0	12.7	38.7	6.1	2.1
Reader C	162.4	38.1	200.5	5.7	6.4

National Taiwan University

Case #1

- Reader B
  - Not marked at step 1 but marked at step 2 (CAD)
  - BI-RADS 4a
- Readers A and C
  - Marked at step 1

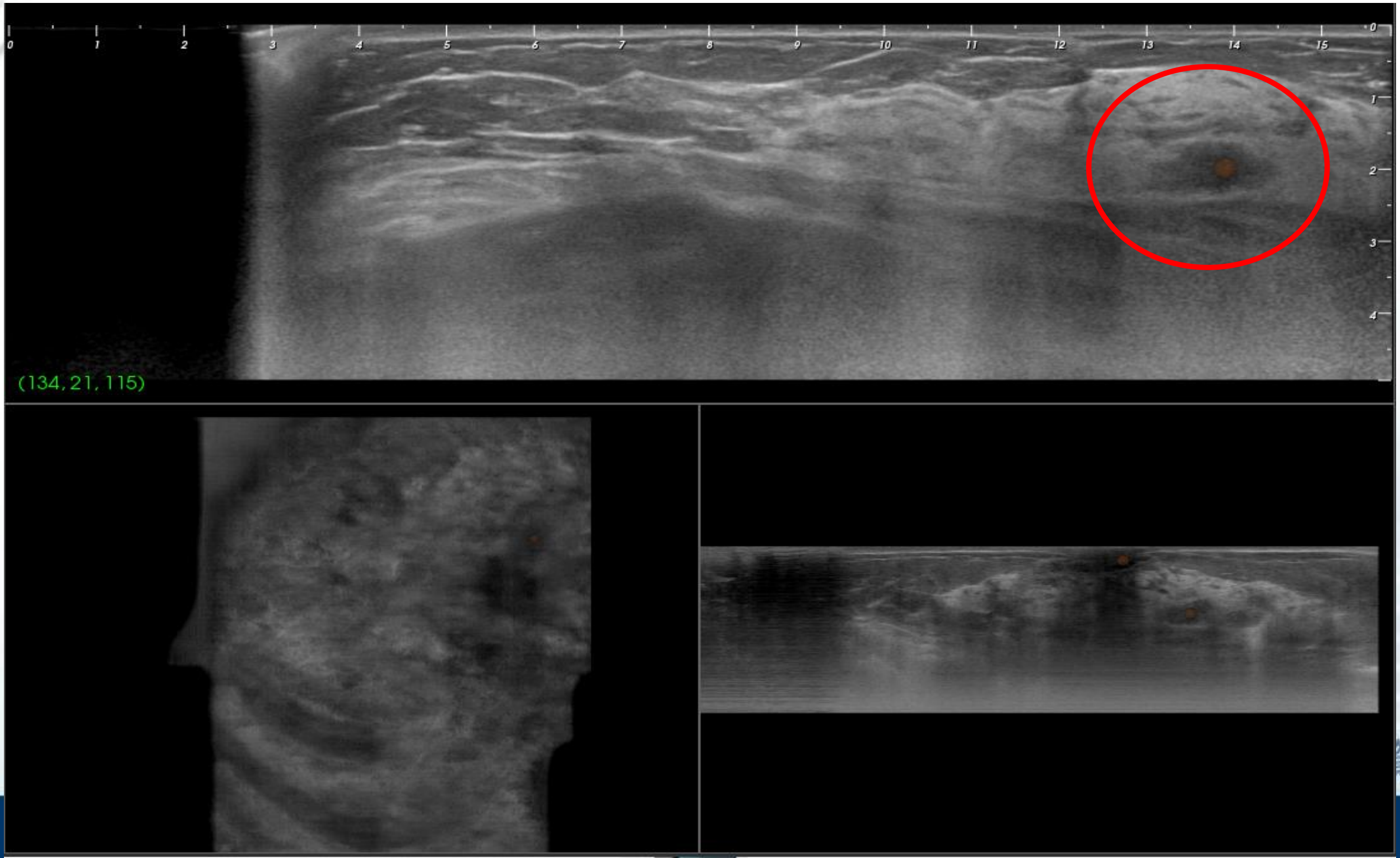

Case #2

- Reader B
  - Not marked at step 1 but marked at step 2 (CAD)
  - BI-RADS 3
- Readers A and C
  - Not marked at step 1

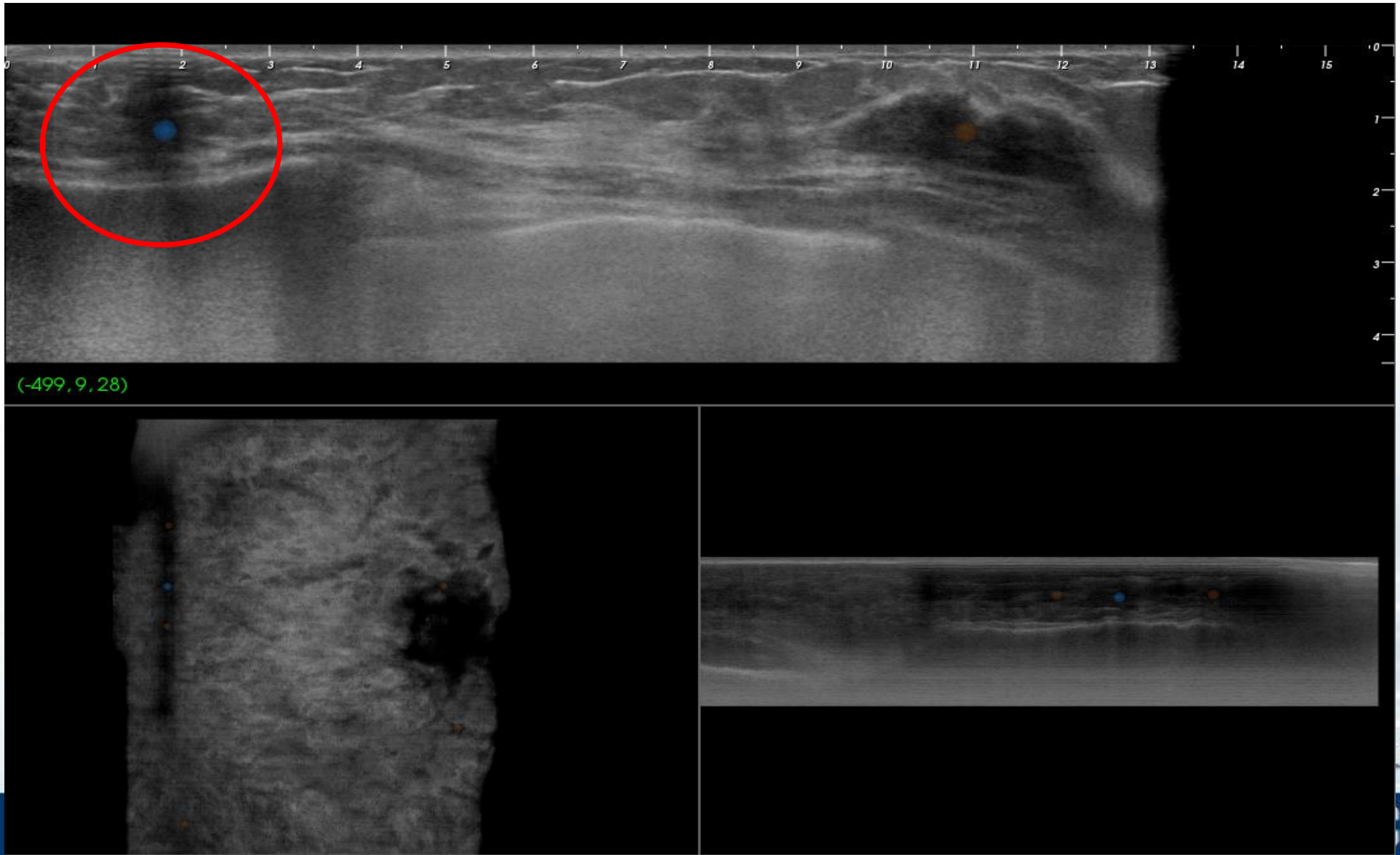

Case #3

- Reader B
  - Not marked at step 1 but marked at step 2 (CAD)
  - BI-RADS 3
- Readers A and C
  - Marked at step 1

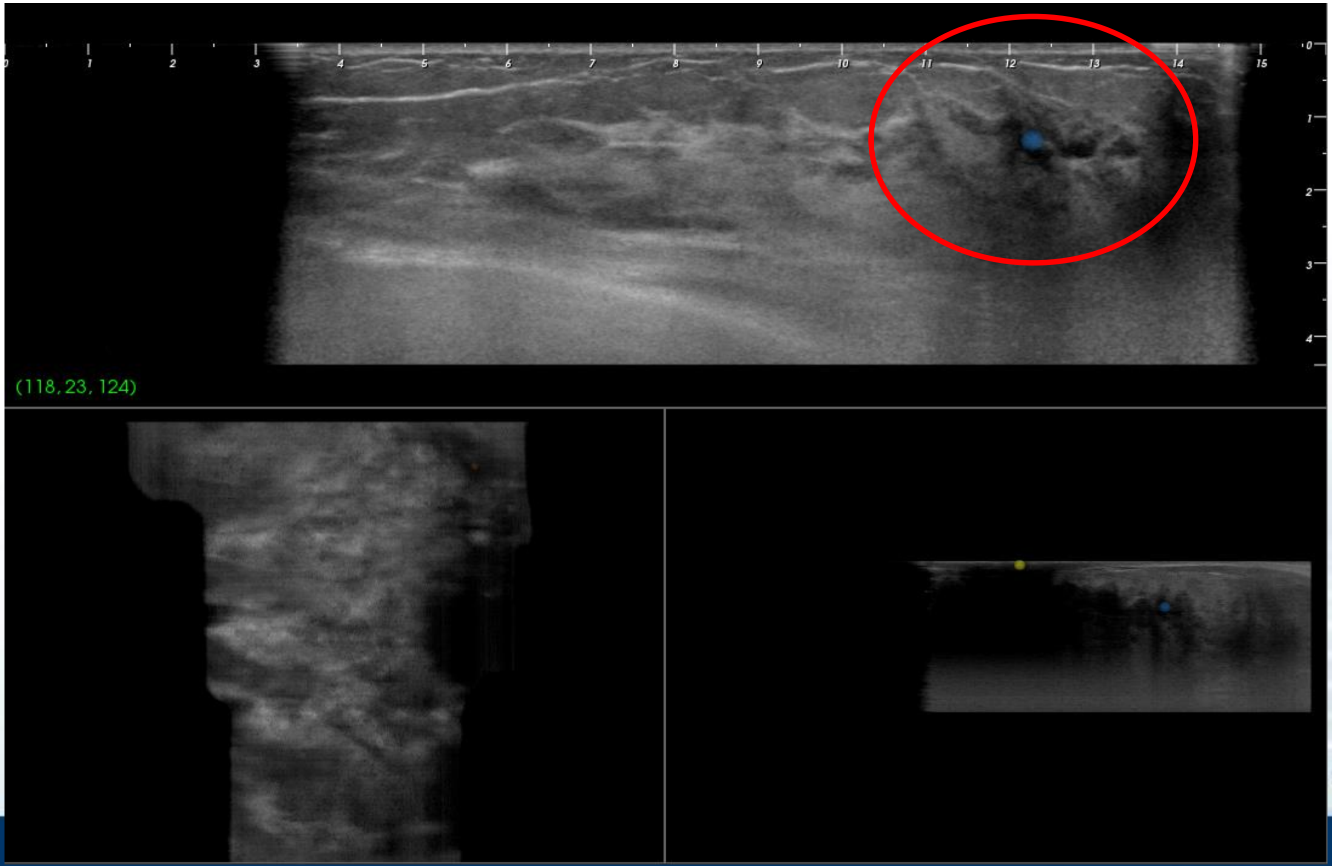

Case #4

- Readers A and B
  - Not marked at step 1 but marked at step 2 (CAD)
  - BI-RADS 5
- Reader C
  - Marked at step 1

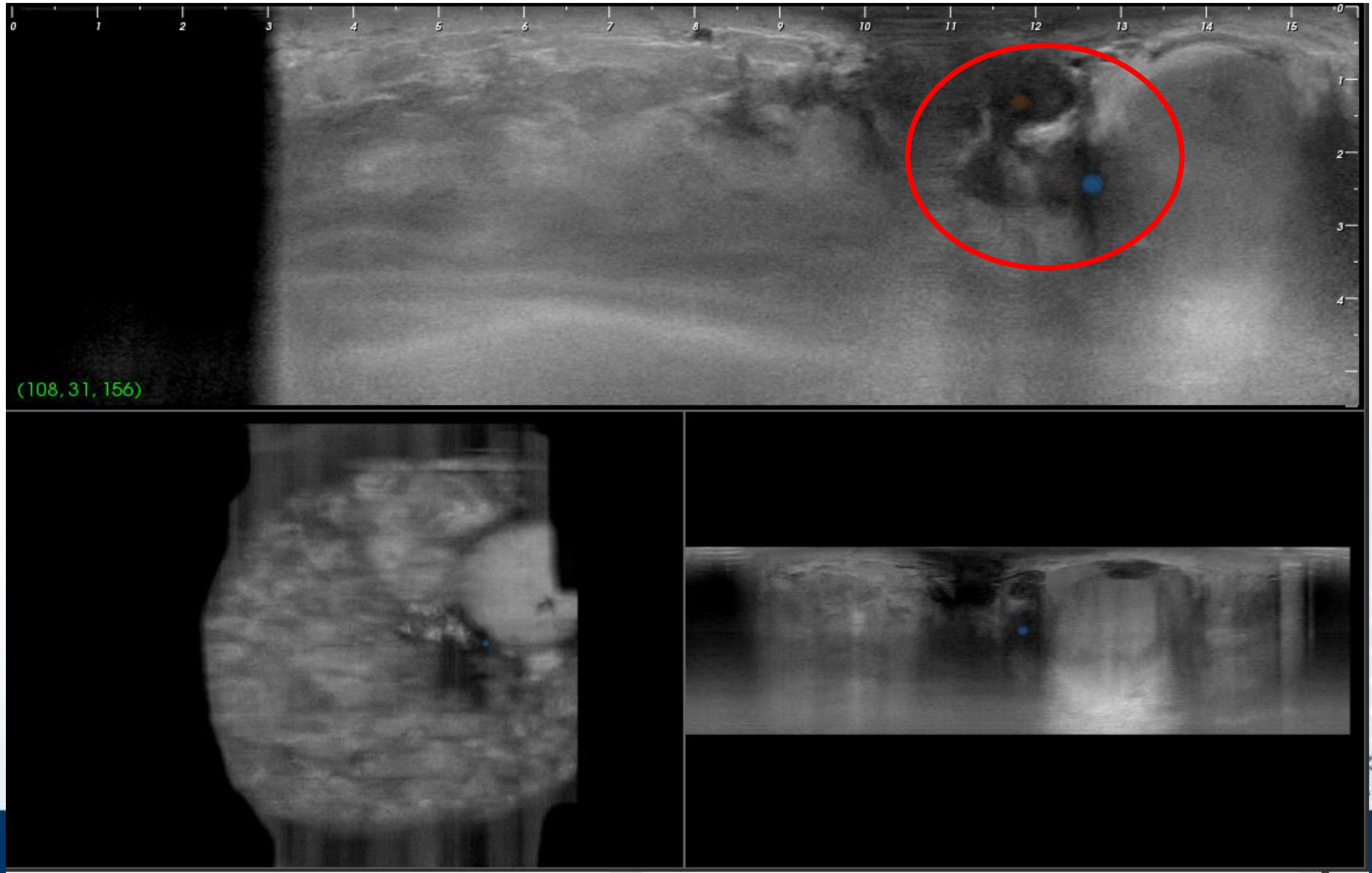

Free-hand Whole Breast US

- Using magnetic tracker and image capturing, the conventional US can be used to scan the whole breast, like ABUS.

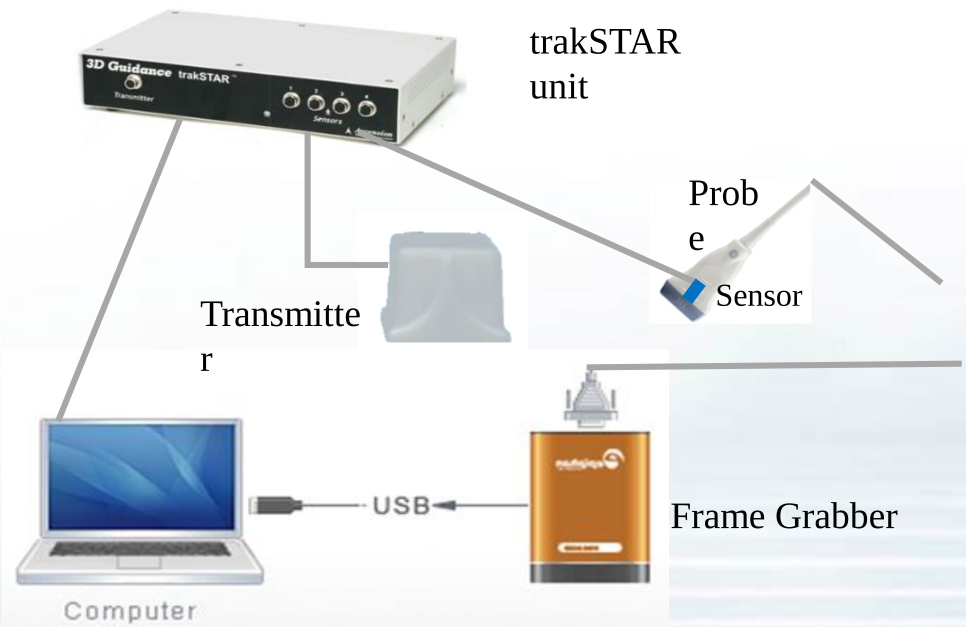

Magnetic Trackers

Hitachi

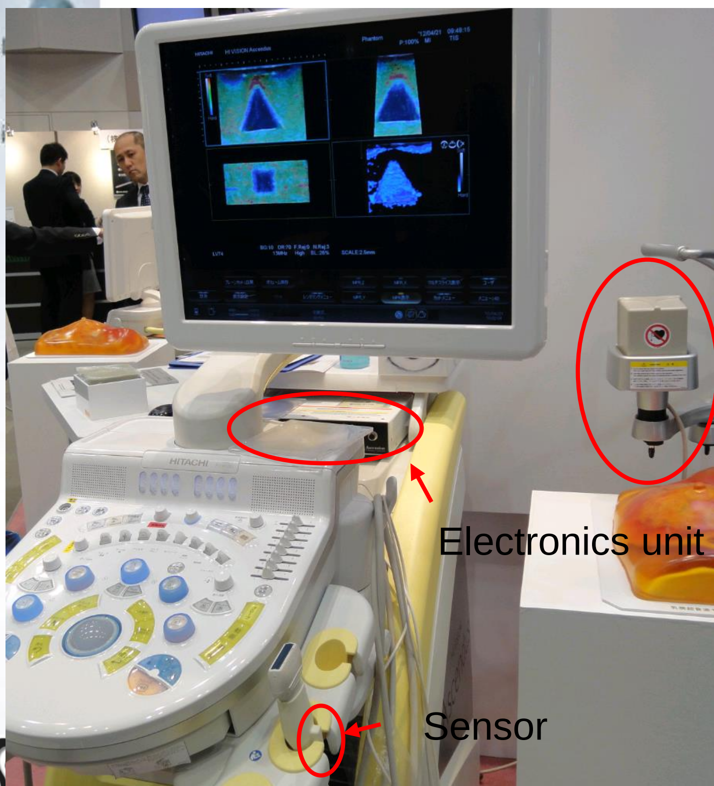

GE

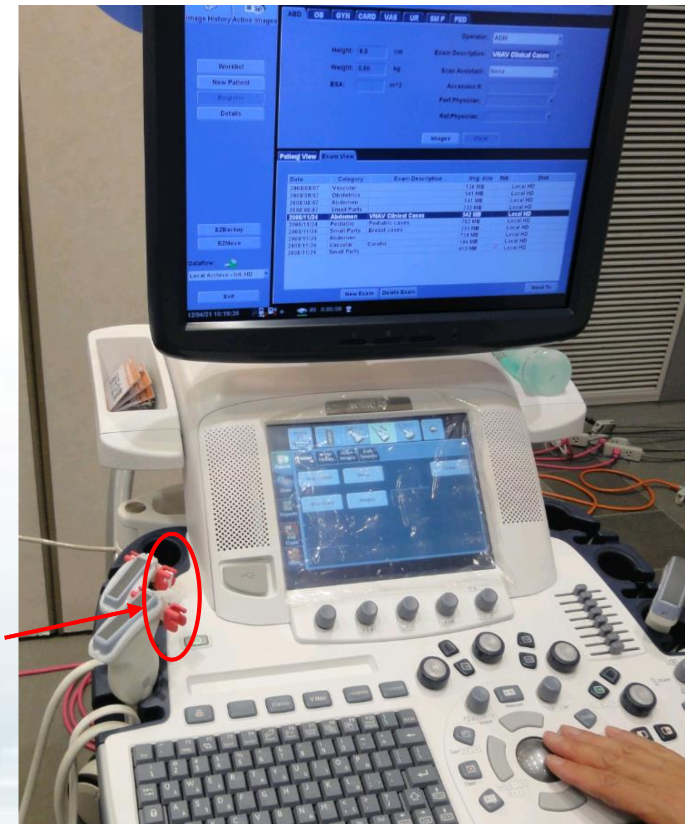

Free-hand WBUS System

- The free-hand GPS system has been tried in the NTUH Breast Center and NTUH Yun-Lin Branch.
  - The free-hand system will be compared with ABUS.
- In the viewing system, the user can select any location to reviewing the images at that location.

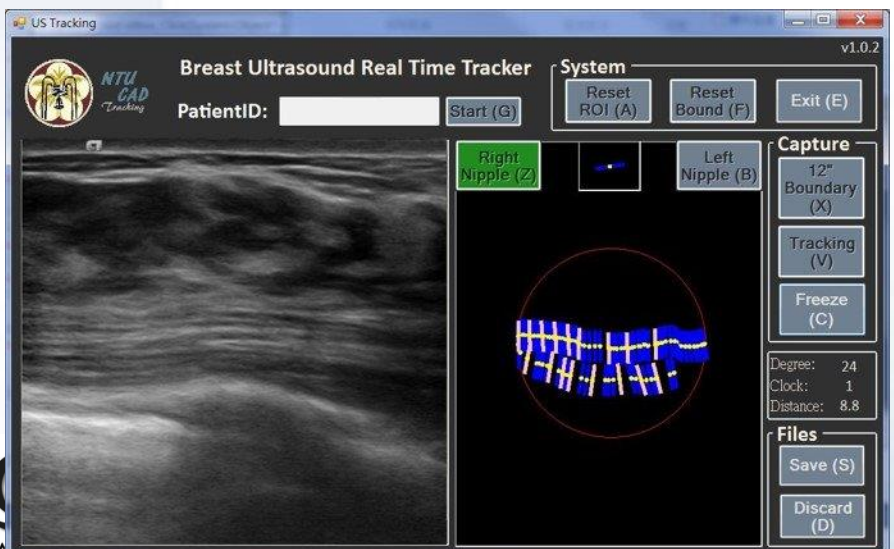

Free-hand GPS Image Recorder

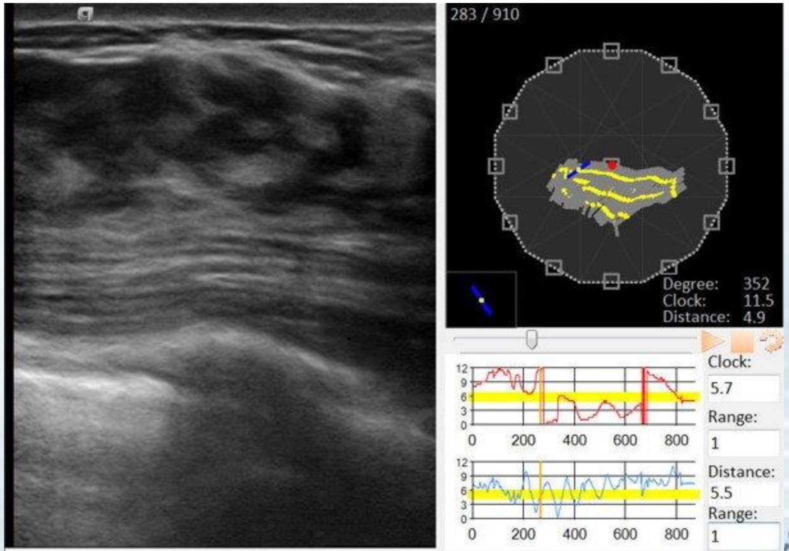

Free-hand GPS Image Player

ABVS/MRI/TOMO Density Analysis

- RIB SHADOW FOR FINDING BREAST REGION

"Breast density analysis for whole breast ultrasound images", Medical Physics, Vol. 36, No. 11, pp. 4933-4943, Nov. 2009.

"Comparative study of density analysis using automated whole breast ultrasound and MRI", Medical Physics, Vol. 38, No. 1, pp. 382-389, Jan. 2011.

"Breast Density Analysis with Automated Whole-Breast Ultrasound: Comparison with 3-D Magnetic Resonance Imaging," Ultrasound in Med. & Biol., vol. 42, no.5, pp. 1211-1220, 2016.

Aloka Whole Breast Density Analysis

- Breast density measured from mammograms and whole breast US

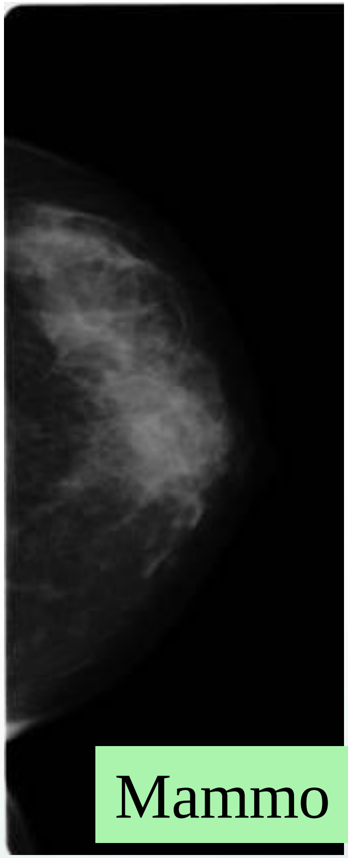

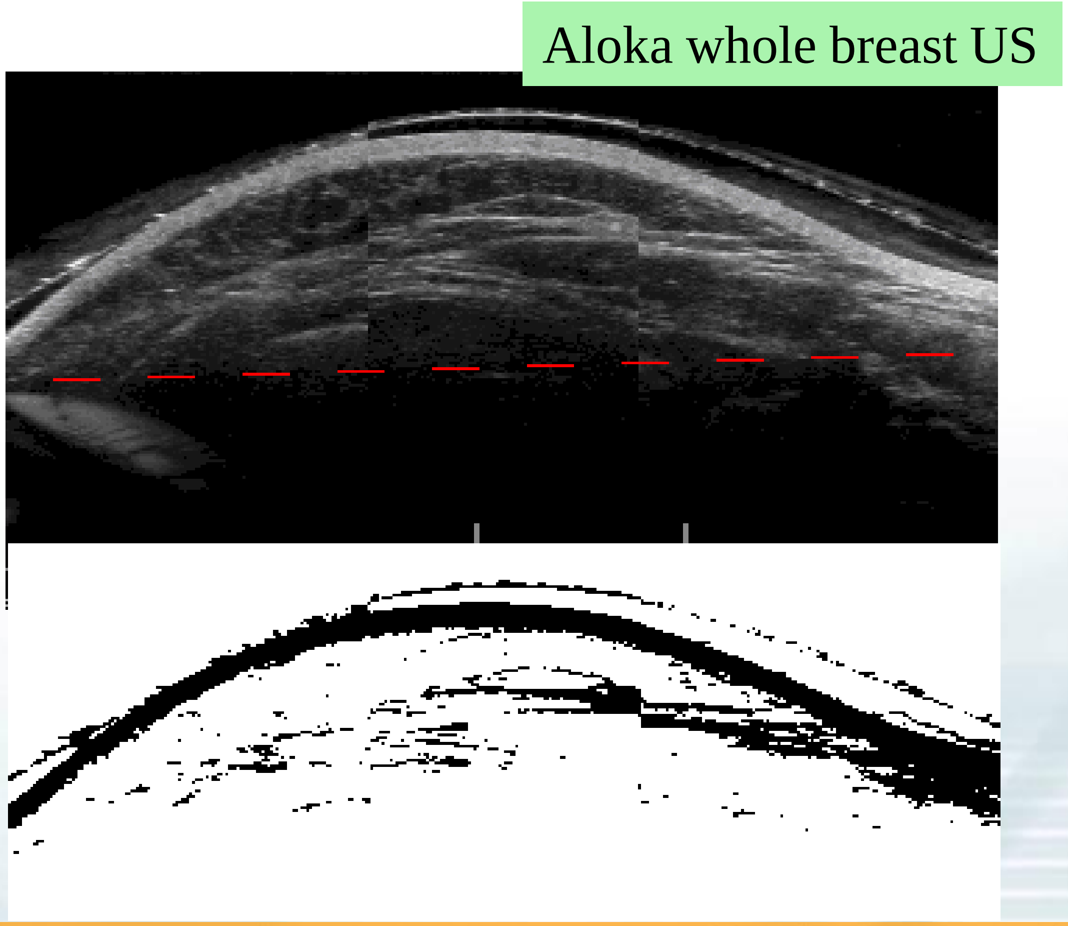

"Breast density analysis for whole breast ultrasound images", Medical Physics, Vol. 36, No. 11, pp. 4933-4943, Nov. 2009.

Whole Breast US vs. Mammogram

Grade 2

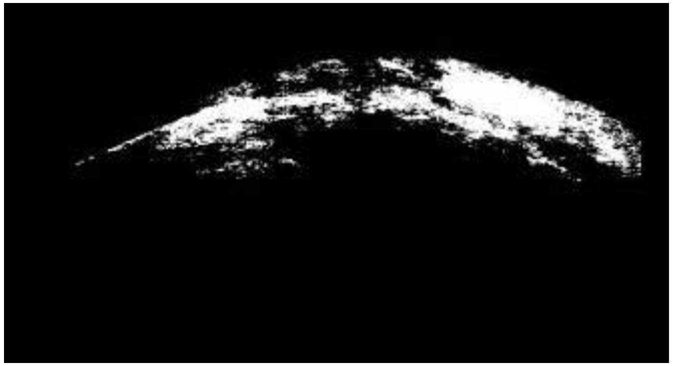

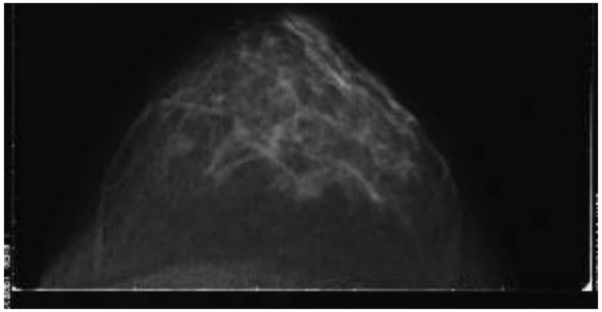

Grade 3

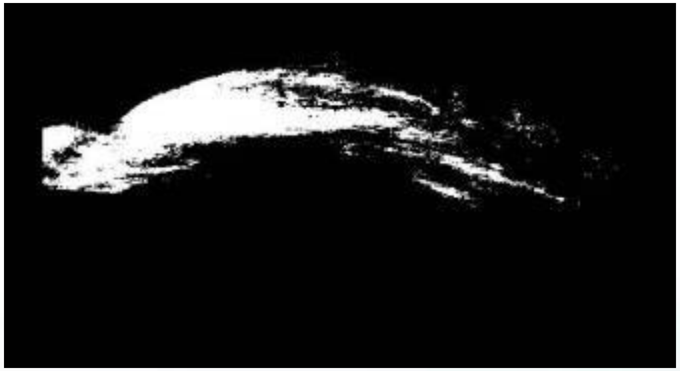

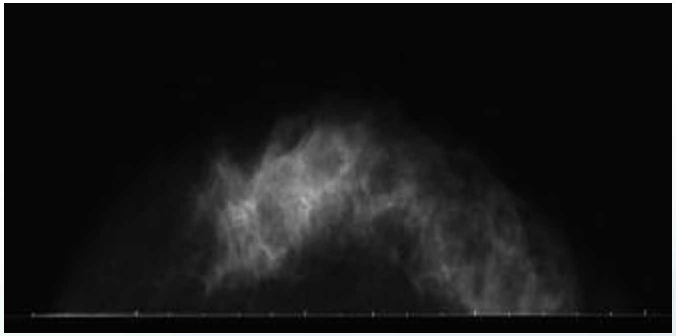

Grade 4

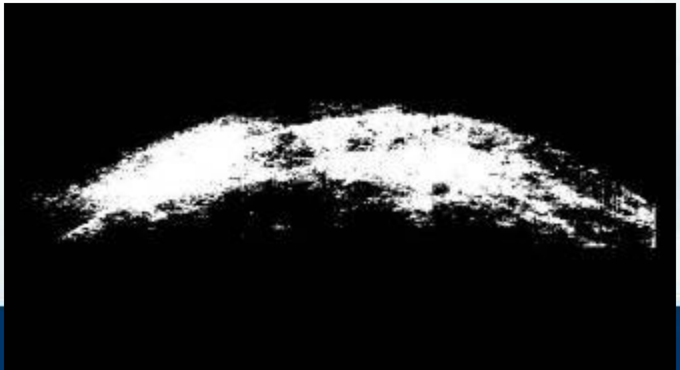

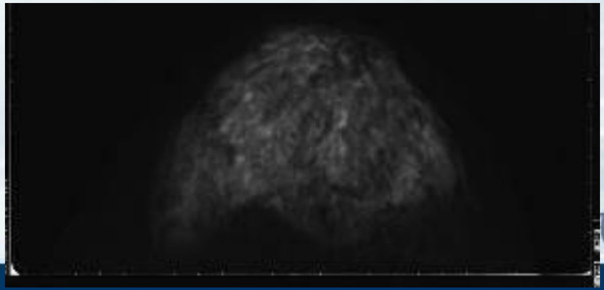

U-systems Whole Breast Density Analysis

- The similar Aloka whole breast density analysis could be applied for the U-systems.

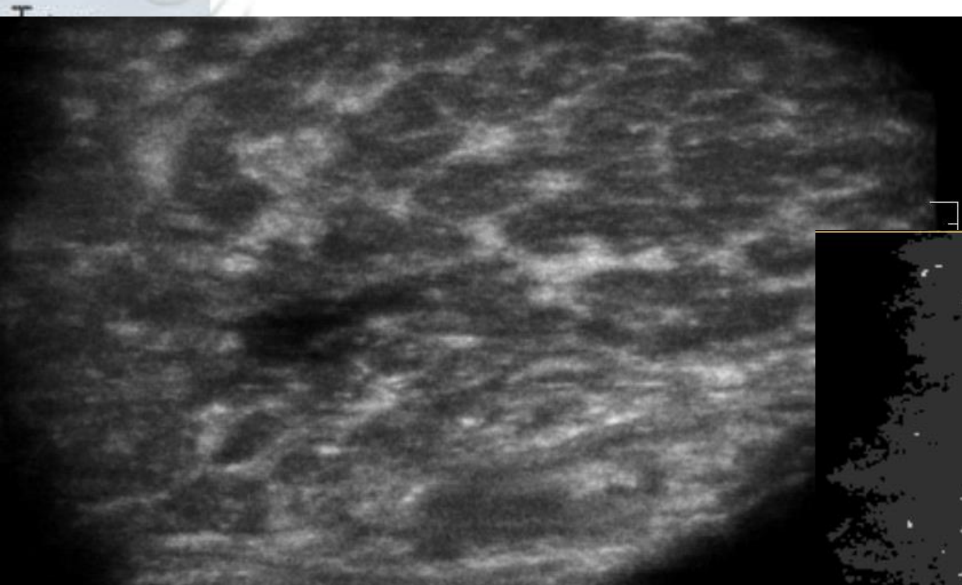

Original C View

Gland/Fat Analysis

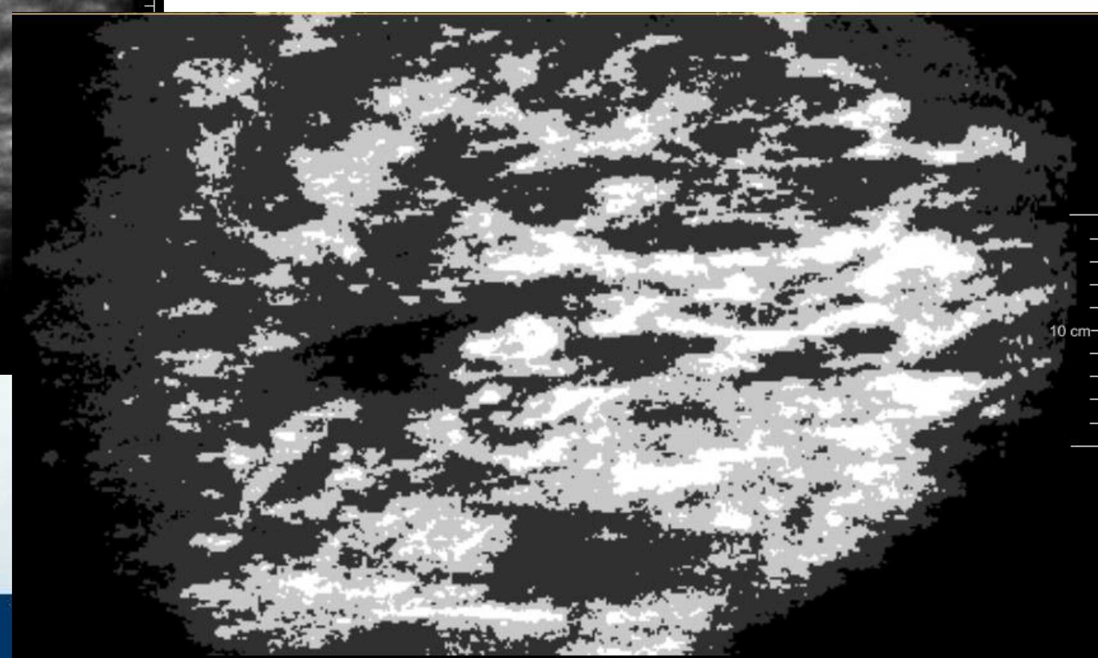

U-Systems Density Analysis

- The U-systems ABUS density and volume is highly correlated with those of MRI.

ABUS

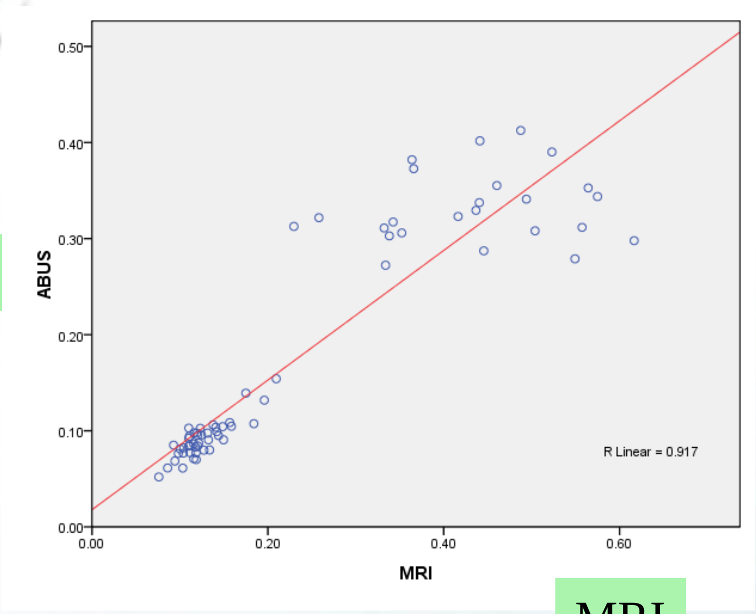

MRI

Density

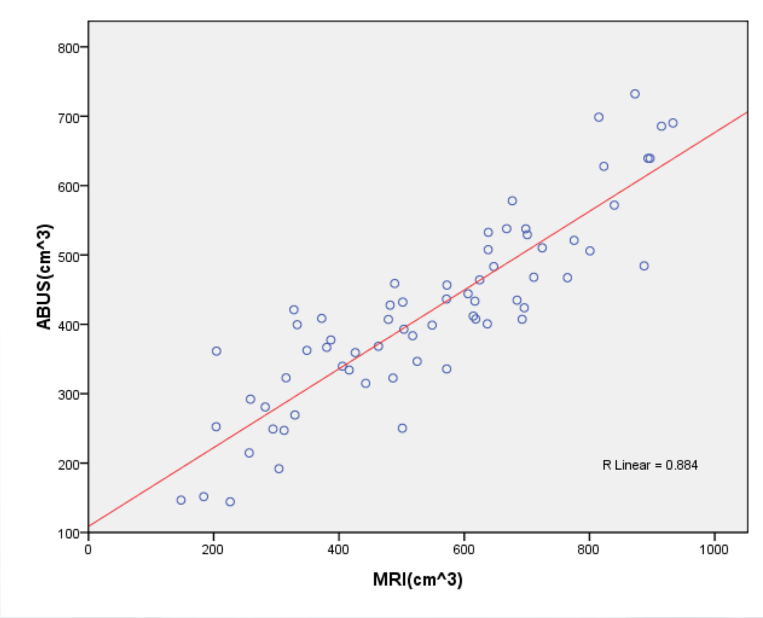

Volume

"Comparative study of density analysis using automated whole breast ultrasound and MRI", Medical Physics, Vol. 38, No. 1, pp. 382-389, Jan. 2011.

FCM Density Analysis

- The fuzzy c-mean (FCM) classifier was used to differentiate the fibroglandular and fatty tissues in ABUS and MRI images

Original

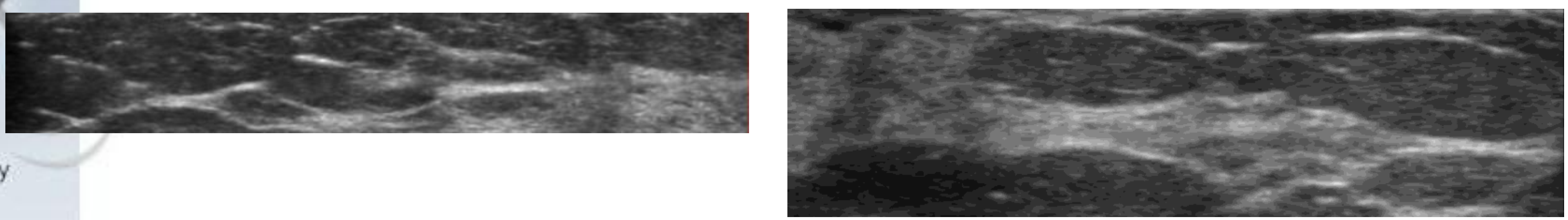

FCM

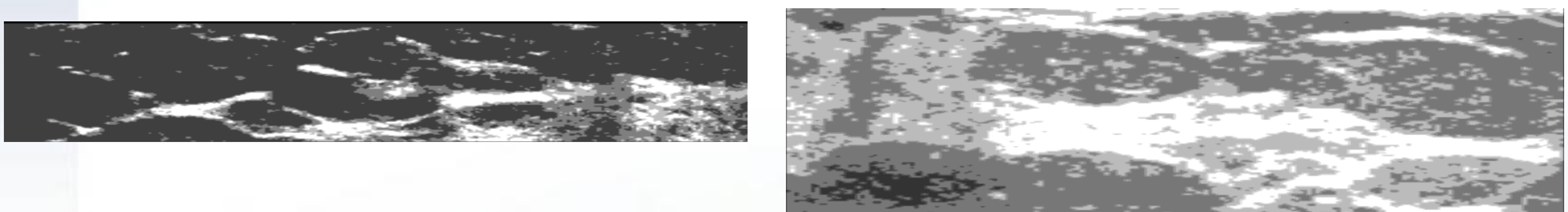

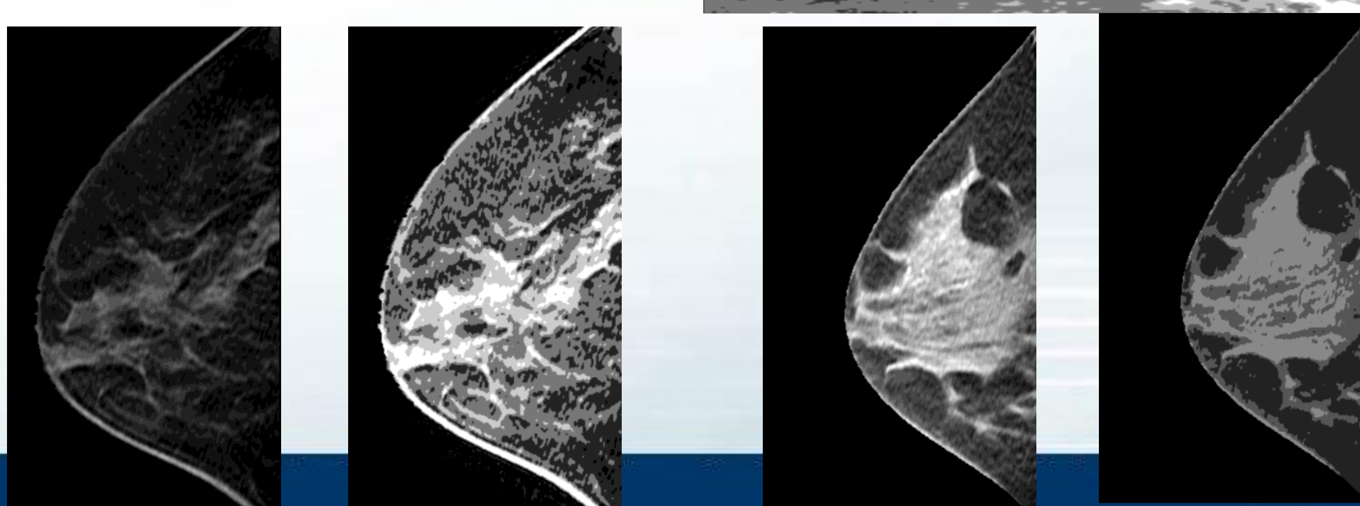

U-Systems Density Analysis

- The U-systems ABUS density and volume is highly correlated with those of MRI.

ABUS

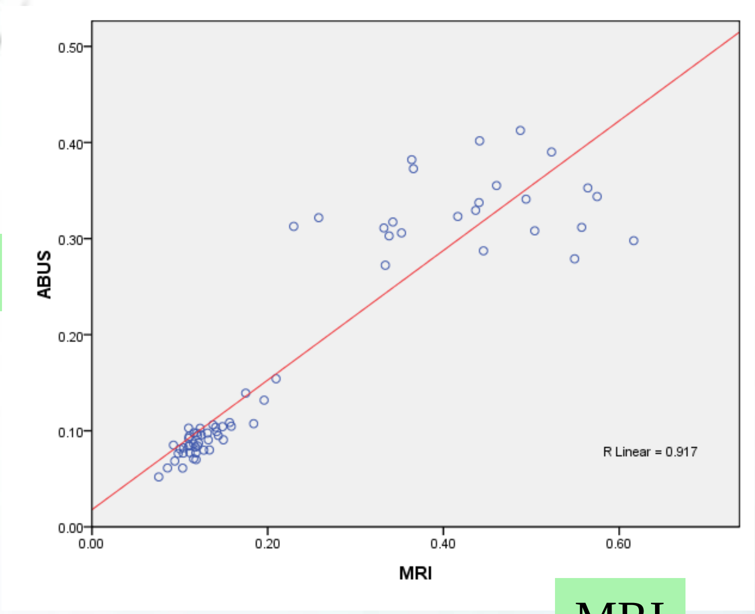

MRI

Density

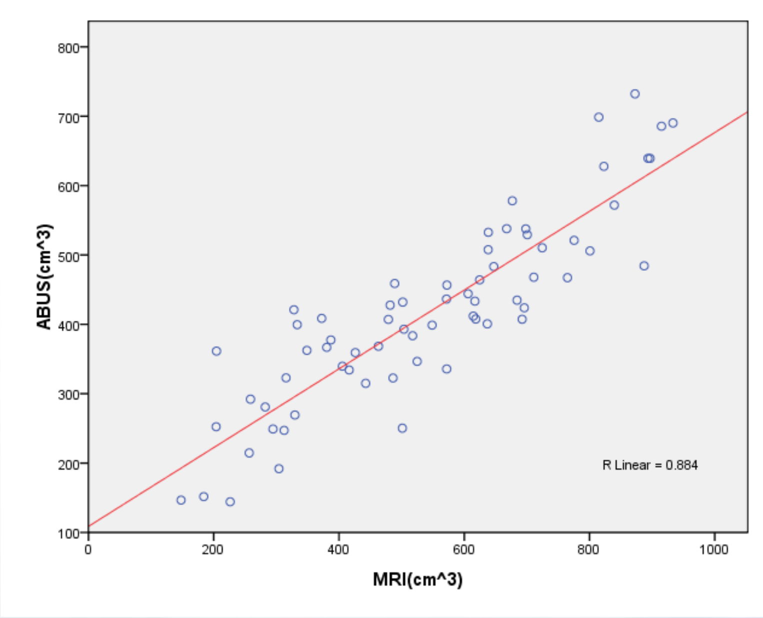

Volume

"Comparative study of density analysis using automated whole breast ultrasound and MRI", Medical Physics, Vol. 38, No. 1, pp. 382-389, Jan. 2011.

Rib Shadow for Finding Breast Region

- For **density analysis**, an automatic breast segmentation method was proposed based on the **rib shadow** to extract breast region from ABUS.

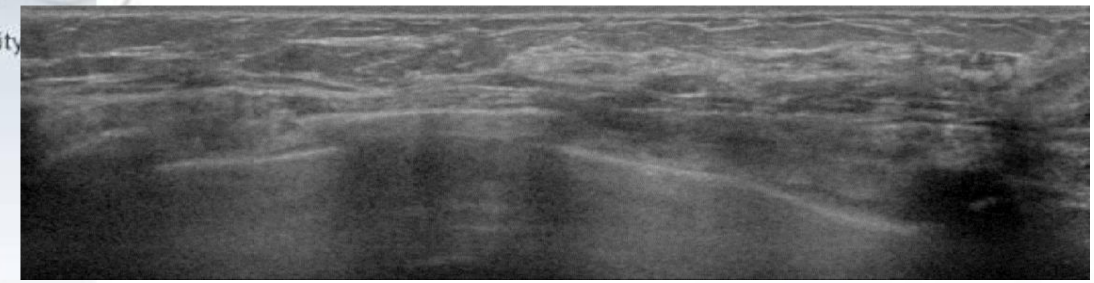

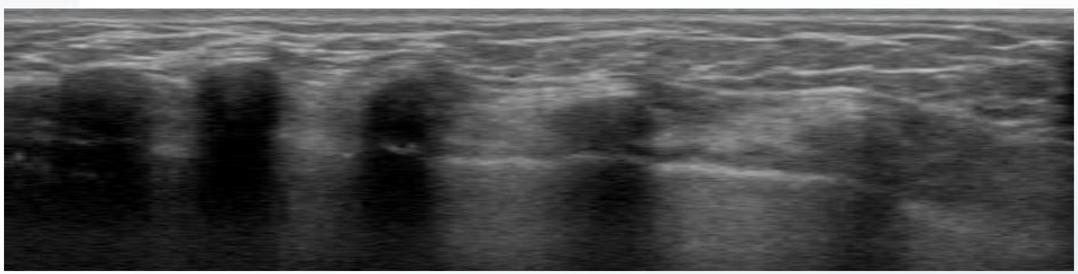

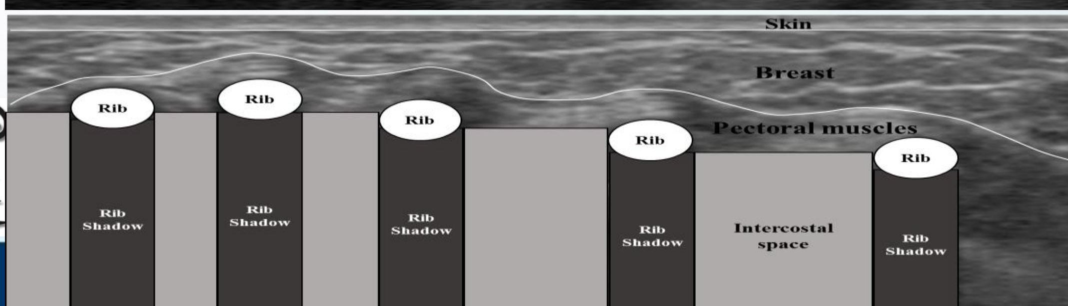

Transverse View

↓

Sagittal View

An Example

- Using rib shadow to extract the chest wall line.

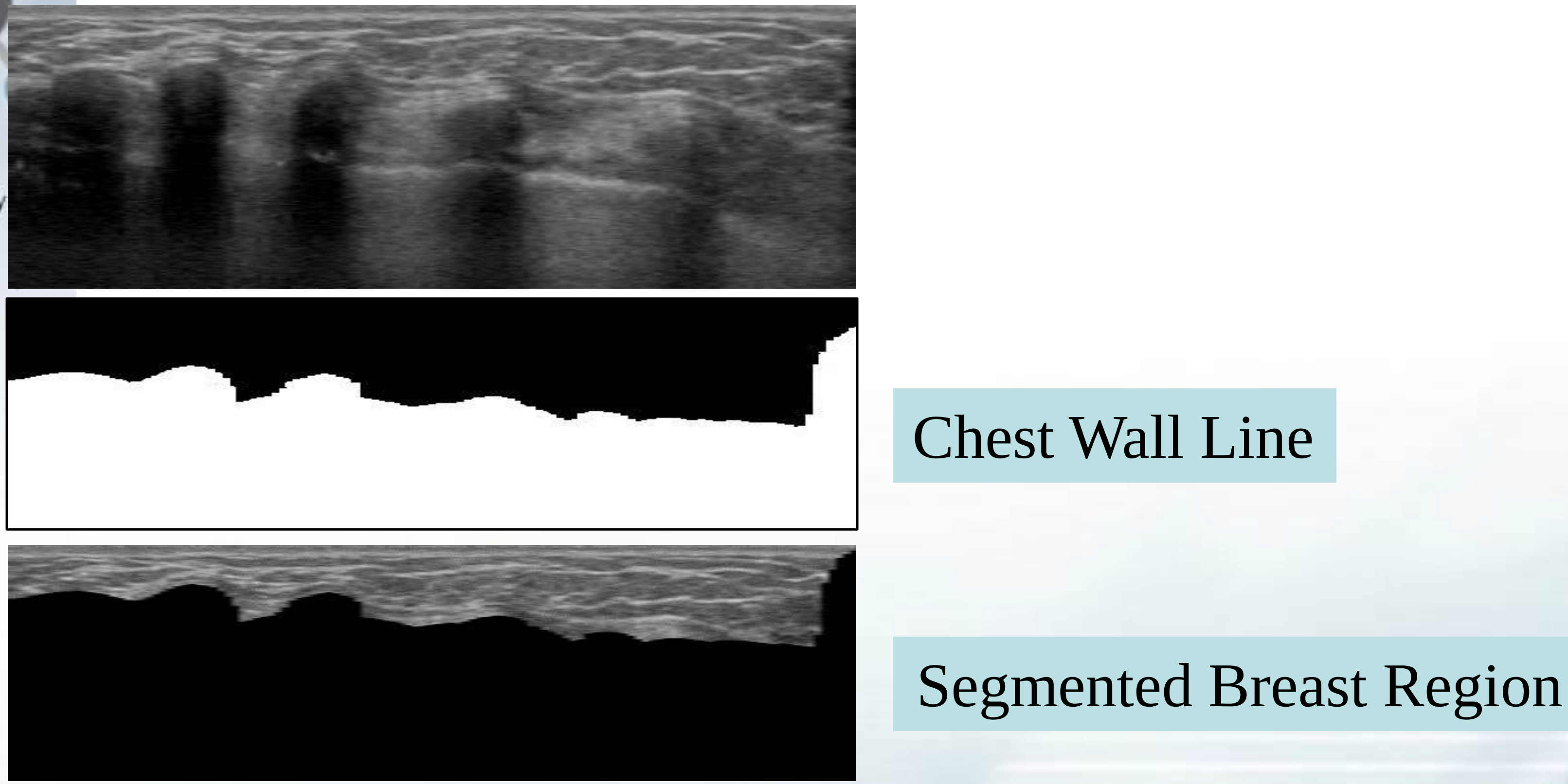

"Breast Density Analysis with Automated Whole-Breast Ultrasound: Comparison with 3-D Magnetic Resonance Imaging," Ultrasound in Med. & Biol., vol. 42, no.5, pp. 1211-1220, 2016.

Experimental Results

- **MRI** and **ABVS** images of 46 breasts from 23 women were collected.
- Our results revealed a high correlation in WBV and BPD between **MRI** and **ABVS**.
- Our study suggests that **ABVS** provides breast density information useful in the assessment of breast health.

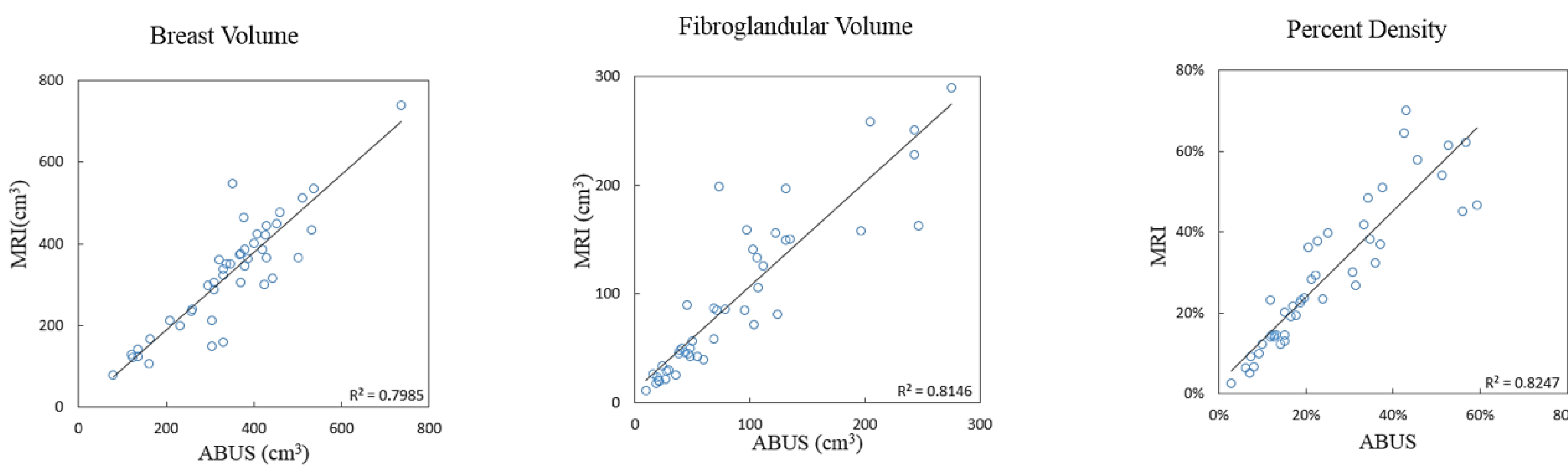

(a)

ABUS-MRI Breast Volume Difference

ABUS-MRI Fibroglandular Volume Difference

ABUS-MRI Percent Density Difference

TOMO Density

From Dr. Moon, SNUH

MRI

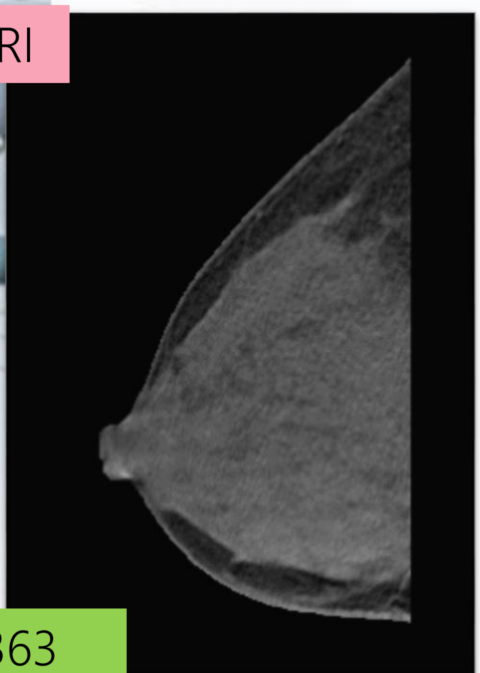

0.3363

TOMO

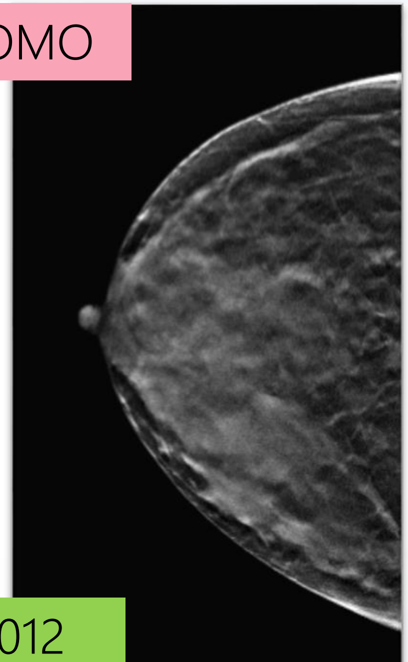

0.2012

2D Mammo

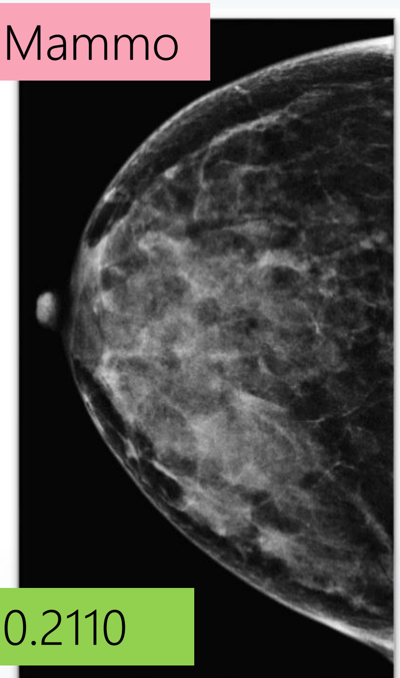

0.2110

BI-RADS=3

LCC

Factor	R	L
Volume of fibroglandular tissue (cm3)	~132	~106
Volume of breast (cm3)	~275	~248
Percentage of fibroglandular tissue (%)	~48	~43

TOMO Density

From Dr. Moon, SNUH

MRI

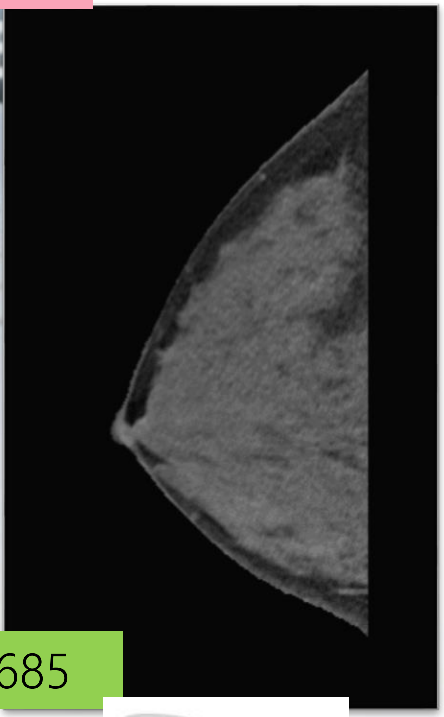

0.3685

TOMO

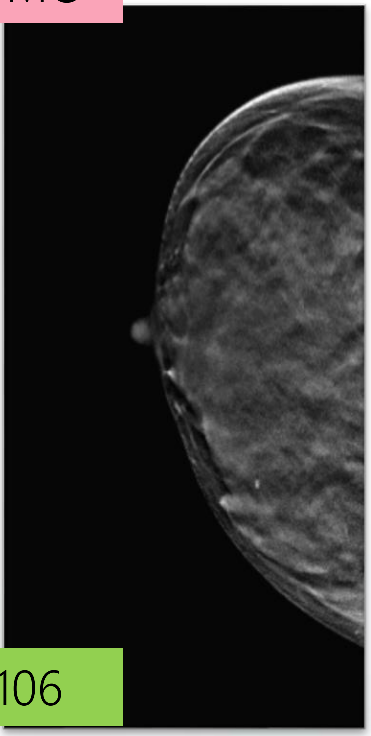

0.2106

2D Mammo

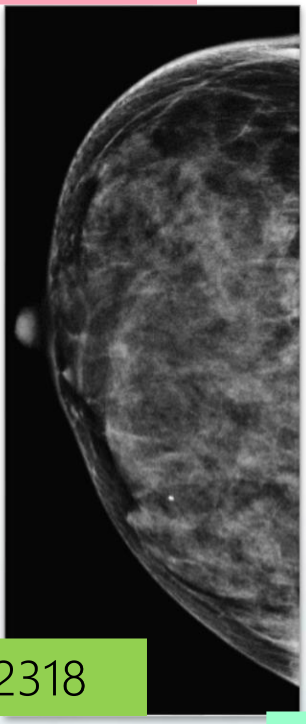

0.2318

BI-RADS=4

LCC

Factor	R	L
Volume of fibroglandular tissue (cm3)	~55	~40
Volume of breast (cm3)	~299	~204
Percentage of fibroglandular tissue (%)	~19	~20

Mammo Volumetric Density

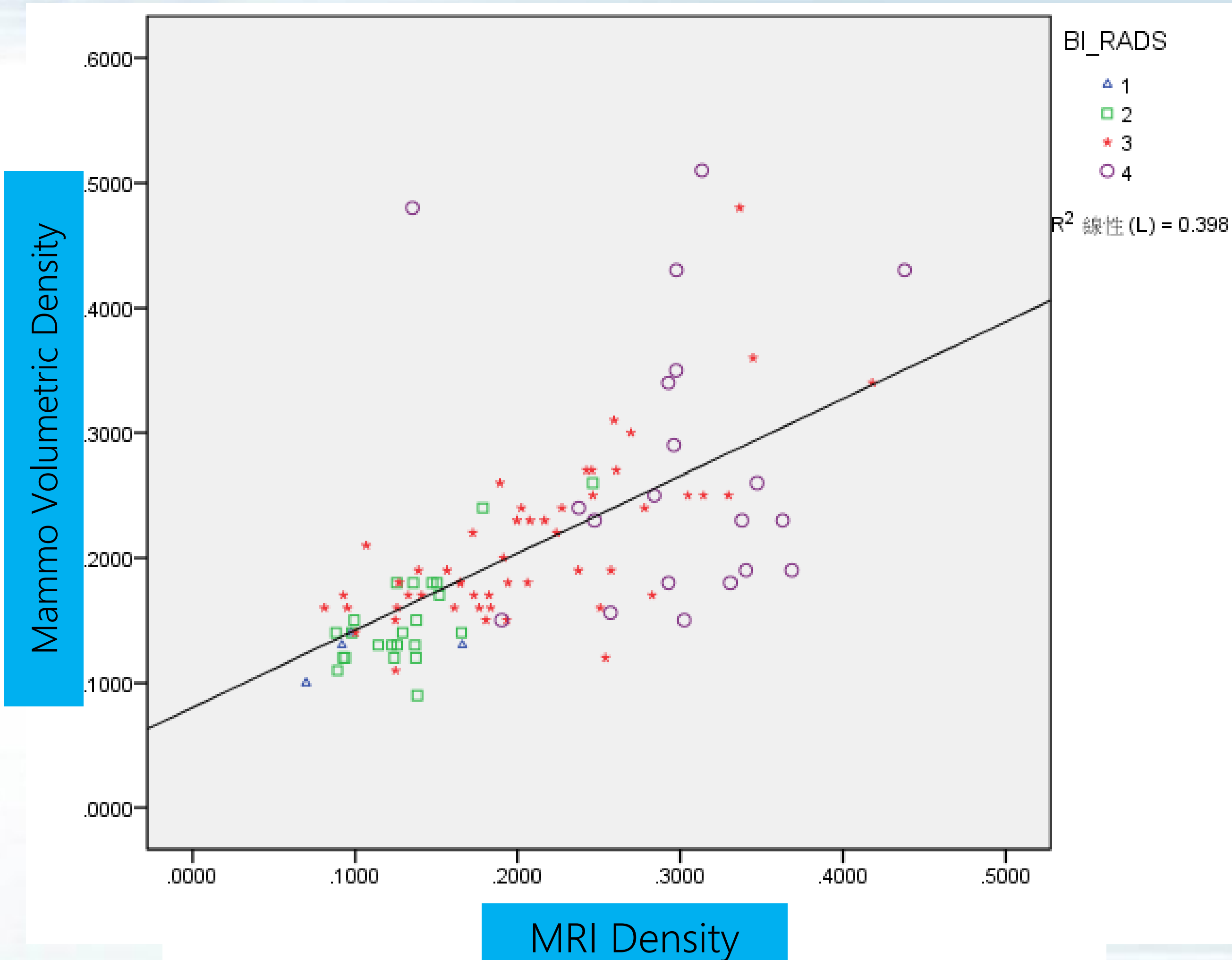

模式	R	R 平方	調過後的 R 平方	估計的標準誤
1	.631[a]	.398	.392	.0657221

a. 預測變數:(常數), MriDens.

MRI CADe/CADx

"Computerized breast lesions detection using kinetic and morphologic analysis for dynamic contrast-enhanced MRI," Magnetic Resonance Imaging, vol. 32, no. 5, pp. 514-522, 2014.

"Computerized breast mass detection using multi-scale Hessian-based analysis for dynamic contrast-enhanced MRI," Journal of Digital Imaging, vol. 27, no. 5, pp. 649-660, 2014.

"Computer-aided diagnosis of mass-like lesion in breast MRI: Differential analysis of the 3-D morphology between benign and malignant tumors," Computer Methods and Programs in Biomedicine, vol. 112, no. 3, pp. 508-517, 2013.

"Computer-aided diagnosis of breast DCE-MRI using pharmacokinetic model and 3-D morphology analysis," Magnetic Resonance Imaging, vol. 32, no. 3, pp. 197-205, 2014.

Hessian-based Detection

- Nonparametric nonuniform intensity normalization algorithm (N4ITK) is used to reduce nonuniformity bias.
- The deformation of thorax to approximate the outline between breast and chest by the Demons deformable algorithm is used to segment the breast region.
- Fuzzy c-means algorithm (FCM) and Hessian algorithm are used to detect the tumors.

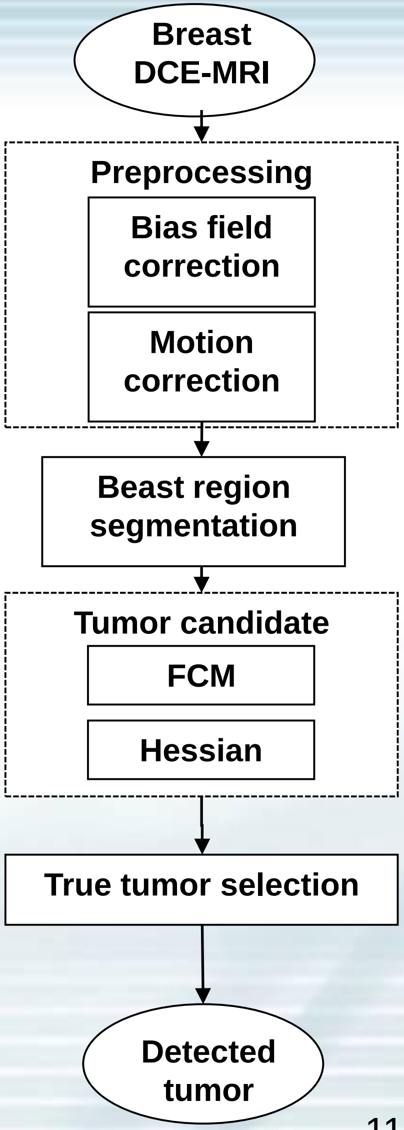

Detection Result

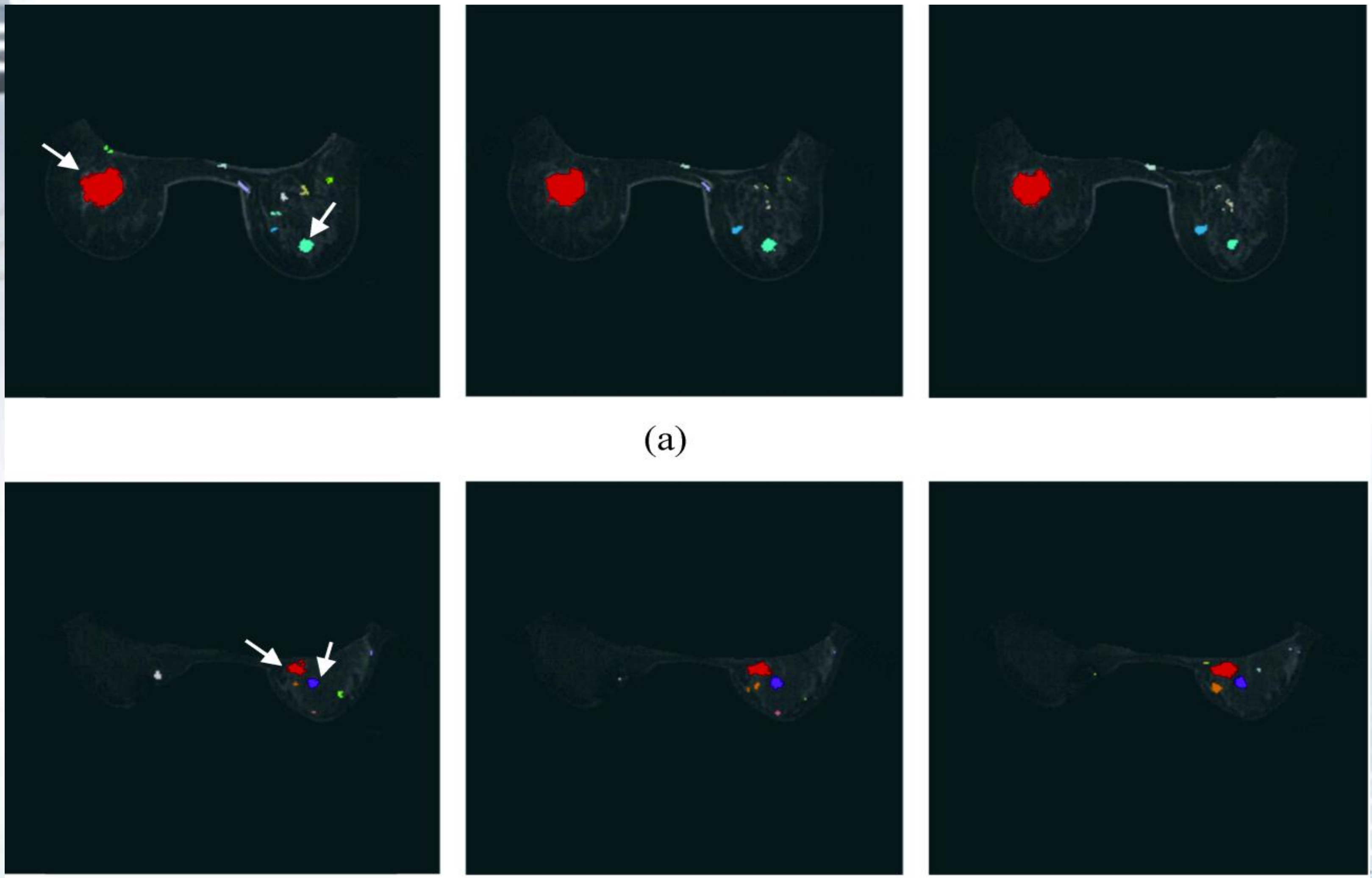

(a)

(b)

Detection performance analysis

- True tumor detection performance
  - The mass detection rates are 100% (61/61) with 15.15 false positives per case and 91.80% (56/61) with 4.56 false positives per case.

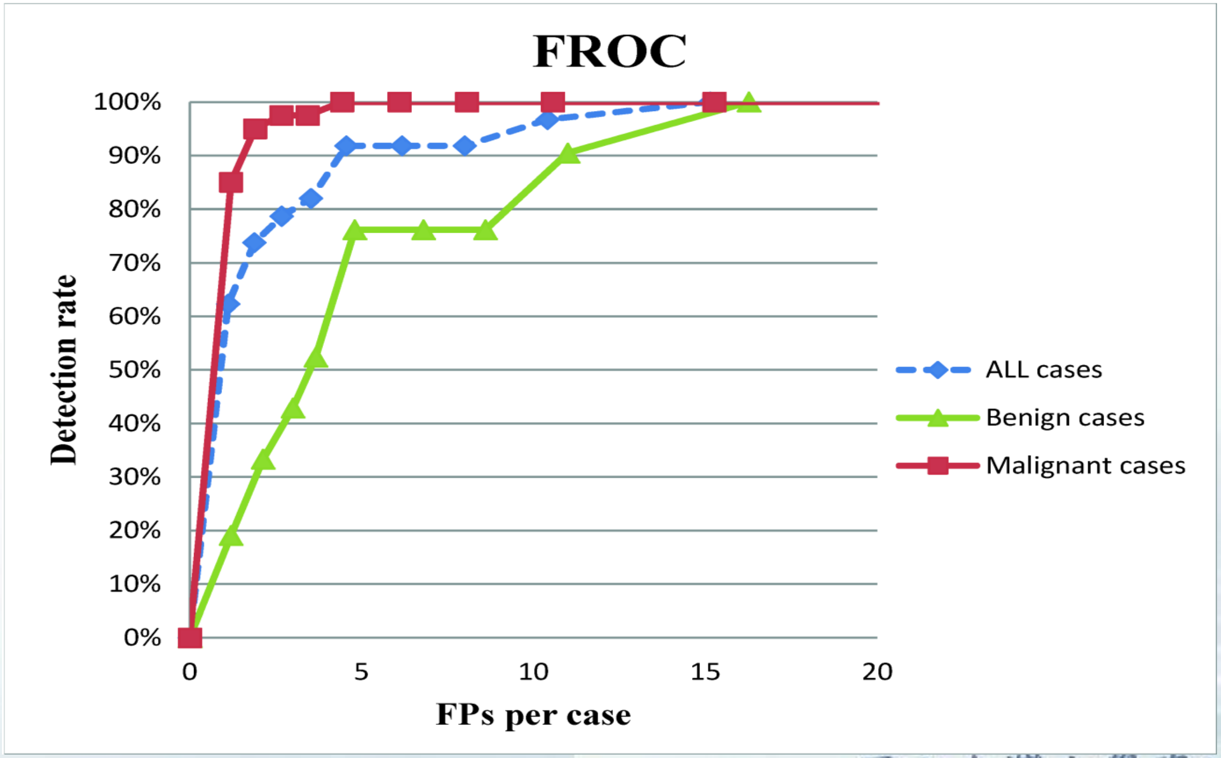

Breast DCE-MRI CADx

- The Pharmacokinetic Model and 3-D morphology Analysis are used to diagnose the tumors in DCE-MRI.

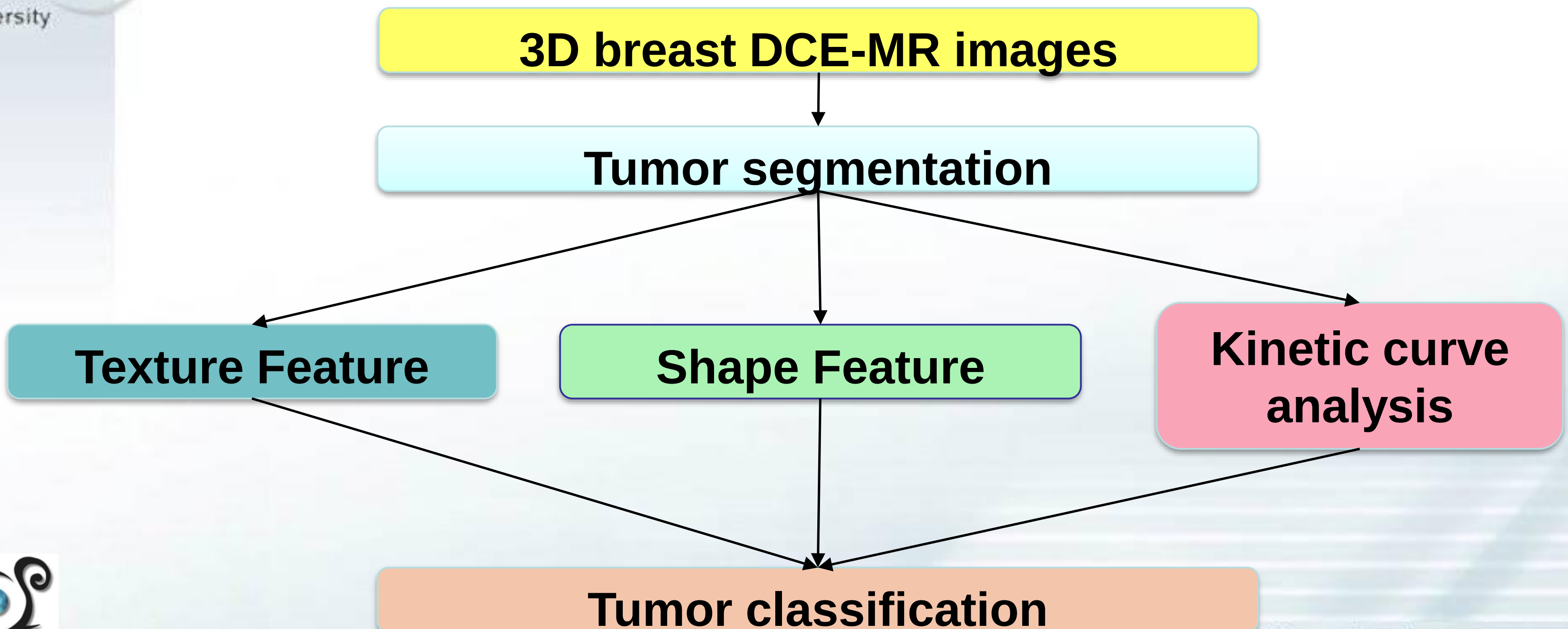

Results

Method Item	Conventional	Tofts model	GLCM	Shape	All
Accuracy (%)	84.85 (112/132)	86.36 (114/132)	81.82 (108/132)	80.30 (106/132)	91.67 (121/132)
Sensitivity (%)	79.71 (55/69)	85.51 (59/69)	81.16 (56/69)	78.26 (54/69)	91.30 (63/69)
Specificity (%)	90.48 (57/63)	87.30 (55/63)	82.54 (52/63)	82.54 (52/63)	92.06 (58/63)
PPV (%)	90.16 (55/61)	88.06 (59/67)	83.58 (56/67)	83.08 (54/66)	92.65 (63/68)
NPV (%)	80.28 (57/71)	84.62 (55/65)	80.00 (52/65)	77.61 (52/66)	90.63 (58/64)

Dynamic Contrast-Enhanced Tomosynthesis

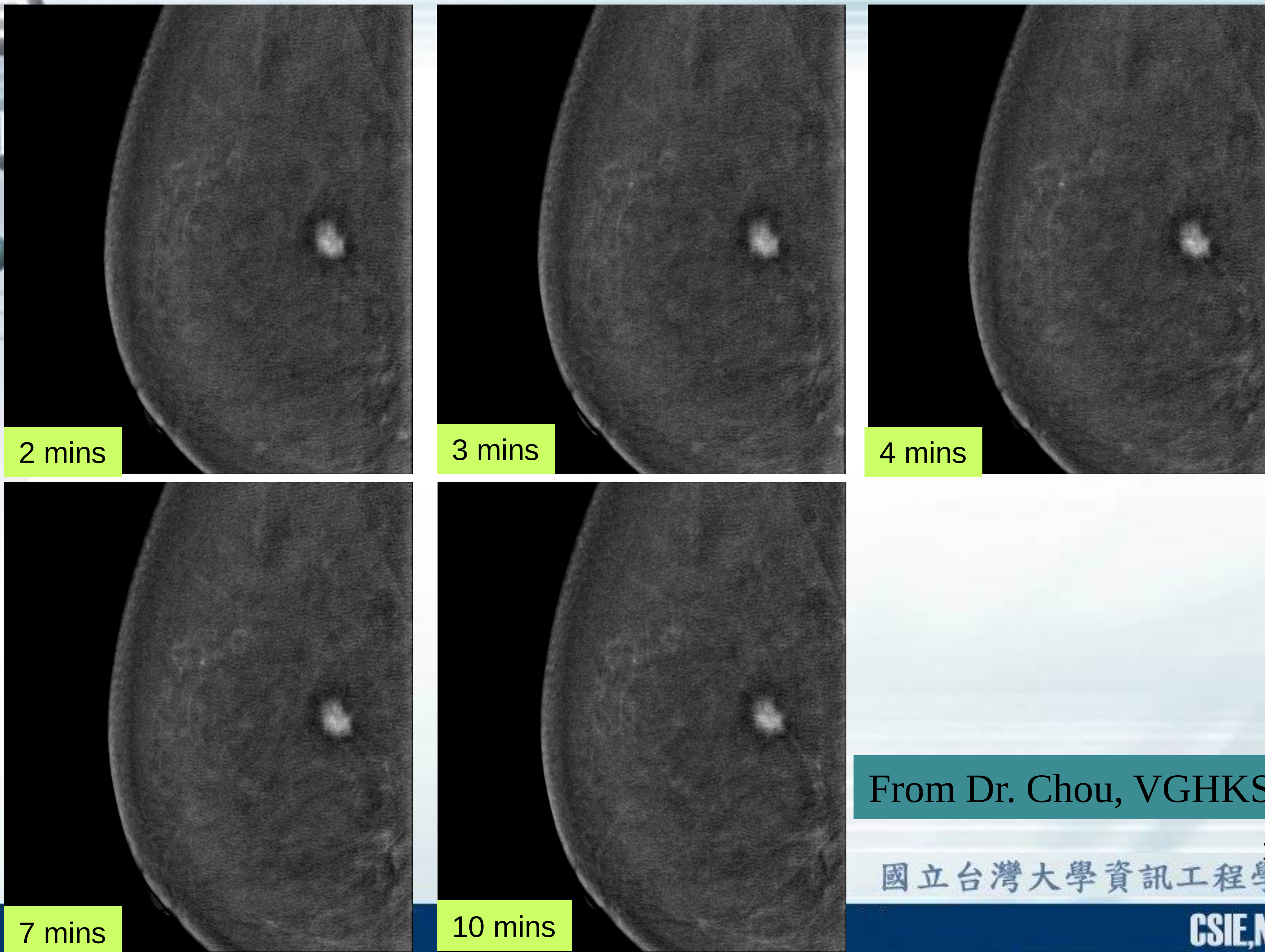

From Dr. Chou, VGHKS

Thanks for Your Attention!!